Crystallographic and Biochemical studies on Dissimilatory Sulfite Reductases

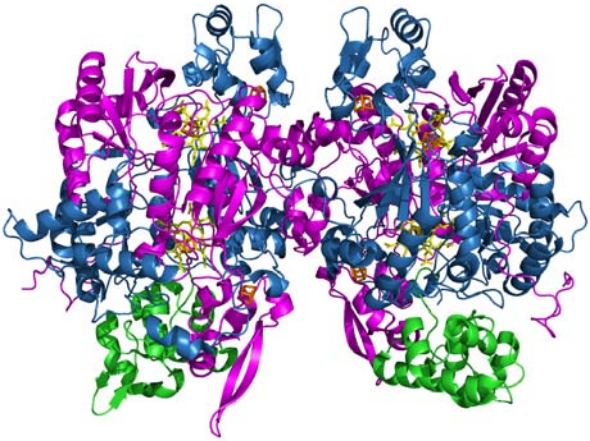

Tânia Filipa Oliveira

Thesis dissertation presented to obtain a PhD degree in Biochemistry at Instituto de Tecnologia Química e Biológica, Universidade Nova de Lisboa

Oeiras, 2011

Scientific Advisers

Doctor Margarida Archer

Doctor Inês Pereira

Doctor Amir Khan

Finantial support for this work was provided by a Fellowship (SFRH/BD/29519/2006) ***from Fundação para a Ciência e Tecnologia, and partial support was also provided by Dr. Amir Khan at Trinity College Dublin***

Acknowledgements

I owe a great deal of thanks to many people. First of all, I would like to thank my two direct supervisors, Doctor Margarida Archer and Doctor Inês Pereira for creating the conditions which made this work possible. For their teaching, guidance, critical discussions, and most importantly, for being there in decisive moments and supporting me, I convey my sincere thanks.

I want to particularly thank Dra Margarida Archer, for receiving me in her lab in the early stages of my scientific career, and for encouraging me through this PhD adventure. Thanks, for all the motivation and help in overcoming the difficulties I encountered, for your guidance and friendship and for supporting all my decisions. It was a great privilege to work so closely with you.

I would like to thank all my colleagues in the Bacterial Energy Metabolism laboratory, with special mention to Sofia Venceslau, for all her teaching in the biochemistry oriented part of my work, for her patience, motivation and friendship.

To my Membrane Protein Crystallography Lab colleagues, thanks for all the support, friendship and work discussions, as well as for the lovely and relaxing afternoon breaks.

Thanks to José, for sharing all your knowledge and for being always available to help me.

I cannot forget, Dr. Pedro Matias for the precious support in the Linux and non-trivial crystallography software world, as well as for the teaching and motivation during data collections at Synchrotron sources. I really feel fortune to have been taught by you. And of course, I cannot forget the uncountable answers to my ´help´ emails. Thanks a lot for everything.

To Diana and David, thanks for your friendship and for all the good moments that we have shared together.

To Luisa a special thanks for her patience and for being such a nice teacher in the crystallization/crystallography field. Moreover, I would like to thank her for listening to me so many times and for being my friend.

In Trinity College I really have to thank Dr. Amir Khan for receiving me in his lab. It was a very enriching and pleasant experience to work with you. Thanks for the opportunity to embrace new projects and for all the advice during my work. For all the members of his lab, most of all, thanks for making me feel home.

To Beto, thanks a lot for always being there for me, and for helping me so many times.

I would like to warmly thank Ed for the countless English lessons and corrections and for all the patience and support, but most of all, for being such a good friend.

To my godparents, thanks for all the interest showed along these years and for believing and supporting me.

A huge thanks to my parents, for always believing and supporting me when needed, and for creating the conditions and the environment which allowed me to pursue my education. To my father, thanks for all the invaluable advise. Your passion for the studies and your intense search for knowledge, created a wonderful model for me. For my mother, more than special thanks for all her love and supporting during my life. Thanks for understanding my decisions and for always being there for me.

Finally, I thank Ricardo for all his patience and support, and for the hundreds of pages that he has printed for me, but most of all, for all his love and for being by my side.

To my Father with all my love

Abstract

Life on earth is only possible through tightly interwoven material transformations through various cycles. Carbon, nitrogen, fosforous and sulfur, with a special interest in the latter, are essential components of all living organisms and represent the most important elements circulating within the biosphere.

During this circulation, sulfur can be found in various oxidation states with transformations occurring both biological and chemically. Dissimilatory sulfate reduction is one of those reactions, where sulfate is reduced to the final product sulfide in order to obtain energy for their metabolism. Sulfate reduction however, is not a favourable energetic reaction, and so sulfate is initially activated to adenosine-5'-phosphosulfate (APS) by ATP sulfurylase. APS is then reduced to sulfite by APS reductase allowing the sulfite reductase to reduce sulfite to the final product sulfide in a six electron transfer reaction. This last step can occur in an assimilatory or dissimilatory way.

This work was focused on the last step of sulfate reduction, particularly in the enzymes involved in the dissimilatory sulfite

reduction. Although theses enzymes have been extensively studied for decades, many questions still remain open. Four major types of dissimilatory sulfite reductases can be classified according to their ultraviolet/visible absorption spectra and other characteristics: desulfoviridin, desulforubidin, desulfofuscidin and P582. Understanding the differences in terms of structures, their assembly, cofactor content and reaction mechanisms was the main goal of this work.

The presented PhD dissertation is divided into five chapters, in which the first consists of a general introduction on the importance of sulfur and sulfate reducing organisms in nature, followed by a more detailed description of sulfite reducing organisms, their classification and reaction mechanism.

Following this, chapters are presented based on the published articles, with an overview of the material and methods used, the results obtained and a discussion of the most important results presented.

The second chapter describes the purification, crystallization and preliminary structure characterization of dissimilatory sulfite reductase (dSir) from *Desulfovibrio vulgaris* Hildenborough, which

belongs to the desulfoviridin class. DSir is bound to DsrC, a crucial protein for the sulfite reduction mechanism.

The third chapter presents a detailed structural description of *D. vulgaris* dSir. This structure revealed novel features and a mechanism for sulfite reduction is proposed.

The fourth chapter consists of structural and biochemical studies of a dissimilatory sulfite reductase from *Desulfomicrobium norvegicum* classified as desulforubidin. A comparison between the two structures from the different classes (desulfoviridin *versus* desulforubidin) is performed with predictions on the structural properties for the other classes - desulfofuscidin and P582. In addition, mass spectrometry analysis identified different stoichiometry complex arrangements of dSiRs which enhance our understanding on the DsrC function.

Finally, in chapter five, a brief conclusion of the work is presented with the major structural and functional features along with future work strategies in the field.

Sumário

A vida no planeta Terra tornou-se uma realidade, devido às múltiplas e intensivas transformações de materiais nos diversos ciclos biológicos. O carbono, nitrogénio, fósforo e enxofre são componentes essenciais existentes em todas as células dos organismos, representando os elementos mais importantes que circulam na biosfera. No estudo seguidamente apresentado, o enxofre e as reacções em que se encontra envolvido assumem um interesse especial.

Durante a circulação do enxofre na biosfera, este pode ser encontrado em diferentes estados de oxidação, sendo que a transformação entre estes mesmos estados pode ocorrer tanto biologica como quimicamente. A redução dissimilativa do sulfato é uma das reacções mais importantes, em que o sulfato é reduzido a sulfureto de modo a que os organismos consigam obter energia para manter o seu metabolismo activo.

No entanto, a redução do sulfato é uma reacção energeticamente desfavorável, pelo que o sulfato tem de ser primeiramente activado a adenosina-5'-fosfosulfato (APS) pela enzima APS sulforilase. O APS formado é então reduzido a sulfito pela enzima APS reductase

permitindo deste modo que a sulfite reductase possa catalizar a redução (envolvendo a transferência de 6 electrões) do sulfito a sulfureto. Esta última reacção pode ocorrer assimilativa ou dissimilativamente. Embora estas enzimas (sulfite reductase) tenham sido alvo de intensivos estudos nas últimas décadas, muitas questões continuam ainda por esclarecer relativamente às proteínas envolvidas na reacção.

As sulfito reductases dissimilativas podem ser classificadas com base nos máximos de absorção no espectro ultravioleta/vísivel e algumas características moleculares nas seguintes classes: Desulfoviridina, Desulforubidina, Desulfofuscidina e P582.

No trabalho de doutoramento aqui apresentado o principal objectivo consistiu na determinação das estruturas tri-dimensionais de duas sulfito reductases de diferentes classes, que permitiu elucidar várias questões como a sua arquitectura, caracterização dos cofactores (natureza e número), tendo sido proposto mecanismo para a redução do sulfito.

O trabalho apresentado na presente dissertação encontra-se dividido em cinco capítulos, sendo que o primeiro consiste numa introdução geral sobre a importância do enxofre e dos organismos

envolvidos na redução de compostos deste elemento e sua influência na natureza, seguida de uma descrição mais detalhada sobre os organismos redutores de sulfito, sua classificação e mecanismo de reacção.

Nos capítulos seguintes é feita uma apresentação do trabalho realizado, baseado nos artigos publicados com uma descrição dos materiais e métodos, seguida dos resultados obtidos e discussão de questões mais relevantes.

No 2ª capítulo é descrito o trabalho de purificação, cristalização e resolução preliminar da estrutura da sulfito reductase (dSiR) de *Desulfovibrio vulgaris* Hildenborough, que pertencente à classe das desulfoviridinas. Esta estrutura encontra-se ligada à DsrC, uma proteína que assume um papel importante no mecanismo de redução do sulfito.

No 3º capítulo é apresentada uma descrição detalhada da estrutura com destaque para as suas características mais relevantes. Ao longo deste capítulo é efectuada uma comparação entre as diferentes classes desulfoviridina e desulforubidina, com uma previsão das propriedades estruturais das classes desulfofuscidina e P582.

No 4º capítulo é feita a caracterização da dSiR isolada de *Desulfomicrobium norvegicum*, que pertence à classe das

dessulforubidinas. São apresentados os resultados de espectroscopia de massa que revelam diferentes formas estequiométricas das subunidades do complexo que ajudam a compreender a importância e envolvimento da proteína DsrC na redução de sulfito.

Para finalizar, é efectuado um breve resumo do trabalho realizado com ênfase nas características estruturais e funcionais mais relevantes, com sugestões de trabalho importante a realizar nesta área de investigação.

Abbreviations:

SRB – sulfate reducing bacteria

SRP – sulfate reducing prokaryotes

alSiR - assimilatory sulfate reductase type

SiR – sulfite reductase

rSiR – reverse sulfite reductase

asrC – anaerobic sulfite reductases

aSiR – assimilatory sulfite reductase

dSiR – dissimilatory sulfite reductase

dsr – gene coding for the dissimilatory sulfite reductase

Dsr – dissimilatory sulfite reductase

DsrA – alpha subunit of dissimilatory sulfite reductase

DsrB - beta subunit of dissimilatory sulfite reductase

DVir – dissimilatory sulfite reductase from *Desulfovibrio vulgaris* Hildenborough

Drub - dissimilatory sulfite reductase from *Desulfomicrobium* (*Dm*) *Norvegicum*

SRH – sirohydrochlorin

SRM – siroheme

FDX – ferredoxin

APS – adenosine-5'-phosphosulfate

ATPS - ATP sulfurylase

PAPS – phosphoadenosine phosphosulfate

PPi – pyrophosphate

PEG – poliethylenoglycol

SDS – sodium dodecyl sulfate

PAGE – polyacrylamide gel electrophoresis

SPR – surface Plasmon resonance

Table of Contents

Chapter 1

Introduction

1.1 Sulfur in the Environment – A General Introduction

Everything has a beginning, and when the earth was formed around 4.5 billion years ago [1], the scene was set for the fascinating story of the evolution of the species. All life requires energy, and through the eons organisms have had to adapt to diverse and changing environments, to eke out energy from sometimes very limited sources and with varying degrees of success. Initially, the environmental conditions were very anoxic with atmospheric gases such as ammonia, methane, hydrogen, nitrogen, sulfur and carbon dioxide predominating, and it is hard to comprehend how our 'aerobic' life emerged from such a different world [2].

Prokaryotes are among the oldest known organisms having fossil records from as early as 3.5 billion years ago, only about 1 billion years after the formation of the Earth's crust [3],[4]. These organisms were chemotrophs that developed a multiplicity of strategies to attain nutrients and an energy source from the very elemental resources available and without the involvement of oxygen. These organisms evolved not only various fermentation pathways, but also the capacity to couple the oxidation of organic substrates to the reduction of inorganic compounds to conserve energy for anaerobic growth [5]. Through time, organism evolution led to the selection of metabolic pathways, many of which certainly modified the surface chemistry of the Earth, providing new

metabolic opportunities, which in turn promoted further evolutionary progression [5].

There is still uncertainty amongst biologists regarding the origin and position of eukaryotes in the overall scheme of evolution, with three different hypotheses being put forward; a) eukaryotes evolved from prokaryotes; b) were of contemporaneous origin; c) prokaryotes evolved from eukaryotic ancestors through a process of simplification [6]. Despite all the controversy, since the 1990's, organisms have been classified into three principal domains: Archaea (archaebacteria), Bacteria, and the Eucarya [7].

The Bacteria domain, encompasses the majority of the prokaryotes with which we are most familiar. These organisms conduct an enormous range of metabolic pathways including: fermentation, acetogenesis, sulfate reduction, elemental sulfur reduction, metal oxide reduction, denitrification, nitrification, aerobic respiration, oxygenic and anoxygenic photosynthesis, and a whole range of chemolithoautotrophic reactions using oxygen, nitrate, and metal oxides, as electron acceptors [4]. It has been estimated that sulfate reduction accounts for more than 50% of the organic mineralization in marine sediments [8]. This emphasizes the importance of sulfur reducing bacteria (SRB) in both the sulfur and carbon cycles, and consequently, why SRB are the subjects of such extensive studies.

1.2 The Sulfur Cycle

On Earth, tectonics and atmospheric photochemical processes are continuously supplying substrates and removing products based on redox reactions, successive transfers of electrons and protons from a relatively limited set of chemical elements in a cyclical manner. The six major elements – H, C, N, O, S and P constitute the major building blocks for all biological macromolecules and their biological fluxes are driven largely by microbially catalyzed, thermodynamically constrained redox reactions which are important components of the Earths elemental cycles [2].

Sulfur is among the most abundant elements on the earth and an essential element for maintaining life. The ocean is a major reservoir for sulfur, having large quantities in the form of dissolved sulfate and sedimentary minerals such as gypsum ($CaSO_4$) and pyrite (FeS_2) in rocks and sediments ($7.8x10^{18}$ g) and seawater ($1.28x10^{18}$ g) [9]. Sulfur has also an obligatory presence in the organisms constitution, occurring mainly as components of proteins (S-containing amino-acids, cysteine and methionine), but also in coenzymes (e.g. coenzyme A, biotin, thiamine), and in the form of iron-sulfur clusters in metalloproteins, all assuming significant roles in the structural, enzymatic and electron transport components of all living cells [10].

In the Earth´s crust, sulfur is cycled by biological processes on such a profound scale that the effects are evident globally. It has been estimated that at least 75% of crustal sulfur has been

biologically cycled and that 4 to $5x10^{12}$ kg of sulfate is cycled through living cells every year [11].

During sulfur circulation, it can be found in various oxidation states ranging from S^{2-} (completely reduced) in sulfide and reduced organic sulfur, to S^{6+} (completely oxidized) in sulfate, and it can be transformed both chemically and biologically as it is cycled [10],[12]. In this regard, micro-organisms play an important role in sulfur transformations and consequently are vital for the cycling of sulfur in our planet. They can use inorganic sulfur, mainly sulfate and reduce it to sulfide which is then incorporated into sulfur-containing amino acids and enzymes in an energy-dependent process referred to as assimilation. Alternatively, many bacteria and archaea can use sulfur in a series of oxidation and reduction reactions for the generation of metabolic energy in the dissimilatory metabolism [10].

The biological sulfur cycle consists of oxidative and reductive sides, where sulfate on the reductive side functions as an electron acceptor and is converted to sulfide, and on the oxidative side, reduced sulfur compounds like sodium sulfide serve as an electron donor for phototrophic or chemolithothrophic bacteria which convert these compounds to elemental sulfur or sulfate [13]. Apart from the above reactions, an energy generating process – sulfur disproportionation, can occur with elemental sulfur or thiosulfate serving both as electron donor and electron acceptor and resulting in the formation of sulfate and sulfide [12]. A simplified scheme of the microbial sulfur cycle demonstrating the fundamental reactions is presented in Figure 1.

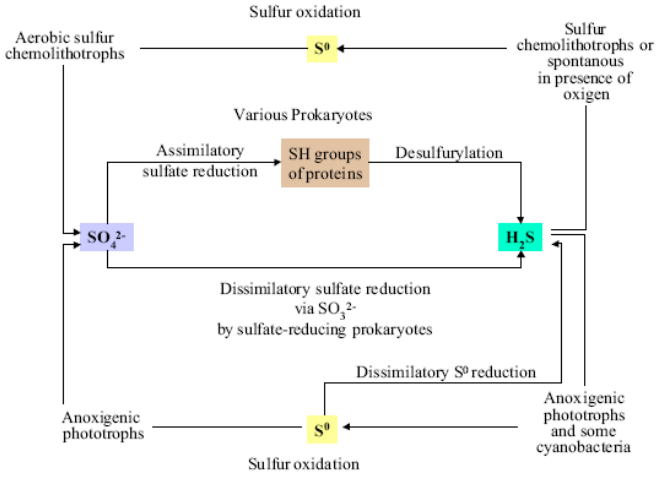

Figure 1. Schematic representation of sulfur transformations (Adaptation of the sulfur cycle image from [9]).

In addition, the sulfur cycle is closely related with other chemical cycles, such as the carbon and nitrogen cycles [9]. Sulfate is the most stable form of sulfur in today's oxygenated environment, being readily found in rocks sediments, which are consequently responsible for the presence of sulfate in the ocean. Also, the reduced inorganic forms of sulfur are quite common in anoxic environments, with sulfur compounds of mixed valency (thiosulfate (IV) and dithionate (III and IV)) produced transiently [10, 14]. During the sulfur cycle (Figure 2), the natural release of volatile organic sulfur compounds from the ocean, mainly as dimethyl sulfide (DMS), facilitates the transfer of sulfur from the ocean to

land, where plants and microorganisms take up sulfate via anaerobic assimilatory sulfate reduction, and animals are only able to take up reduced sulfur compounds through their diet. In the atmosphere, DMS is oxidized to acidic aerosol particles which affects cloud properties and the amount of solar radiation reflected back into space, thereby influencing the atmospheric chemistry and the climate system [10].

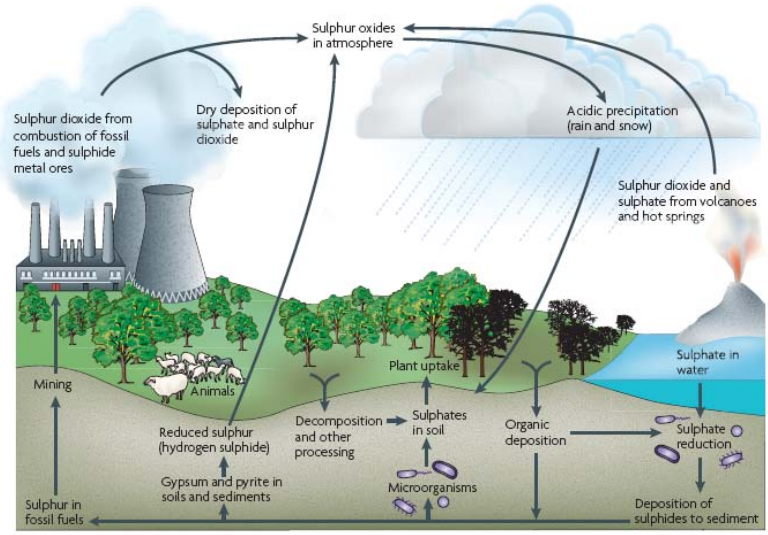

Figure 2: Schematic view of the sulfur cycle depicting the flow of sulfur compounds in the environment. Sulfate is taken up by microorganisms and plants, and subsequently by animals. Decomposition of dead organisms in the absence of oxygen releases the sulfur again as hydrogen sulfide. The combustion of fossil fuels and emission of volcanic fumes releases sulfur dioxide into the atmosphere, where it

reacts with water which forms sulfuric acid and results in acid rain. Image taken from [9].

1.3 Sulfate Reducing Bacteria

Anaerobic sulfate reduction represents an ancient, but evolutionary successful metabolic system in some prokaryotes. Molecular evidence has suggested that dissimilatory sulfate reduction is ancient [15] and geochemical data indicate the occurrence of microbial sulfate reduction 3.47 billion years ago [16].

Despite its long evolutionary history, the anaerobic sulfate respiration pathway seems to be restricted to a rather small group of very specialized microbes, termed the sulfate-reducing prokaryotes (SRP).

SRP obtain their energy by oxidizing organic compounds or molecular hydrogen H_2 while reducing sulfates to sulfides. They are mainly found in the Bacteria and Archaea domains, with a greater incidence falling into the phylogentic lineages of mesophilic delta-proteobacteria and thermophilic gram-positive bacteria, this being the reason why SRP are commonly refered to as sulfate reducing bacteria (SRB) [9].

They can be identified as a mixed group of morphologically (cocci, rods, curved type, cell aggregates, and multicellular gliding filaments) and nutritionally diverse, chemoorganotrophic organisms that generally use sulfate as the terminal electron acceptor for the degradation of organic compounds in their energy metabolism [14].

SRB may use other electron acceptors besides sulfate for the anaerobic respiration, namely elemental sulfur, fumarate, nitrate, dimethylsulfoxide, Mn (IV) and Fe (III), or even fermented substrates in the absence of inorganic acceptors. Therefore, the prevalence/existence of SRB in an environment does not necessarily imply the occurrence of sulfate reduction. Sulfate reducers can reduce other sulfur compounds (thiossulfate, sulfite and sulfur) to sulfide or can reduce nitrate and nitrite to ammonium [10]. Some organisms have been shown capable of aerobic respiration; providing energy basically for their maintenance [14], although in some cases they were able to grow in the presence of oxygen [17]. SRB have been detected or isolated from a variety of anaerobic niches, such as soil, marine environments, mud and sediments of freshwaters (rivers, lakes), hydrothermal vents, hydrocarbon seeps and mud volcanoes, industrial waste waters, and are abundantly present in hypersaline microbial mats [9],[18],[19]. They can also grow in inhospitable habitats of extreme pH values, such as acid-mine drainage sites (pH is around 2) and in soda lakes (pH can be as high as 10) [9]. Their presence was also detected in oil fields, rice paddies and technical aqueous systems (sludge digesters, oil tanks or vats in the paper-making industry) [14], on the deep sub-surface, and in the rhizosphere of plants, in aquifers and in engineered systems, such as anaerobic water-water treatment plants [9]. SRB were also found in the gastrointestinal tract of man and animals, where the sulfate concentrations is relatively low [20]. The basic metabolic process of SRB is the anaerobic reduction of sulfates to sulfide, in which sulfate is the electron acceptor [13]. Considering

the inorganic or organic character of the energy source there are two types of anaerobic respiration of sulfates [13]:
1 – Autotrophic reduction of sulfates – the energy source is gaseous hydrogen, and the carbon source is CO_2, and the reaction proceeds according to the equation $4H_2 + SO_4^{2-} \rightarrow S^{2-} + 4H_2O$
2 – Heterotrophic reduction of sulfates – the energy sources are simple organic substances, such as lactate, fumarate, pyruvate and some alcohols. Depending on the final product (oxidation state of organic substrate), the reduction process can be classified as incomplete or complete with the final products being acetate (CH_3COO^-) or carbon dioxide (CO_2) plus H_2O respectively [13].

$2CH_3CHOHCOO^- + SO_4^{2-} \rightarrow 2CH_3COO^- + 2HCO_3^- + H_2S$

$4CH_3COCOONa + 5MgSO_4 \rightarrow 5MgCO_3 + 2Na_2CO_3 + 5H_2S + 5CO_2 + H_2O$

These organisms are probably responsible for most of the H_2S production on Earth at temperatures below 100ºC [21], with their activities being detected under a wide range of environmental conditions (+350 to -500 mV; pH 4.2-10.4; 0.1-100 MPa; 0-104ºC and salinity from less than 1% to saturated NaCl) [11]. When sulfate is reduced by these bacteria there is a net release of free energy which is utilized for growth, and because of the low energy yield, under optimum conditions large quantities of sulfate are reduced [11]. It has been estimated that sulfate reduction can account for more than 50% of the organic carbon mineralization, which

indicates the importance of sulfate reducers in both sulfur and carbon cycles, and consequently, why SRB are under extensive scrutiny [8-9].

1.4 Sulfate Reduction and Evolution

It appears to be clear from geochemical (sulfur isotopic) evidence that the process of biological sulfate reduction is evolutionary ancient, being one of the oldest microbial pathways on earth [22],[11] . In order to understand how life has evolved from this ancient microbial pathway, several phylogenetic studies on SRB have been undertaken. A basic assumption made is that all modern organisms originated from an ancestor, meaning that all organisms contain remnants of their ancient history, facilitating comparative divergent sequence analysis [14].

A variety of techniques have been used to understand the evolutionary relationships among organisms, their diversity and activity. One of the oldest techniques used for this purpose is cultivation. This technique, although useful has limitations, as only a small fraction (less than 1%) of naturally occurring SR organisms can be cultured [9]. Another technique used, but having taxonomic resolution limitations is the phospholipid fatty acids analysis [9]. To overcome these problems, the application of culture independent molecular methods for SRP detection in environmental samples was applied [23].

Most information on the diversity of SRP in both natural and engineered ecosystems has been obtained from the use of marker genes, in particular by direct comparison of the small subunit (16S subunit) of the ribosomal RNA molecule (rRNA) [9],[4],[20] which is moderately to highly conserved across great phylogenetic distances allowing widely different organisms to be compared. Another reason for the preferentially use of 16S rRNA is the slow but functionally neutral mutations that accumulate over time [14],[20] . Based on the 16S rRNA sequence analysis life can be divided into three principal Domains; Bacteria, Archaea and Eucarya, with the first two depicting the most important historical developments in sulfur metabolism [4]. This division as illustrated in the tree of life (Figure 3) emphasizes the genetic diversity of prokaryotes and shows that the history of life on Earth is largely a history of prokaryotic evolution.

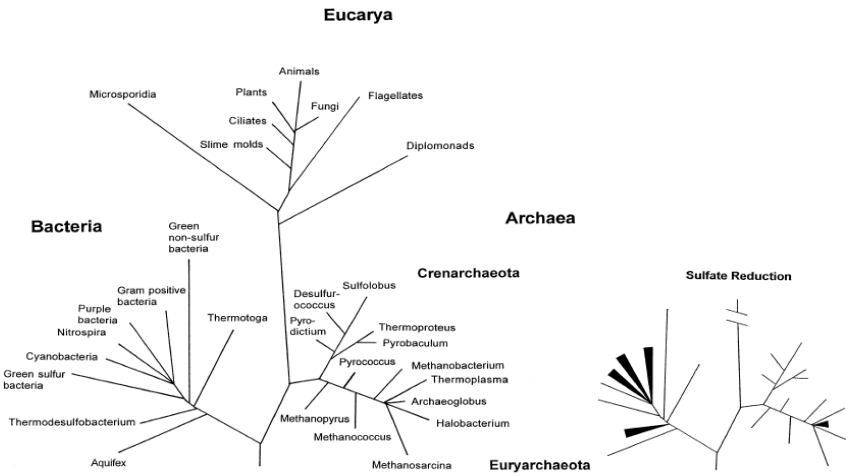

Figure 3. Principal lineages within the 'Tree of Life' determined from the comparison of 16S rRNA sequences, with particular relevance on the lineages within Bacteria and Archaea domains involved in the sulfate reduction. Figure was taken from [4].

There is also a major problem with 16S rRNA sequence based classification, which is still unresolved. The 16S rRNA sequences available do not contain information on the physiology of the respective organism, and this can be problematic due to the wide presence of SRP in the phylogenetic tree (where lineages also contain organisms with other modes of energy utilization and conservation). The close relationship of SRP with other bacterial 16S rRNA targeted probes, can lead to an ambiguous identification of an SRP [14].

Consequently is necessary to identify and exploit additional phylogenetic genetic markers which allow one to specifically detect and identify SRP. The *dsrA* and *dsrB* genes code for two subunits (DsrAB) of the dissimilatory sulfite reductase and are well-suited phylogenetic marker molecules for dissimilatory sulfate reducing organisms, since the DsrAB is present in all dissimilatory sulfate-reducing organisms investigated so far [24],[23]. The genes encoding the two subunits are found adjacent to each other in the respective genomes and probably arose from the duplication of an ancestral gene [25]. Comparative amino acid sequences of the dissimilatory sulfite reductase genes (*dsrAB*) have then been used to investigate the evolutionary history of anaerobic sulfate (sulfite) respiration, suggesting a single ancestral progenitor present before the split between the *Bacteria, Archaea* and *Eucarya* domains [25].

The comparison of results from phylogenetic analysis of 16sRNA sequences and *dsrAB* databases yielded similar tree topologies, suggesting that comparative DsrAB sequence analysis allows specific yet independent identification of SRB. Based on the phylogenetic analysis, SRB can be organized into five major branches as presented in Figure 4. There are 3 branches within the Bacteria and 2 branches within the Archaea domains, where in the Bacteria most of the sulfate reducers belong to the delta-proteobacteria class (more than 35 genera), followed by the gram-positive SRB genus (*Desulfotomaculum*, *Desulfitobacterium* and *Desulfosporosinus* species). The third branch comprises solely thermophilic organisms, which can be organized in three different lineages: Nitrospirae phylum (*Thermodesulfovibrio* genus);

Thermodesulfobacterium phylum (*Thermodesulfobacterium* genus) and Thermodesulfobiaceae (*Thermodesulfobium* genus). Separately from the Bacteria domain, SR can also be found within the Archaea domain, with organisms belonging to the genus *Archaeoglobus* in the Euryarchaeota, and to the genera *Thermocladium* and *Caldirvirga* in the Crenarchaeota [26],[9], [12].

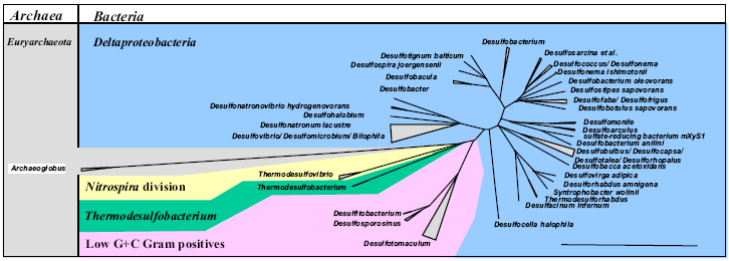

Figure 4. 16S rRNA gene based tree containing all recognized phyla of sulfate-reducing organism. Different phyla are color coded. Figure accordingly with [27] and [28].

All the characterized enzymes catalyzing either the oxidative or reductive (dissimilatory or assimilatory) transformations between sulfite and sulfide appear to be related suggesting a vertical transmission in the evolution of SR organisms. However, comparison of phylogenetic relationships among *dsr* gene sequences and 16S rRNAs (Figure 5) shows that despite a general consistency between the data, there is good evidence that there has been some episodes of lateral transfer [26],[15],[29].


Archaeoglobus profundus
Archaeoglobus fulgidus
Archaeoglobus veneficus
Thermodesulfobio islandicus
Thermodesulfovibrio yellowstonii
Thermodesulfobacterium commune
Thermodesulfobacterium mobile
Desulfosporosinus orientis
Desulfitobacterium dehalogenans
Desulfitobacterium hafniense
Desulfotomaculum geothermicum
Desulfotomaculum thermosapovorans
Desulfotomaculum kuznetsovii
Desulfotomaculum thermolaternum
Desulfotomaculum thermoacetoxidans
Desulfotomaculum thermobenzoicum
Desulfotomaculum acetoxidans
Desulfotomaculum alkaliphilum
Desulfotomaculum halophilum
Desulfotomaculum aeronauticum
Desulfotomaculum ruminis
Desulfotomaculum nigrificans
Desulfotomaculum putei
Desulfohalobium retbaense
Desulfonatronovibrio hydrogenovorans
Desulfomicrobium orale
Desulfomicrobium escambiense
Desulfomicrobium baculatum
Desulfobacterium macestii
Desulfomicrobium apsheronum
Desulfomicrobium norvegicum
Desulfonatronum lacustre
Desulfovibrio burkinensis
Desulfovibrio fructosovorans
Desulfovibrio desulfuricans El Agheila Z
Desulfovibrio africanus
Desulfovibrio longus
Desulfovibrio aespoeensis
Desulfovibrio halophilus
Desulfovibrio oxystinae
Desulfovibrio gigas
Desulfovibrio cuneatus
Desulfovibrio vulgaris
Desulfovibrio sp. PT-2
Desulfovibrio termitidis
Bilophila wadsworthii
Desulfovibrio piger
Desulfovibrio desulfuricans Essex 6
Desulfovibrio intestinalis
Desulfocurvus vexinensis
Thermodesulforhabdus norvegica
Syntrophobacter wolinii
Desulforhabdus amnigena
Desulfovigga adipica
Syntrophobacter fumaroxidans
Desulfobulbus sp. 3pr10, DSM2058
Desulfobulbus rhabdoformis
Desulfobulbus elongatus
Desulfobulbus propionicus
Desulfotalea psychrophila
Desulforhopalus vacuolatus
Desulfurella glycolicus
Desulforhopalus singaporensis
Desulfobacca acetoxidans
Desulfarculus baarsii
Desulfomonile tiedjei
Desulfobacterium anilini
sulfate-reducing bacterium mXyS1
Desulfobacterium oleovorans
Sulfate reducing bacterium HxdI
Sulfate-reducing bacterium AK-01
Desulfococcus multivorans
Desulfonema limicola
Desulfobacterium cetonicum
Desulfosarcina variabilis
Sulfate reducing strain oXyS1
Desulfocella halophila
Desulfobotulus sapovorans
Desulfofaba gelida
Desulfomusa hansenii
Desulfobacterium autotrophicum
Desulfobacterium vacuolatum
Desulfotignum balticum
Desulfotignum phosphitoxidans
Desulfospira joergensenii
Desulfobacula phenolica
Desulfobacula toluolica
Desulfobacter postgatei
Desulfobacter curvatus
Desulfobacter latus
Desulfobacter vibrioformis

Figure 5: Phylogenetic tree based on comparative 16S rRNA gene sequence and *dsrAB* sequence analysis. Phylogenetic groups are color coded: *Thermodesulfovibrio* – red, *Archaeoglobus* – magenta, *Thermodesulfobacterium* – yellow, Gram-positives (*Desulfotomaculum*, *Desulfitobacterium*, *Desulfosporosinus*) – green and *Deltaproteobacteria* – blue. Figure adapted from [29].

Some discrepant 16S rRNA and *dsrAB* gene phylogenies are found for the thermophilic bacterial genus *Thermodesulfobacterium* and several, mostly thermophilic, gram-positive sulfate-reducing *Desulfotomaculum* species [11]. These discrepancies reflect either a differential loss of ancestral paralogs or a lateral transfer between lineages and between species belonging to different bacterial divisions[30],[29],[15],[22]. This hypothesis would also explains why sulfate respiration is not widespread among known *Archaea* but is instead phylogenetically restricted to *A. fulgidus* and close relatives [15],[29]. Regarding the evolution of the assimilatory and dissimilatory processes, the isotopic signal of microbial sulfate reduction and a depletion of biogenic sulfides of the heavy sulfur isotope ^{34}S is detectable through-out the Proterozoic, and reaches back into the Archaean [11]. The sulfur isotopic records suggest that dissimilatory sulfate-reducing bacteria could have existed 2.7-3.47 billion years ago. For the dissimilatory process, independent paleoisotopic data is available, and it is believed that the assimilatory process must be at least of similar age [26]. In view of this information it is unlikely that dissimilatory sulfite reductases preceded the assimilatory versions, since assimilatory sulfite reductases are essential enzymes that provide sulfur for central biosynthetic pathways, such as biosynthesis of sulfur-containing

amino acids and acetyl-coA [26]. After the separation of dissimilatory and assimilatory pathways, a deep archaeal/bacterial divergence probably occurred. According to a study performed by Dhillon *et al.* on phylogenetic topologies of *dsrAB* genes, the symmetry shown between domains indicate that ancestral gene duplication occurred within or prior to the last common ancestor of Bacteria and Archaea [26].

Phylogenetic analysis performed on assimilatory and dissimilatory genes provides evidence for a common existence of a siroheme domain, whereas a ferredoxin domain only appears in the dissimilatory enzymes. Based on topology analysis, speculations on a likely progenitor and evolution led to the hypothesis that the assimilatory sulfite reductases are more ancient than dissimilatory reductases, which appeared as a result of the insertion of a ferredoxin domain and gene duplication event (Figure 6). The proposed insertion probably occurred before the Archaea-Bacteria divergence, since the ferredoxin-like sequences are located at the same positions in the *dsrAB* sequences of both domains [26].

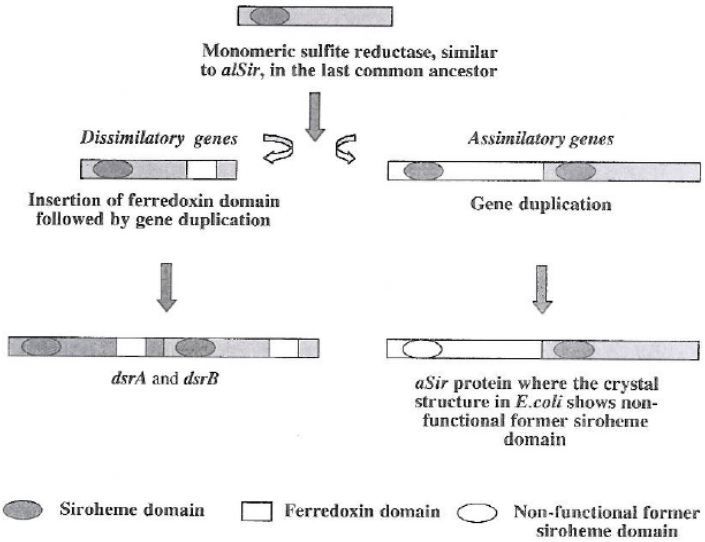

Figure 6: Hypothetical model for the evolution of dissimilatory and assimilatory sulfite reductases. Image adopted from [26].

1.5 Sulfite Reductase and Cofactors

Cofactors are used for a variety of functions in a diverse set of biological scenarios. One of the most familiar examples of these molecules is the protoporphyrin IX-derived macrocycles like the iron-containing hemes [11].

Siroheme (Figure 7a) is an isobacteriochlorin, meaning that its central ring is more reduced than the protoporphyrin IX-derived macrocycles like heme, and more closely related to cobinamide, the corrin ring of cobalamin (vitamin B12) [31].This molecule, derived from early intermediates in heme synthesis and most likely evolved before the cytochromes, is commonly characterized as a heme-like prosthetic group, and is used by some enzymes to mediate the six-electron reduction of sulfur and nitrogen [31],[32],[14],[33].

Sequence analysis of *dsr* genes shows they belong to redox superfamily characterized by a cofactor structure common to sulfite [32],[34] and nitrite reductases [35]. This superfamily also includes assimilatory nitrite and sulfite reductases from higher plants [36], fungi [37], algae, and bacteria, the small monomeric sulfite reductase [38], and reverse sulfite reductases [39],[40],[26].

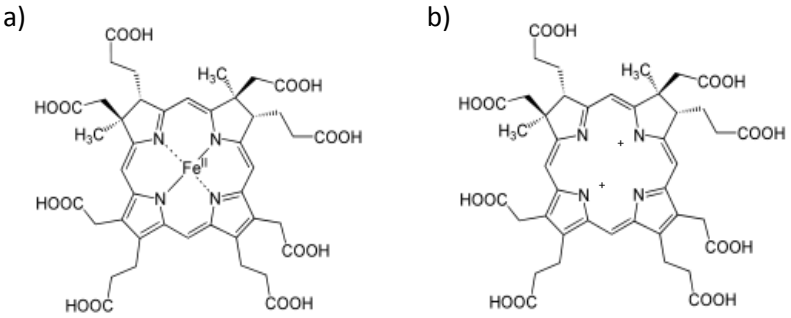

Figure 7: Schematic representation of (a) siroheme and (b) sirohydrochlorin molecules. Images were adopted from [31].

A derivative of the first intermediate in heme biosynthesis, is the iron tetrahydroporphyrin of the isobacteriochlorin type (where adjacent pyrrole rings are reduced) which contain eight carboxylic acid groups, and is named sirohydrochlorin (Figure 7b) [33]. This prosthetic group has been detected in *Desulfovibrio vulgaris* and has been associated with a UV-visible maximum absorbance at 628 nm [41]. Remarkably, in dissimilatory and assimilatory reductases and nitrate reductases the siroheme/sirohydrochlorin molecules are bridged to an iron sulfur-cluster [4Fe4S] by a sulfur atom forming a characteristic complex cofactor as shown in Figure 8 [42],[43],[44]. The active redox center comprising the two metallo-cofactor complexes is involved in the transfer of electrons to the substrate [14].

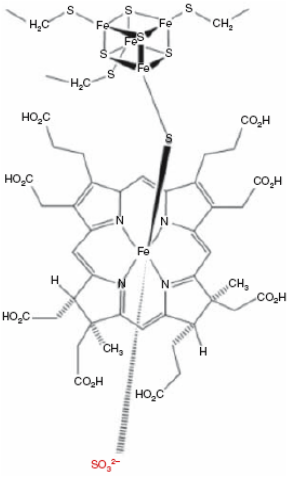

Figure 8: Schematic representation of siroheme-[4Fe4S] cluster covalently coupled via a sulfur bridge. The sulfite molecule is also represented, associating with the iron atom of the siroheme molecule on the non-bridging side. Image was adapted from [14].

1.6 Sulfite Reduction

Sulfite reduction to sulfide is a widespread reaction in nature, and is performed by different types of sulfite reductases, like, the assimilatory sulfite reductase (aSiR), dissimilatory sulfite reductase (dSiR), nitrite reductases, anaerobic sulfite reductase (asrC) (for example *Salmonella typhimurium* and *Clostridium* species) and assimilatory sulfate reductase type alSiR. There is also a reverse dissimilatory sulfite reductase which can be found in some sulfide and sulfur oxidizing bacteria[26].
Despite having different biological roles, dSiR, aSiR and NiRs (nitrite reductases) belong to a super family of enzymes, where a strictly conserved functional unit called the SNiRR (sulfite or nitrite reductase repeat), plays a crucial role in the six-electron reduction [14],[31],[45-46].

1.6.1 Assimilatory Sulfite Reductases

Assimilatory sulfite reductases (aSiRs) can be isolated from both Prokaryotic (bacteria) and Eucaryotic (plants and fungi) organisms, and is primarily concerned with the assimilation of sulfur into cellular material, for the biosynthesis of organosulfur compounds, such as sulfur-containing amino acids and enzyme cofactors [26].

The aSiRs have a low molecular mass and are comprised of a single polypeptide chain with a simple oligomeric structure,

containing the characteristic chromophore with an absorption peak at 580-590 nm, due to the siroheme- [4Fe4S] cluster coupled cofactor per polypeptide chain. In addition to the UV/visible maximum peak observed due to the presence of the SRM molecule, the aSiRs are characterized by UV/visible spectra with maximums also at 545 and 405 nm [47]. Electro Paramagnetic Resonance (EPR) and Mossbauer studies on aSiRs have shown that the siroheme has a low-spin ferric status, S=1/2, exhibiting EPR resonances at g=2.44, 2.36 and 1.77 [47]. Regarding the sulfite reduction reaction, these enzymes produce sulfide in a single six-electron step, with no intermediate sulfur compounds being released and form a complex with carbon monoxide (CO) or cyanide which inhibits activity [48],[31],[49].

The first aSiR structure from *Escherichia coli* was solved in 2001 [46] (PDB code 1AOP), revealing a tri-lobed protein with pseudo two-fold symmetry, where three separate domains can be identified (see Figure 11). Domains 1 (residues 1-145 and 347-421) and 2 (residues 146-346), contribute residues whose side chains form hydrogen bonds with acetyl and propionyl groups from the siroheme, and domain 3 (residues 422-570) from which 4 cysteine residues (Cys 434, 440, 479 and 483) coordinate the [4Fe4S] cluster bound to the siroheme molecule. The cofactor was shown to be placed at the junction of the three domains and to be composed of a siroheme-[4Fe4S] cluster (as described in Section 1.5).

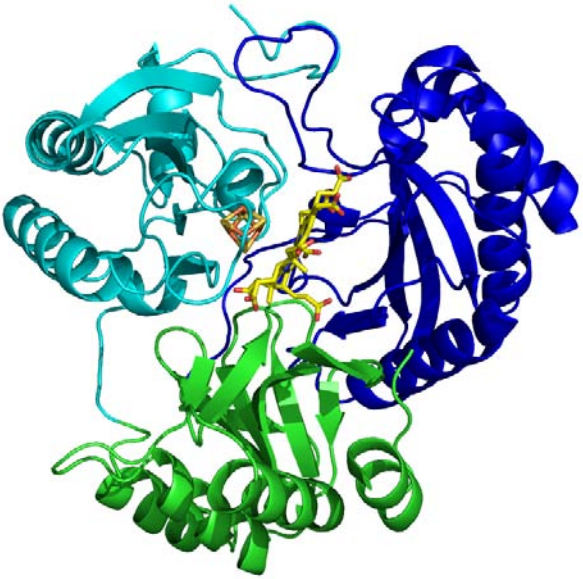

Figure 11. Cartoon representation of aSiR with the tri-lobed domains colored differently. Domain 1 is green, domain 2 blue, and domain 3 cyan. A stick representation of the cofactor content is also shown, SRM (C- yellow, O- red, Fe- brown) and [4Fe4S] (Fe- orange, S- gold). The figure was generated using Pymol [50].

1.6.2 Dissimilatory Sulfite Reductases

Dissimilatory sulfite reductases (dSiRs) are found in morphological and metabolically diverse sulfate and sulfite reducing Bacteria and some species of thermophilic Archaea. The sulfite

reductase activity occurs in the terminal step of the respiratory electron transfer chain [51]. They are distinguished from aSiRs by their molecular composition (larger molecular mass and subunit composition) and their propensity to primarily produce incomplete reduced sulfur species in the form of trithionate and to a lesser extent thiosulfate [51]. Additionally, dSiRs usually do not form complexes with CO and cyanide and so are not inhibited by these small molecules [49]. There are some exceptions however, such as the *Desulfotomaculum nigrificans* and *Desulfovibrio desulfuricans* Norway 4 strains, which readily form complexes resulting in activity inhibition by CO and cyanide [52].

The physical properties of the various dissimilatory sulfite reductases are overall quite similar, although they differ in finer details. They form large oligomers assembled in $\alpha_2\beta_2$ arrangements with molecular masses ranging from 145 to 225 kDa [14]. Their optical spectra show typical siroheme bands in the region of 540-580 nm and around 400 nm with a high-spin ferric state of S=5/2 [49],[53],[54],[55] and S = 9/2 in *Desulfovibrio vulgaris* Hildenborough [56].

Analysis of the cofactor content by heme extraction experiments result in a characteristic siroheme type spectrum with a ratio of two sirohemes per 240 kDa molecular mass. The iron content, determined calorimetrically, was shown to be much higher than that observed in aSiRs, with each enzyme containing multiple [Fe-S] clusters, resulting in 14 to 21 nonheme irons, plus equivalent sulfide content per molecule [54],[57],[58].

1.7 dSir Classification

On the basis of UV/visible absorption spectroscopy, and other molecular properties, four major types of dissimilatory sulfite reductases are distinguished in sulfate reducing-bacteria [14]. In 1965, desulfoviridins were the first class to be described with the identification of a green pigment [59]. It was isolated from several species such as *Desulfovibrio* (*D.) gigas*, *D. salexigens* and *D. vulgaris* and is easily distinguishable from the other dSiR classes by the characteristic sirohydrochlorin maximum spectra at 628 nm [49],[53],[60]. The second class was named Desulforubidin [52] and when isolated displayed a characteristic reddish brown color, with characteristic maximum absorption at 545 nm. Proteins from this class have been isolated from *Desulfovibrio desulfuricans* strain Norway 4, which has been renamed to *Desulfomicrobium baculatus* Norway 4 [61], and *Desulfovibrio* DSM 1743 [62]. The two remaining classes, classified as Desulfofuscidin and P582, have a characteristic brown color, and are distinguished by the maximum absorption spectra at 576 and 582 nm, respectively. In 1965 the Desulfofuscidin protein was first identified in the *Desulfomaculum* genus [63], and has now been isolated from a host of different species, such as *Desulfovibrio thermophilus* and *Thermodesulfobacterium commune*, both thermophilic sulfate reducers [58]. Finally from the P582 class, proteins from *Desulfotomaculum (Dt.) ruminis* and *Dt. nigrificans* have been identified [64]. In addition to these four bacterial dSiR classes, one

archaeal dSiR has been purified [25]. The various dissimilatory sulfite reductases share many similarities. Besides their high molecular weight and $\alpha_2\beta_2$ assembly [51], they all contain a reduced porphyrin of the isobacteriochlorin class – SRM which is covalently coupled to an iron-sulfur cluster [4Fe4S] to form the electronically integrated metallocofactor for delivering electrons to substrate at the active site [65].
Despite years of intensive analysis on cofactor content of dSiRs there is still some disparity for the different classes (see Table 1).

Table 1. Physico-chemical and composition of dissimilatory sulfite reductases [58].

Property	Desulfofuscidin		Desulfoviridin (D. gigas)	Desulforubidin (Dsm. Baculatum DSM 1741)	P582 (Dm. Nigrificans)
	T. commune	*T. mobile*			
Molecular Mass (kDa)	167	190	200	225	194
Subunit structure	$\alpha_2\beta_2$	$\alpha_2\beta_2$	$\alpha_2\beta_2$	$\alpha_2\beta_2$	$\alpha_2\beta_2$
Absorption maxima (nm)	389, 576, 693	392, 578, 700	390, 408, 580, 628	392, 545, 580	392, 582, 700
Iron content	20-21	32	16.5	16.6	16
Labile sulfide	16	ND	14	14.7	14
Siroheme	4	4		2	1.3
Sirohydroporphyrin			2		
[4Fe4S]	4	8	4	4	4
Reaction with CO	+	+	-	+	+

A third subunit (γ) has been observed in a desulfoviridin-type of dSiR from *D. vulgaris* [66],[67] and *D. desulfuricans* strain Essex [68], corresponding to the *dsrC* gene. This protein was suggested to be a subunit the dSiR protein and to be arranged as $\alpha_2\beta_2\gamma_2$. The γ-

subunit however, is not encoded on the same operon as the α and β subunits and there is no coordinated expression with the α and β subunits [67], which is an interesting feature.

1.8 The Mechanism of Sulfate Reduction

1.8.1 Sulfate Reduction

The reduction of sulfate can be divided in two phases; the reduction of sulfate to sulfite and the reduction of sulfite to sulfide [69],[14]. However, from a chemical point of view, sulfate is an unfavorable electron acceptor for microorganisms. The sulfate-sulfite couple redox potential ($E^{0'}$) is -516mV, too negative to allow reduction by the intracellular electron mediators present in sulfate reducers such as ferredoxin or NADH ($E^{0'}$ of -398 mV and -314 mV, respectively). As a result, prior to reduction, inorganic sulfate (SO_4^{2-}) has to be activated by an ATP sulfurylase (ATPS), which covalently attaches a sulfate ion at the *a*-phosphate site of ATP to form adenosine-5'-phosphosulfate (APS) and inorganic phosphate (PPi) [70]. The breaking of a phosphodiester bond in ATP provides the energy required for the formation of APS and PPi (hydrolyzed by pyrophosphatase to 2-phosphate). The $E^{0'}$ of the redox couple APS-sulfite plus AMP is -60 mV, allowing the reduction of APS. At this point, the assimilatory and dissimilatory reduction of sulfite

reductase presents some differences. In the dissimilative reduction, the sulfate moiety of APS is reduced directly to sulfite with concomitant release of AMP by the enzyme APS reductase [71], [72]. On the other hand, in the assimilative reduction, another phosphorous atom is added to APS by APS kinase phosphorylase to form phosphoadenosine-5´-phosphosulfate (PAPS), before reduction by PAPS reductase to sulfite [9, 12] (see Figure 9).

In both cases the product of sulfate reduction is sulfite, which is further reduced to sulfide by the assimilatory or dissimilatory sulfite reductases, with an $E^{0'}$ of the redox couple sulfite-sulfide of -116 mV. In the assimilatory reduction a single six electron reaction performed by aSiR takes place [14]. For the dissimilatory process, the number of reactions, as well as the number of electrons involved in each step remains unclear and has been the subject of intense studies and debate for many years [14].

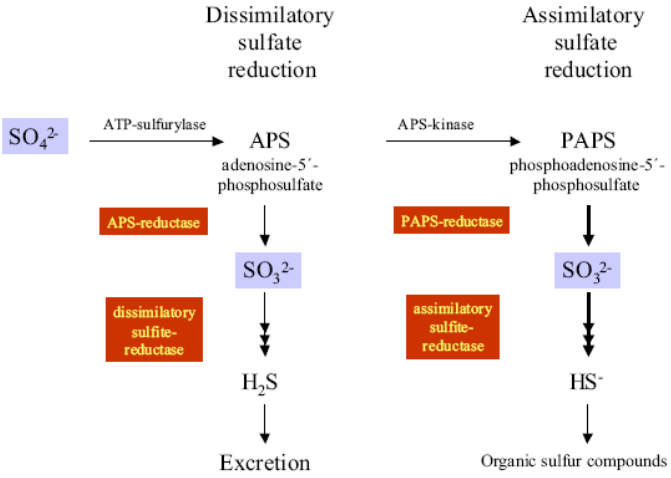

Figure 9: Schematic representation of dissimilatory and assimilatory reduction mechanisms. Figure according to [73].

1.8.2 Sulfite Reduction Pathway

The assimilatory reduction occurring in bacteria involves the direct reduction of sulfite to sulfide without the formation of any detectable intermediates by aSiR. In contrast, a series of complex reactions have been proposed for the dissimilatory pathway leading to the formation of a mixture of products, such as sulfide, trithionate and thiossulfate.

In 1969, the finding of a thiosulfate producing system during reduction experiments in *D. vulgaris* [74],[75],[76], led to a period of intense work on sulfite reduction and its products, with an initial suggestion of bisulfite (HSO_3^-) as the actual substrate instead of sulfite (SO_3^{2-}) [74]. Around the same period, it was reported that trithionate [77],[61],[64] and thiosulfate [76],[78],[74] were formed as a product reaction in *D. vulgaris* and *Desulfotomaculum nigrificans* [79],[80] extracts. Further studies revealed the presence of thiosulfate reductase activity and the isolation of the enzyme from several sulfate reducing organisms which established the importance of thiosulfate in dissimilatory reduction [81]. Ishimoto and Kobayashi [60] postulated that several reductases, such as bisulfate reductase [60],[82],[83],[61], thiosulfate reductase [81],[84],[85] and trithionate reductase [83] may be involved in the dissimilatory reduction of sulfite by sulfate reducing bacteria. However, trithionate reductase seems not to be distributed uniformly amongst the *Desulfovibrio* species, being absent in *D. gigas* [77]. They proposed a three consecutive reductions of two electrons each to achieve complete reduction to sulfide. Sulfite is

reduced by bisulfate reductase to trithionate, which remains in the active site while being reduced by thritionate reductase to thiosulfate, which is then further reduced to sulfide by thiosulfate reductase (Figure 10).

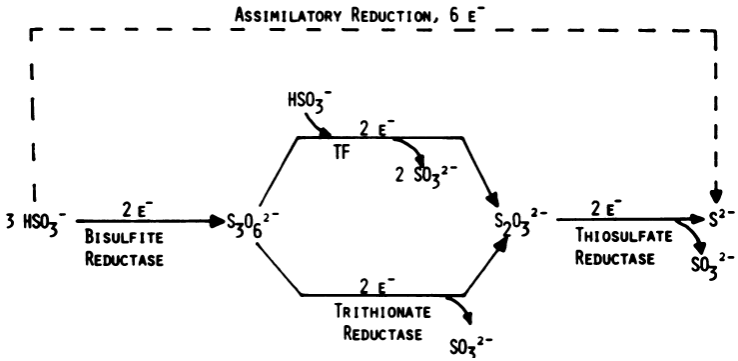

Figure 10: The proposed pathway for the reduction of bisulfate to sulfide occurring in three consecutive two electron steps, with the formation of trithionate and thiossulfate as reaction intermediates. Diagram was adopted from [75].

In addition to this reaction scheme, Drake and Akagi [83] suggested a model for the bisulfite reductase, in which the active site contains 3 adjacent sites, A, B and C available to bind bisulfite. Once bisulfite binds to site C, is reduced to sulfoxylate (two electrons). When available, another bisulfate binds to site B forming a two-sulfur intermediate. A third bisulfite binds at site A and then reacts with the two-sulfur intermediate forming trithionate.

However, if the concentration of the electron donor is high enough, the two-sulfur intermediate may undergo a reduction to thiosulfate. As the reaction proceeds and bisulfite is depleted, site A becomes empty and the reduction of the two-sulfur intermediates predominates with the formation of thiossulfate. When the bisulfite concentration is almost entirely depleted, the sulfoxilate intermediate is reduced to sulfide [83] (Figure 11).

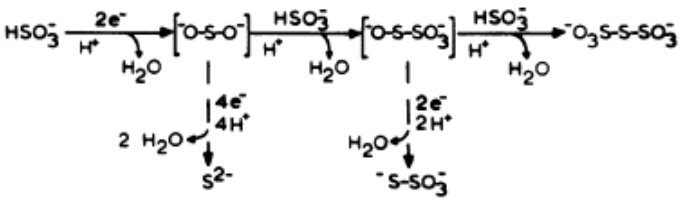

Figure 11: The proposed pathway of bisulfate reduction at the active site of bisulfate reductase [86].

This hypothesis explains the isolation of the intermediate products and explains the apparent lack of trithionate accumulation in reaction mixtures [87]. Although some studies confirm the presence of thiossulfate and trithionate as intermediate products in sulfite reduction, there are some contradictory reports where thiosulfate or trithionate were not shown to be the normal intermediates in the reduction pathway [77]. For this reason, and although a pathway through trithionate and thiosulfate would allow a reduction in three two-electron reduction steps, reduction in a six-electron reduction step cannot be ruled out [9].

1.9 Environmental and Biotechnological importance of SRB

In addition to their relevance in the biogeochemical sulfur cycle, the sulfate reducing bacteria (SRB) have considerable economic and environmental impact. As a result of their metabolic actions, SRB can have positive and negative impacts on the environment, with significant economic losses, environmental dangers, and health and safety risks [12],[13],[88]. The next few paragraphs are dedicated to the presentation of some of these impacts.

In the process of anaerobic respiration SRB produce a considerable amount of the toxic, odorous and corrosive gas hydrogen sulfide (H_2S) which reacts in an aqueous medium with heavy metal cations thereby forming mainly insoluble metal sulfides [13]. A negative consequence of such SRB activity is found in the petro-chemical industry, where SRB are responsible for extensive corrosion of drilling, pumping machinery and storage tanks due to hydrogen sulfide formation [69],[9],[89],[90],[91]. Furthermore, the contamination of crude oil with such microorganisms causes the release of hydrogen sulfide into petroleum products, thereby increasing the sulfur content of the crude oil. So in a number of indirect ways SRB contribute to the safety concerns for personnel who are involved in offshore drilling activities [9],[13].

Other negative effects of SRB activity can be found in paper industries, where as a result of SRB activity, iron sulfides contaminate water processing and causes paper blackening [92].

Moreover, SRB can also be a major problem in health. Sulfate reducing bacteria are normal inhabitants of the intestine in humans and animals. SRB have been implicated in a number of gastrointestinal diseases, such as cholecystitis and abdominal abscesses. In some cases, the increase of SRB in the human tract is related with other illnesses, like spondylitis and colorectal cancer [20]. Regarding the latter, it is suggested that the formation of sulfide activates a number of biochemical pathways believed to be involved in the initiation of the disease [20]. Moreover, at physiological concentrations, sulfide has been shown to protect colon cancer cells from drugs such as β-phenyl ethyl isocyanate for the promotion of tumor genesis. Intense inflammation of the large bowel mucosa (underlying epithelial cell surfaces) may also develop. Symptoms vary between individuals, but in general, the disease is associated with bloody diarrhea, abdominal pain, weight loss, urgency to defecate, and arthritic [20]. Ulcerative colitis is one of the two major forms of idiopathic inflammatory bowel disease and represents a highly disabling incurable condition. Current maintenance therapies rely on anti-inflammatory drugs and steroids, but in severe cases, partial or complete surgical removal of the bowel is necessary [20].

In contrast to the negative consequences of SRB colonization, sulfate reduction can be applied beneficially to biotechnology, when involved in the removal of heavy metals and sulfur compounds from

groundwater, industrial waste waters and contaminated soils [9]. This application takes advantage of differences in the chemical properties of metal sulfates and sulfides. Metal sulfates (cadmium, cobalt, copper, iron, nickel and zinc) are highly soluble, but the corresponding metal sulfides have low solubility, allowing precipitation of the metal sulfides through sulfate reduction. The metals can even be recovered and reused from the precipitate [9],[69]. Another important implication of SRB is biocorrosion or microbiologically influenced corrosion (MIC), where the organisms, both in man-made and natural environments surface-associated microbial growth or 'biofilms', influence the physico-chemical condition and interaction between metals and environment, frequently leading to deterioration of the metal [93],[91].

1.10 References:

1. Newman, W., *Age of the Earth.* Publications Services, USGS, 2007.
2. Falkowski, P.G., T. Fenchel, and E.F. Delong, *The microbial engines that drive Earth's biogeochemical cycles.* Science, 2008. **320**(5879): p. 1034-9.
3. Rabus, R., T. Hansen, and F. Widdel, *Dissimilatory Sulfate- and Sulfur-Reducing Prokaryotes*, in *The Prokaryotes*, M.e.a. Dworkin, Editor. 2007, Springer-Verlag, New York. p. 659-768.
4. Canfield, D.E. and R. Raiswell, *The Evolution of the Sulfur Cycle.* American Journal of Science, 1999. **299**: p. 627-723.
5. Canfield, D.E., M.T. Rosing, and C. Bjerrum, *Early anaerobic metabolisms.* Philos Trans R Soc Lond B Biol Sci, 2006. **361**(1474): p. 1819-34; discussion 1835-6.
6. Martin W., *Who is the Tree of Life. In Microbial Phylogeny and Evolution. Concepts and Controversies.* Oxford University Press, 2005. **139**.
7. Woese C., Kandler O., and W. M., *Towards a natural system of organisms: proposal for the domains Archaea, Bacteria and Eucarya.* Proc Natl Acad Sci USA 1990. **87**(12): p. 4576-9.
8. Jorgensen B. B., *Mineralization of organic matter in the sea bed—the role of sulphate reduction.* Nature, 1982. **296**: p. 643-645.

9. Muyzer, G. and A.J. Stams, *The ecology and biotechnology of sulphate-reducing bacteria.* Nat Rev Microbiol, 2008. **6**(6): p. 441-54.
10. Sievert, S.M., R.P. Kiene, and H. Schiulz-Vogt, *Microbes and major elemental cycles.* Oceanography, 2007. **20**(2): p. 117-123.
11. Skyring, G.W. and T.H. Donnelly, *Precambrian sulfur Isotopes and a possible role for sulfite in the evolution of biological sulfate reduction.* Precambrian Research, 1982. **17**: p. 41-61.
12. Tang, K., V. Baskaran, and M. Nemati, *Bacteria of the Sulphur Cycle: An overview of microbiology, biokinetics and their role in petroleum and mining industries.* Biochemical Engineering Journal, 2009. **44**: p. 73-94.
13. Luptakova, A., *Importance of Sulphate-Reducing Bacteria in Environment.* Nova Biotechnologica, 2007. **VII-I**: p. 17-22.
14. Rabus, R., T. Hansen, and F. Widdel, *The Prokaryotes. Dissimilatory Sulfate- and Sulfur- Reducing Prokaryotes* Springer New York, 2006.
15. Wagner, M., et al., *Phylogeny of dissimilatory sulfite reductases supports an early origin of sulfate respiration.* J Bacteriol, 1998. **180**(11): p. 2975-82.
16. Shen, Y.N. and R. Buicks, *The antiquity of microbial sulphate reduction.* Earth-Science Reviews, 2004. **64**: p. 243-272.
17. Lobo, S.A., et al., *The anaerobe Desulfovibrio desulfuricans ATCC 27774 grows at nearly atmospheric oxygen levels.* FEBS Lett, 2007. **581**(3): p. 433-6.
18. LeGall, J. and G. Fauque, eds. *Biology of Anaerobic Microorganisms*. Dissimilatory Reduction of Sulfur Compounds 1988, John Willey and Sons. 587-639.

19. Peck, H.D. and J. LeGall, *Biochemistry of dissimilatory sulphate reduction.* Philos Trans R Soc Lond B Biol Sci, 1982. **298**(1093): p. 443-66.
20. Barton, L.L. and W.A. Hamilton, *Sulphate-reducing Bacteria.* Cambridge University Press, 2007.
21. Trudinger, P.A. and D.J. Swaine, eds. *The biological sulfur cycle*. Biogeochemical Cycling of Mineral-Forming Elements. Vol. 293-313. 1979 Elsevier: Amsterdam.
22. Stahl, D.A., et al., *Origins and diversification of sulfate-respiring microorganisms.* Antonie Van Leeuwenhoek, 2002. **81**(1-4): p. 189-95.
23. Wagner, M., et al., *Functional marker genes for identification of sulfate-reducing prokaryotes.* Methods Enzymol, 2005. **397**: p. 469-89.
24. Loy, A., S. Duller, and M. Wagner, *Evolution and Ecology of Microbes Dissimilating Sulfur Compounds: Insights from Siroheme Sulfite Reductases*, in *Microbial Sulfur Metabolism*, C. Dahl and C. Friedrich, Editors. 2007, Springer Berlin Heidelberg. p. 46-59.
25. Dahl, C., et al., *Dissimilatory sulphite reductase from Archaeoglobus fulgidus: physico-chemical properties of the enzyme and cloning, sequencing and analysis of the reductase genes.* J Gen Microbiol, 1993. **139**(8): p. 1817-28.
26. Dhillon, A., et al., *Domain evolution and functional diversification of sulfite reductases.* Astrobiology, 2005. **5**(1): p. 18-29.
27. Woese, C.R., *Bacterial evolution.* Microbiol Rev, 1987. **51**(2): p. 221-71.
28. Widdel F. and H.T. A., *The dissimilatory sulfate- and sulfur bacteria*. 2nd ed. The Prokaryotes, ed. A. Balows, et al. 1992, New York, : Springer-Verlag.

29. Klein, M., et al., *Multiple lateral transfers of dissimilatory sulfite reductase genes between major lineages of sulfate-reducing prokaryotes.* J Bacteriol, 2001. **183**(20): p. 6028-35.
30. Zverlov, V., et al., *Lateral gene transfer of dissimilatory (bi)sulfite reductase revisited.* J Bacteriol, 2005. **187**(6): p. 2203-8.
31. Stroupe, M.E., *Making and Using Siroheme: the X-ray Crystallographic Structures of Siroheme Synthase and Sulfite Reductase*. 2002, The Scripps Research Institute: California.
32. Murphy, M.J. and L.M. Siegel, *Siroheme and sirohydrochlorin. The basis for a new type of porphyrin-related prosthetic group common to both assimilatory and dissimilatory sulfite reductases.* J Biol Chem, 1973. **248**(19): p. 6911-9.
33. Murphy, M.J., et al., *Reduced nicotinamide adenine dinucleotide phosphate-sulfite reductase of enterobacteria. II. Identification of a new class of heme prosthetic group: an iron-tetrahydroporphyrin (isobacteriochlorin type) with eight carboxylic acid groups.* J Biol Chem, 1973. **248**(8): p. 2801-14.
34. Schedel, M., J. Legall, and J. Baldensperger, *Sulfur metabolism in Thiobacillus denitrificans evidence for the presence of a sulfite reducatase activity.* Arch Microbiol, 1975. **105**(3): p. 339-41.
35. Jackson, R.H., A. Cornish-Bowden, and J.A. Coles, *Prosthetic groups of the NADH-dependent nitrite reductase from Escherichia coli K12.* Biochemical Journal, 1981. **193**(3): p. 861-867.

36. Hucklesby D. P., et al., *Properties of nitrite reductase from Cucurbita Pepo* Phytochemistry, 1976. **15**: p. 599-603.
37. Vega, J.M. and R.H. Garrett, *Siroheme: a prosthetic group of the Neurospora crassa assimilatory nitrite reductase.* J Biol Chem, 1975. **250**(20): p. 7980-9.
38. Tan, J. and J.A. Cowan, *Enzymatic redox chemistry: a proposed reaction pathway for the six-electron reduction of SO3(2-) to S2- by the assimilatory-type sulfite reductase from Desulfovibrio vulgaris (Hildenborough).* Biochemistry, 1991. **30**(36): p. 8910-7.
39. Schedel, M. and H.G. Truper, *Purification of Thiobacillus denitrificans siroheme sulfite reductase and investigation of some molecular and catalytic properties.* Biochim Biophys Acta, 1979. **568**(2): p. 454-66.
40. Schedel, M., M. Vanselow, and H.G. Trüper, *Siroheme-sulfite reductase isolated from Chromatium vinosum. Purification and investigation of some molecular and catalytic properties.* Archives of Microbiology, 1979. **121**(1): p. 29-36.
41. Kobayashi, K., E. Takahashi, and M. Ishimoto, *Biochemical studies on sulfate-reducing bacteria. XI. Purification and some properties of sulfite reductase, desulfoviridin.* J Biochem, 1972. **72**(4): p. 879-87.
42. Christner, J.A., et al., *Mossbauer evidence for exchange-coupled siroheme and [4Fe-4S] prosthetic groups in Escherichia coli sulfite reductase. Studies of the reduced states and of a nitrite turnover complex.* J Biol Chem, 1983. **258**(18): p. 11147-56.
43. Christner, J.A., et al., *Exchange Coupling between Siroheme and [4Fe-4S] Cluster in E. Coli Sulfite Reductase. Mössbauer Studies and Coupling Models for a 2- Electron Reduced*

Enzyme State and Complexes with Sulfide. Journal of the American Chemical Society, 1984. **106**: p. 6786-6794.

44. Crane, B.R., L.M. Siegel, and E.D. Getzoff, *Structures of the siroheme- and Fe4S4-containing active center of sulfite reductase in different states of oxidation: heme activation via reduction-gated exogenous ligand exchange.* Biochemistry, 1997. **36**(40): p. 12101-19.
45. Postgate, J.R., *Sulphate Reduction by Bacteria.* Annual Review of Microbiology, 1959. **13**: p. 505-520.
46. Crane, B.R., L.M. Siegel, and E.D. Getzoff, *Sulfite reductase structure at 1.6 A: evolution and catalysis for reduction of inorganic anions.* Science, 1995. **270**(5233): p. 59-67.
47. Moura, I., et al., *Low-spin sulfite reductases: a new homologous group of non-heme iron-siroheme proteins in anaerobic bacteria.* Biochem Biophys Res Commun, 1986. **141**(3): p. 1032-41.
48. Murphy, M.J., L.M. Siegel, and K. H., *An Iron Tetrahydroporphyrin Prosthetic group common to both Assimilatory and Dissimilatory Sulfite Reductases.* Biochemical and Biophysical Research Communications, 1973. **54**(1): p. 82-88.
49. Lee, J.P., J. LeGall, and H.D. Peck, Jr., *Isolation of assimilatroy- and dissimilatory-type sulfite reductases from Desulfovibrio vulgaris.* J Bacteriol, 1973. **115**(2): p. 529-42.
50. DeLano, W.L., *The PyMOL Molecular Graphics System, Version 1.2r3pre, Schrödinger, LLC.* 2002.
51. Crane, B.R. and E.D. Getzoff, *The relationship between structure and function for the sulfite reductases.* Curr Opin Struct Biol, 1996. **6**(6): p. 744-56.
52. Lee, J.P., et al., *Isolation of a New Pigment, Desulforubidin, from Desulfovibrio desulfuricans (Norway Strain) and Its*

Role in Sulfite Reduction Journal of Bacteriology, 1973. **115**(1): p. 453-455.

53. Lui, S.M., A. Soriano, and J.A. Cowan, *Electronic properties of the dissimilatory sulphite reductase from Desulfovibrio vulgaris (Hildenborough): comparative studies of optical spectra and relative reduction potentials for the [Fe4S4]-sirohaem prosthetic centres.* Biochem J, 1994. **304 (Pt 2)**: p. 441-7.
54. Wolfe, B.M., S.M. Lui, and J.A. Cowan, *Desulfoviridin, a multimeric-dissimilatory sulfite reductase from Desulfovibrio vulgaris (Hildenborough). Purification, characterization, kinetics and EPR studies.* Eur J Biochem, 1994. **223**(1): p. 79-89.
55. Huynh, B.H., et al., *Characterization of a sulfite reductase from Desulfovibrio vulgaris. Evidence for the presence of a low-spin siroheme and an exchange-coupled siroheme-[4Fe-4S] unit.* J Biol Chem, 1984. **259**(24): p. 15373-6.
56. Pierik, A.J. and W.R. Hagen, *S = 9/2 EPR signals are evidence against coupling between the siroheme and the Fe/S cluster prosthetic groups in Desulfovibrio vulgaris (Hildenborough) dissimilatory sulfite reductase.* Eur J Biochem, 1991. **195**(2): p. 505-16.
57. Seki, Y., K. Kobayashi, and M. Ishimoto, *Biochemical studies on sulfate-reducing bacteria. XV. Separation and comparison of two forms of desulfoviridin.* J Biochem, 1979. **85**(3): p. 705-11.
58. Hatchikian, E.C., *Desulfofuscidin: dissimilatory, high-spin sulfite reductase of thermophilic, sulfate-reducing bacteria.* Methods Enzymol, 1994. **243**: p. 276-95.
59. Postgate, J.R., *Cytochrome C3 and Desulfoviridin; Pigments of the anaerobe Desulphovibrio Desulphovibrio*

desulphuricans. 1956. **14**(Journal of General Microbiology): p. 545-572.

60. Kobayashi, K., Y. Seki, and M. Ishimoto, *Biochemical studies on sulfate-ruducing bacteria. 8. Sulfite reductase from Desulfovibrio vulgaris--mechanism of trithionate, thiosulfate, and sulfide formation and enzymatic properties.* J Biochem, 1974. **75**(3): p. 519-29.
61. Lee, J.P. and H.D. Peck, *Purification of the Enzyme Reducing Bisulfite to Trithionate from Desulfovibrio gigas and its Identification as Desulfoviridin.* Biochemical and Biophysical Research Communications, 1971. **45**(3): p. 583-589.
62. Moura, I., et al., *Characterization of two Dissimilatory Sulfite Reductases (Desulforubidin and Desulfoviridin) from the Sulfate-Reducing Bacteria. Mössbauer and EPR Studies.* Journal of the American Chemical Society, 1988. **110**: p. 1075-1082.
63. Campbell, L.L. and J.R. Postgate, *Classification of the spore-forming sulfate-reducing bacteria.* Bacteriol Rev, 1965. **29**(3): p. 359-63.
64. Akagi, J.M. and V. Adams, *Isolation of a bisulfite reductase activity from Desulfotomaculum nigrificans and its identification as the carbon monoxide-binding pigment P582.* J Bacteriol, 1973. **116**(1): p. 392-6.
65. Miller, J.D. and A.M. Saleh, *A Sulphate-Reducing Bacterium Containing Cytochrome C3 but Lacking Desulfoviridin.* J Gen Microbiol, 1964. **37**: p. 419-23.
66. Pierik, A.J., et al., *The third subunit of desulfoviridin-type dissimilatory sulfite reductases.* Eur J Biochem, 1992. **205**(1): p. 111-5.

67. Karkhoff-Schweizer, R., R.M. Bruschi, and G. Voordouw, *Expression of the gama-subunit gene of Desulfoviridin-type dissimilatory sulfite reductase and of the alfa and beta subunit gene is not coordinatellt regulated.* European Journal of Biochemistry, 1993. **211**: p. 501-507.
68. Steuber, J., et al., *Molecular properties of the dissimilatory sulfite reductase from Desulfovibrio desulfuricans (Essex) and comparison with the enzyme from Desulfovibrio vulgaris (Hildenborough).* Eur J Biochem, 1995. **233**(3): p. 873-9.
69. Postgate, J.R., *Recent advances in the study of the sulfate-reducing bacteria.* Bacteriol Rev, 1965. **29**(4): p. 425-41.
70. Akagi, J.M. and L.L. Campbell, *STUDIES ON THERMOPHILIC SULFATE-REDUCING BACTERIA III. : Adenosine Triphosphate-sulfurylase of Clostridium nigrificans and Desulfovibrio desulfuricans.* J Bacteriol, 1962. **84**(6): p. 1194-201.
71. Ishimoto, M. and T. Yagi, *Biochemical studies on sulphate-reducing bacteria. IX. Sulfite reductase.* The Journal of Biochemistry, 1961. **49**: p. 103-109.
72. Fritz, G., et al., *Structure of adenylylsulfate reductase from the hyperthermophilic Archaeoglobus fulgidus at 1.6-A resolution.* Proc Natl Acad Sci U S A, 2002. **99**(4): p. 1836-41.
73. Lengeler, J.W., Drews G., and S.H. G., *Biology of the prokaryotes*. 1999, Stuttgart, Germany: Thieme Verlag.
74. Suh, B. and J.M. Akagi, *Formation of thiosulfate from sulfite by Desulfovibrio vulgaris.* J Bacteriol, 1969. **99**(1): p. 210-5.
75. Drake, H.L. and J.M. Akagi, *Dissimilatory reduction of bisulfite by Desulfovibrio vulgaris.* J Bacteriol, 1978. **136**(3): p. 916-23.

76. Findley, J.E. and J.M. Akagi, *Evidence for thiosulfate formation during sulfite reduction by Desulfovibrio vulgaris.* Biochem Biophys Res Commun, 1969. **36**(2): p. 266-71.
77. Chambers, L.A. and P.A. Trudinger, *Are thiosulfate and trithionate intermediates in dissimilatory sulfate reduction?* J Bacteriol, 1975. **123**(1): p. 36-40.
78. Findley, J.E. and J.M. Akagi, *Role of Thiosulfate in Bisulfite Reduction as Catalyzed by Desulfovibrio vulgaris.* Journal of Bacteriology, 1970. **103**(3): p. 741-744.
79. Akagi, J.M., *Reduction of bisulfite by the trithionate pathway by cell extracts from Desulfotomaculum nigrificans.* Biochem Biophys Res Commun, 1983. **117**(2): p. 530-5.
80. Akagi, J.M., M. Chan, and V. Adams, *Observations on the bisulfite reductase (P582) isolated from Desulfotomaculum nigrificans.* J Bacteriol, 1974. **120**(1): p. 240-4.
81. Haschke, R.H. and L.L. Campbell, *Thiosulfate reductase of Desulfovibrio vulgaris.* J Bacteriol, 1971. **106**(2): p. 603-7.
82. Drake, H.L. and J.M. Akagi, *Product analysis of bisulfite reductase activity isolated from Desulfovibrio vulgaris.* J Bacteriol, 1976. **126**(2): p. 733-8.
83. Drake, H.L. and J.M. Akagi, *Characterization of a novel thiosulfate-forming enzyme isolated from Desulfovibrio vulgaris.* J Bacteriol, 1977. **132**(1): p. 132-8.
84. Hatchikian, E.C., *Purification and properties of thiosulfate reductase from Desulfovibrio gigas.* Arch Microbiol, 1975. **105**(3): p. 249-56.
85. Nakatsukasa, W. and J.M. Akagi, *Thiosulfate reductase isolated from Desulfotomaculum nigrificans.* J Bacteriol, 1969. **98**(2): p. 429-33.

86. Drake, H.L. and J.M. Akagi, *Bisulfite reductase of Desulfovibrio vulgaris: explanation for product formation.* J Bacteriol, 1977. **132**(1): p. 139-43.
87. Kim, J.H. and J.M. Akagi, *Characterization of a trithionate reductase system from Desulfovibrio vulgaris.* J Bacteriol, 1985. **163**(2): p. 472-5.
88. Hamilton, W.A., *Sulphate-reducing bacteria and anaerobic corrosion.* Annu Rev Microbiol, 1985. **39**: p. 195-217.
89. Seth, A.D. and R.G.J. Edyvean, *The function of sulfate-reducing bacteria in corrosion of potable water mains*. 2006, Department of Chemical and Process Engineering, University of Sheffield, Sheffield, UK.
90. Pereira, A.S., et al., *Characterization of representative enzymes from a sulfate reducing bacterium implicated in the corrosion of steel.* Biochem Biophys Res Commun, 1996. **221**(2): p. 414-21.
91. Beech, I.B., *Sulfate-reducing bacteria in biofilms on metallic materials and corrosion.* Microbiology, 2003. **30**: p. 115-117.
92. Soimajärvi J., Pursiainen M., and K. J., *Sulphate-reducing bacteria in paper machine waters and in suction roll perforations.* Applied Microbiology and Biotechnology, 1978. **5**(2): p. 87-93.
93. Beech, I., et al., *Study of Parameters Implicated in the Biodeterioration of Mild Steel in the Presence of Different Species of Sulphate-reducing Bacteria.* International Biodeterioration & Biodegradation, 1994: p. 289-303.

Chapter 2

Purification, crystallization and preliminary crystallographic analysis of a dissimilatory DsrAB sulfite reductase in complex with DsrC

This Chapter was published in:

Oliveira, T. F.; Vonrhein, C.; Matias, P. M.; Venceslau, S. S.; Pereira, I. A. C.; (2008), Purification, crystallization and preliminary crystallographic analysis of a dissimilatory DsrAB sulfite reductase in complex with DsrC. Journal of Structure Biology, 164, 236-239

Note: SSV and TFO purified the protein samples, TFO crystallized the protein, TFO and PM collected X-ray diffraction data, TFO solved the phase problem with the help of CV and PM. TFO wrote the manuscript with IACP and MA

2.1 Abstract

Dissimilatory sulfite reductase (dSiR, DsrAB) is a key protein in several types of dissimilatory sulfur metabolism, one of the earliest types of energy metabolism to be traced on earth. dSirs are large oligomeric proteins around 200 kDa forming an $\alpha_2\beta_2$ arrangement and including a unique siroheme-[4Fe-4S] coupled cofactor. Here, we report the purification, crystallization and preliminary X-ray diffraction analysis of dSir isolated from *Desulfovibrio vulgaris* Hildenborough, also known as desulfoviridin. In this enzyme the DsrAB protein is associated with DsrC, a protein of unknown function that is believed to play an important role in the sulfite reduction. Crystals belong to the monoclinic space group $P2_1$ with unit cell parameters a=122.7, b=119.4 and c=146.7 Å and diffract X-rays to 2.8 Å on a synchrotron source.

2.2. Introduction

Reduction of sulfite is a crucial biological reaction both in assimilatory pathways, which lead to incorporation of sulfur into amino-acids and other cellular metabolites, or in dissimilatory pathways used by anaerobic microorganisms that respire sulfur compounds [1]. Both assimilatory and dissimilatory sulfite reductases (SiR) contain in the active site a unique combination of cofactors that includes a reduced porphyrin of the isobacterichlorin class, termed siroheme, that is coupled through its cysteine axial ligand to a [4Fe4S] iron-sulfur cluster [2-4]. Furthermore, these two classes of enzymes belong to a superfamily of coupled siroheme-[4Fe4S] containing enzymes that include also assimilatory and dissimilatory nitrite reductases that reduce nitrite to ammonia [1]. The assimilatory sulfite reductases (aSiRs) have been extensively investigated and serve as models for this family of proteins since they are structurally well characterized [2, 5], In contrast, many questions remain regarding dissimilatory sulfite reductases dSiRs, which are apparently more diverse based on distinct spectroscopic properties [6]. One of the most distinguishing factors of dSiRs include the fact that *in vitro* they reduce sulfite incompletely to mainly trithionate and some thiosulfate and sulfide, whereas aSiRs reduce sulfite completely to sulfide [7]. The aSiRs are monomeric and share low sequence similarity to dSiRs, which are large oligomeric proteins with a molecular mass in the order of 200 kDa and minimally composed of two different types of subunits in a $\alpha_2\beta_2$ arrangement [8]. The number of cofactors in some proteins is

also not clear with studies reporting from two to four sirohemes and 10 to 32 non-heme irons per $\alpha_2\beta_2$ module [4, 9-11]. Although some authors propose that the cubane-siroheme cofactor arrangement of dSiRs is similar to that found in aSiRs [4, 10], other authors have proposed the presence of higher nuclearity high-spin iron-sulfur clusters [10-12].

One of the most studied dSiRs is the protein desulfoviridin (Dvir) present in *Desulfovibrio* spp. [7, 13]. This protein is particularly intriguing since it is reported that up to 80% of its siroheme is not metallated but is in the form of sirohydrochlorin [4, 11, 14], although this has been disputed [10]. Another interesting aspect of Dvir is that it forms a stable complex with a smaller protein of 11 kDa, initially classified as a third subunit of dSiR [15], but later identified as the DsrC protein. DsrC is encoded separately from DsrAB, the two subunits of dSiR and their expression is not coordinately regulated [16]. It is actually one of the most highly expressed proteins in *Desulfovibrio vulgaris* Hildenborough, with twice the expression level of DsrAB [17]. This indicates that it plays a crucial role in energy metabolism, but that it is more than a subunit of the dSiR complex. DsrC is also found in sulfite or thiosulfate reducing organisms and is one of the few genes of the *dsr* cluster that is also present in sulfur-oxidizing organisms [18], which contains the *dsrAB* genes coding for a reverse dissimilatory sulfite reductase (rSiR) that is related to dSiRs [19-20]

The dSiRs are very important enzymes for our understanding of biological evolution, since they catalyze a key energy-conserving

step in organisms that metabolise sulfur compounds. Phylogenetic analysis supports an ancient origin of dSiR [20-22], and evidence for the existence of sulfur-metabolizing organisms dates back to 3.49 Gyr ago in the Early Archaean period [23-24]. It is thus be very important to obtain structural information for dSiR to provide insights into these open questions. We have concentrated our efforts in trying to crystallize the Dvir from *D. vulgaris* as this protein forms a stable complex with DsrC, and its structure will thus not only resolve the questions about its cofactor composition, but will also yield evidence for the mode of interaction between DsrAB and DsrC, and the possible role of this protein in the reduction of sulfite.

2.3 Protein Purification

D. vulgaris Hildenborough (DSM 644) was grown in lactate/sulfate medium, and the soluble cell fraction was obtained as previously described [25]. The purification was performed aerobically at 4ºC. The soluble fraction was loaded on a Q-Sepharose fast-flow column equilibrated with 20 mM Tris-HCl pH 7.6 buffer. A stepwise gradient of increasing NaCl concentration was performed. Two bands were separated (eluting at 300 and 350 mM NaCl) showing the characteristic Dvir absorption peak at 630 nm, as previously described [10]. The first eluting band was further purified

on a Q-Sepharose high performance column by a similar procedure. Analysis of the Dvir-containing fraction by native gel electrophoresis indicated that two forms with distinct pIs were still present and thus the protein was still not homogeneous. We separated these two forms on a preparative scale 9% gel containing 0.1% Triton X-100 under native conditions. The running buffer also contained 0.1% Triton X-100. Without any staining it was possible to identify two separate green bands in the gel, a “slow” form (S) and a “fast” form (F) (Fig. 1A). These bands were cut in small slices and submitted to electroelution on a BioRad electro-eluter Model 422 (9 mA, 5 h, 4 ºC) under native conditions. The electroeluted samples of Dvir were collected, washed and concentrated to 10 $mg.mL^{-1}$ in 10 mM Tris-HCl pH 7.6. Studies are underway to investigate the difference between these two bands, both showing similar sulfite reduction activity. An SDS-PAGE was performed to confirm the presence of both subunits of Dvir (DsrA, DsrB) and DsrC, which form a stable complex in *D. vulgaris* that is not disrupted by the described purification procedure (Fig. 1B).

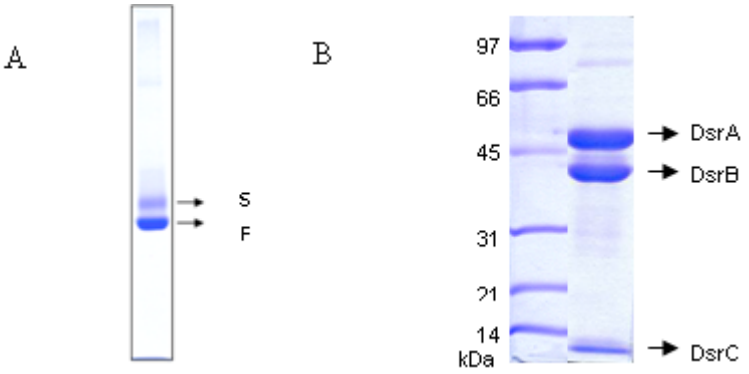

Figure 1 - A) 9% Native-PAGE of Dvir (20 µg) showing two bands: "slow" (S) and "fast" form (F). **B)** 12% SDS-PAGE of the desulfoviridin "slow" form (20 µg) after the electroelution.

2.4. Crystallization

Some initial crystallization screenings from Qiagen and Emerald BioSystems were performed in parallel with both forms (slow and fast) of Dvir at 4 and 20 ºC, using 0.1 µl nanodrops in a Cartesian Dispensing Systems robot from Genomic Solutions (vapor diffusion method with sitting drops). Crystalline material appeared for the fast form of Dvir in conditions #63 (8% PEG 8K, 0.1 M Tris-HCl pH 8.5) and #64 (10% PEG 8K, 0.1 M Hepes pH 7.5) of the Classics suite screening (Qiagen). Further narrower searches were performed around the initial conditions in order to obtain good

quality crystals. After several crystal optimization experiments, small green crystals were grown by mixing 2 µl of protein with 1 µl of reservoir solution containing 12.5% PEG 4000, 0.1 M Tris-HCl pH 8.5, 0.2 M $MgCl_2$. The crystals appeared within two days and grew to maximum dimensions of 0.1x0.1x0.1 mm in one week (Fig. 2). An SDS-PAGE confirmed the presence of DsrA, DsrB and DsrC proteins in the crystals (data not shown). Crystals were cryoprotected with the reservoir solution supplemented with 20% glycerol and were directly flash cooled in liquid nitrogen. However, it was extremely difficult to get suitable crystals for X-ray diffraction experiments, due to the low reproducibility of the crystallization conditions and very poor diffraction quality shown by most screened crystals. Many similar crystallization conditions were set up yielding quite different results, and most of the obtained crystals were pre-screened in our in-house generator prior to shipment to synchrotron sources.

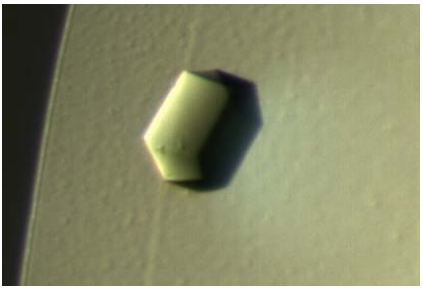

Figure 2 – Crystal of Dvir- DsrC complex grown in 12.5% PEG 4K, 0.1 M Tris-HCl pH 8.5, 0.2 M $MgCl_2$ (dimensions of ~ 0.1x0.1x0.1 mm).

2.5. Data collection

X-ray diffraction data were collected on ID29 at ESRF (Grenoble) to 2.8 Å resolution. A multiple-wavelength anomalous dispersion (MAD) experiment was set up based on the fluorescence scan around the Fe *K*-edge (absorption peak: 1.736 Å; inflection point: 1.742 Å and high-energy remote: 1.033 Å). Diffraction data were recorded at a detector-to-crystal distance of 208.8 mm on an ADSC Q315R detector, with an oscillation range of 1º and an exposure time of 4 s per frame (Fig. 3).

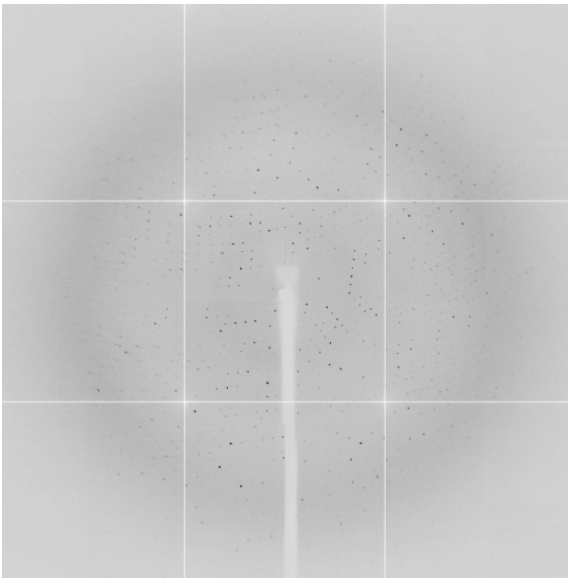

Figure 3 - Diffraction pattern of Dvir-DsrC crystal collected at ID29 at ESRF-Grenoble (resolution limit is ~2.8 Å).

X-ray data were integrated using XDS [26] followed by scaling and merging with SCALA [27] from the CCP4 program suite [28], using all three wavelengths together during the scaling step but keeping them separately during the final merging. During scaling, the peak wavelength showed detectable anomalous signal to about 5 Å, and the inflection to about 8 Å. Crystals belong to the monoclinic space group $P2_1$ with unit-cell parameters of *a*=122.7,

b=119.4 and *c* = 146.68 Å, β = 110.0°, with two $\alpha_2\beta_2\gamma_2$ units of 200 kDa each per asymmetric unit and a solvent content of about 51%. Statistics for the crystallographic data sets are summarized in Table 1.

Table 1. Crystal data and X-ray diffraction statistics

	pk	ip	hrem
Wavelenght (Å)	1.736	1.742	1.033
Space Group	$P2_1$		
Unit Cell Parameters (Å)	a = 122.7, b = 119.4, c = 146.7		
Overall resolution range (Å)	54.79 – 2.76	60.86 - 3.19	35.25 – 3.10
Highest resolution shell (Å)	2.91 – 2.76	3.30 – 2.76	3.30 – 3.13
Total reflections	565149 (60720)	234784 (16108)	255920 (31200)
Unique reflections	101597 (14611)	66048 (6235)	70614 (11135)
I/σ (I)	8.8 (2.1)	5.9 (2.0)	6.2 (2.0)
R_{merge} (%)*	13.6 (50.5)	16.4 (36.5)	15.8 (41.2)
R_{anom} (%)	8.3 (35.5)	12.3 (36.1)	11.4 (37.2)
Completeness[a] (%)	99.8 (98.6)	99.6 (96.6)	98.3 (92.9)
Multiplicity	5.6 (4.2)	3.6 (2.6)	3.6 (2.8)

Anomalous Completeness (%)	98.9 (93.0)	97.9 (84.8)	96.0 (81.1)
Anomalous multiplicity	2.8 (2.1)	1.8 (1.4)	1.8 (1.5)

Values in parenthesis show the statistics of the highest resolution shell

*R_{merge} = $\sum_{hkl} \sum_{i} \left| I_i(hkl) - \overline{I(hkl)} \right| / \sum_{hkl} \sum_{i} \left| I_i(hkl) \right|$ where I_i (hkl) is the i^{th} measurement

2.6 Preliminary Structure Determination

The automated pipeline autoSHARP [29] was used to start the substructure detection and structure solution. Initially it was thought that due to the low resolution of the anomalous signal detectable during data processing, the iron-sulfur cluster might not be resolved into individual atoms - at least not for the substructure solution. Therefore, only 3 sites per monomer were searcher for, each corresponding to one αβγ unit. Although this significantly underestimated the number of Fe sites expected per monomer, SHELXD [30] (as run through autoSHARP) had no problems finding 12 sites. Furthermore, the density modification step using SOLOMON [31] gave a clear indication about the correct enantiomorph for the substructure. This initial modified electron density showed some β-sheet features but would have been difficult to interpret. However, the residual maps automatically

analyzed by autoSHARP showed some clear additional sites for the remaining iron atoms that form the separate iron-sulfur clusters. Therefore, SHARP [32] was used to extend and complete the heavy atom substructure. Additionally, an overall anisotropy correction (as implemented in SHARP) was used, since the data showed some severe anisotropic diffraction. This resulted in far less reflections being rejected during the likelihood analysis in SHARP.

The final heavy atom substructure consisting of 20 sites was given to PROFESSS to detect the non-crystallographic symmetry. There was a clear solution for a dimer of dimers; these initial 4-fold NCS operators were used in DM [33] for density modification including NCS averaging. The resulting map showed clear helical density and several β-sheets. Models for the Fe-S clusters could be placed into this density to accurately describe the heavy-atom substructure.

BUCCANEER [34] was used for automatic building of a starting model. This was subsequently used in iterative density modification to improve the starting map for solvent flipping with SOLOMON followed by NCS-averaging in DM. These steps (model building followed by density modification) were repeated several times. This initial, auto-built model was used to construct a preliminary tetrameric model. Crystallographic refinement is underway.

2.7 Acknowledgements

The authors would like to thank Fundação para a Ciência e Tecnologia for the research grants PTDC/QUI/68368/06 and BIA-PRO/55621/2004 and FCT-POCTI fellowships to TFO (SFRH/BD/29519/2006) and SSV (SFRH/BD/30648/2006). We also would like to thank ESRF and SLS for finantial support for data collection (SLS: European Commission under the 6th Framework Programme through the Key Action: Strenghtening the European Research Area, Research Infrastructures. Contract nº: RII3-CT-2004-506008). CV would like to thank K. Cowtan for making a pre-release of BUCANEER available.

2.8 References

1. Crane, B.R. and E.D. Getzoff, *The relationship between structure and function for the sulfite reductases.* Curr Opin Struct Biol, 1996. **6**(6): p. 744-56.
2. Crane, B.R., L.M. Siegel, and E.D. Getzoff, *Sulfite reductase structure at 1.6 A: evolution and catalysis for reduction of inorganic anions.* Science, 1995. **270**(5233): p. 59-67.
3. Janick, P.A. and L.M. Siegel, *Electron paramagnetic resonance and optical spectroscopic evidence for interaction between siroheme and Fe4S4 prosthetic groups in Escherichia coli sulfite reductase hemoprotein subunit.* Biochemistry, 1982. **21**(15): p. 3538-47.
4. Moura, I., et al., *Characterization of two Dissimilatory Sulfite Reductases (Desulforubidin and Desulfoviridin) from the Sulfate-Reducing Bacteria. Mössbauer and EPR Studies.* Journal of the American Chemical Society, 1988. **110**: p. 1075-1082.
5. Schnell, R., et al., *Siroheme- and [Fe4-S4]-dependent NirA from Mycobacterium tuberculosis is a sulfite reductase with a covalent Cys-Tyr bond in the active site.* J Biol Chem, 2005. **280**(29): p. 27319-28.
6. Rabus, R., T. Hansen, and F. Widdel, *Dissimilatory Sulfate- and Sulfur-Reducing Prokaryotes*, in *The Prokaryotes*, M.e.a. Dworkin, Editor. 2007, Springer-Verlag, http://link.springer-ny.com/link/service/books/10125/. New York. p. 659-768.
7. Lee, J.P., J. LeGall, and H.D. Peck, Jr., *Isolation of assimilatroy- and dissimilatory-type sulfite reductases from Desulfovibrio vulgaris.* J Bacteriol, 1973. **115**(2): p. 529-42.

8. Schiffer, A., et al., *Structure of the dissimilatory sulfite reductase from the hyperthermophilic archaeon Archaeoglobus fulgidus.* J Mol Biol, 2008. **379**(5): p. 1063-74.
9. Fauque, G., et al., *Purification and Characterization of bisulfite reductase (Desulfofuscidin) from Desulfovibrio thermophilus and its complexes with exogenous ligands.* Biochemical and Biophysica acta Pro., 1990. **1040**(1): p. 112-118.
10. Marritt, S.J. and W.F. Hagen, *Dissimilatory sulfite reductase revisited. The desulfoviridin molecule does contain 20 iron ions, extensively demetallated sirohaem, and an S = 9/2 iron-sulfur cluster.* Eur J Biochem, 1996. **238**(3): p. 724-7.
11. Pierik, A.J. and W.R. Hagen, *S = 9/2 EPR signals are evidence against coupling between the siroheme and the Fe/S cluster prosthetic groups in Desulfovibrio vulgaris (Hildenborough) dissimilatory sulfite reductase.* Eur J Biochem, 1991. **195**(2): p. 505-16.
12. Arendsen, A.F., et al., *The dissimilatory sulfite reductase from Desulfosarcina variabilis is a desulforubidin containing uncoupled metalated sirohemes and S = 9/2 iron-sulfur clusters.* Biochemistry, 1993. **32**(39): p. 10323-30.
13. Lee, J.P. and H.D. Peck, *Purification of the Enzyme Reducing Bisulfite to Trithionate from Desulfovibrio gigas and its Identification as Desulfoviridin.* Biochemical and Biophysical Research Communications, 1971. **45**(3): p. 583-589.
14. Murphy, M.J. and L.M. Siegel, *Siroheme and sirohydrochlorin. The basis for a new type of porphyrin-*

related prosthetic group common to both assimilatory and dissimilatory sulfite reductases. J Biol Chem, 1973. **248**(19): p. 6911-9.

15. Pierik, A.J., et al., *The third subunit of desulfoviridin-type dissimilatory sulfite reductases.* Eur J Biochem, 1992. **205**(1): p. 111-5.
16. Karkhoff-Schweizer, R., R.M. Bruschi, and G. Voordouw, *Expression of the gama-subunit gene of Desulfoviridin-type dissimilatory sulfite reductase and of the alfa and beta subunit gene is not coordinatellt regulated.* European Journal of Biochemistry, 1993. **211**: p. 501-507.
17. Haveman, S.A., et al., *Gene expression analysis of energy metabolism mutants of Desulfovibrio vulgaris Hildenborough indicates an important role for alcohol dehydrogenase.* J Bacteriol, 2003. **185**(15): p. 4345-53.
18. Pott, A.S. and C. Dahl, *Sirohaem sulfite reductase and other proteins encoded by genes at the dsr locus of Chromatium vinosum are involved in the oxidation of intracellular sulfur.* Microbiology, 1998. **144 (Pt 7)**: p. 1881-94.
19. Hipp, W.M., et al., *Towards the phylogeny of APS reductases and sirohaem sulfite reductases in sulfate-reducing and sulfur-oxidizing prokaryotes.* Microbiology, 1997. **143 (Pt 9)**: p. 2891-902.
20. Molitor, M., et al., *A dissimilatory sirohaem-sulfite-reductase-type protein from the hyperthermophilic archaeon Pyrobaculum islandicum.* Microbiology, 1998. **144 (Pt 2)**: p. 529-41.
21. Dhillon, A., et al., *Domain evolution and functional diversification of sulfite reductases.* Astrobiology, 2005. **5**(1): p. 18-29.

22. Wagner, M., et al., *Phylogeny of dissimilatory sulfite reductases supports an early origin of sulfate respiration.* J Bacteriol, 1998. **180**(11): p. 2975-82.
23. Philippot, P., et al., *Early Archaean microorganisms preferred elemental sulfur, not sulfate.* Science, 2007. **317**(5844): p. 1534-7.
24. Shen, Y., R. Buick, and D.E. Canfield, *Isotopic evidence for microbial sulphate reduction in the early Archaean era.* Nature, 2001. **410**(6824): p. 77-81.
25. Legall, J., et al., *Localization and Specificity of Cytochromes and Other Electron-Transfer Proteins from Sulfate-Reducing Bacteria.* Biochimie, 1994. **76**: p. 655-665.
26. Kabsch, W., *Automatic processing of rotation diffraction data from crystals of initially inknown symmetry and cell constants.* J. Appl. Crystallogr., 1993. **26**: p. 795-800.
27. Evans, P., *Scaling and assessment of data quality.* Acta Crystallogr D Biol Crystallogr, 2006. **62**(Pt 1): p. 72-82.
28. *Collaborative Computational Project Number 4 - The CCP4 Suite: Programs for Protein Crystallography.* Acta Cryst. D, 1994. **50**: p. 760-763.
29. Vonrhein, C., et al., *Automated structure solution with autoSHARP.* Methods Mol Biol, 2007. **364**: p. 215-30.
30. Schneider, T.R. and G.M. Sheldrick, *Substructure solution with SHELXD.* Acta Crystallogr D Biol Crystallogr, 2002. **58**(Pt 10 Pt 2): p. 1772-9.
31. Abrahams, J.P. and A.G.W. Leslie, *Methods used in the structure determination of bovine mitochondrial F1 ATPase.* Acta Crystallogr D Biol Crystallogr D, 1996. **52**: p. 30-42.

32. Fortelle, E.d.L. and G. Bricogne, *Maximum-Likelihood Heavy-Atom Parameter for the Multiple Isomorphous Replacement and Multiwavelenght Anomalous Diffraction Methods.* Methods in Enzymology, 1997. **276**: p. 472-494.
33. Cowtan, K., *Joint CCP4 and ESF-EACBM.* Newsletter on Protein Crystallography, 1994. **31**: p. 34-38.
34. Cowtan, K., *The Buccaneer software for automated model building. 1. Tracing protein chains.* Acta Crystallogr D Biol Crystallogr, 2006. **62**(Pt 9): p. 1002-11.

Chapter 3

The Crystal Structure of *Desulfovibrio vulgaris* Dissimilatory Sulfite Reductase Bound to DsrC Provides Novel Insights into the Mechanism of Sulfate Respiration

This Chapter was published in:

Oliveira, T. F.; Vonrhein, C.; Matias, P. M.; Venceslau, S. S.; Pereira, I. A. C.; Archer, M., (2008). The Crystal Structure of Desulfovibrio vulgaris Dissimilatory Sulfite Reductase Bound to DsrC Provides Novel Insights into the Mechanism of Sulfate Respiration, (2008). Journal of Biological Chemistry, Vol 283, 49, 34141-9

Note: TFO crystallized the protein, TFO and PM collected X-ray diffraction data, TFO solved and refined the structure with the help of CV, PM and MA. TFO, IACP and MA analyzed the structure and wrote the manuscript

3.1 Abstract

Sulfate reduction is one of the earliest types of energy metabolism used by ancestral organisms to sustain life. Despite extensive studies, many questions remain about the way respiratory sulfate reduction is associated with energy conservation. A crucial enzyme in this process is the dissimilatory sulfite reductase (dSiR), which contains a unique siroheme-[4Fe4S] coupled cofactor. Here, we report the structure of desulfoviridin from *Desulfovibrio vulgaris*, in which the dSiR DsrAB (sulfite reductase) subunits are bound to the DsrC protein. The $\alpha_2\beta_2\gamma_2$ assembly contains two siroheme-[4Fe4S] cofactors bound by DsrB, two sirohydrochlorins, two [4Fe4S] centers bound by DsrA, and another four [4Fe4S] centers in the ferredoxin domains. A sulfite molecule, coordinating the siroheme, is found at the active site. The DsrC protein is bound in a cleft between DsrA and DsrB with its conserved C-terminal cysteine reaching the distal side of the siroheme. We propose a novel mechanism for the process of sulfite reduction involving DsrAB, DsrC and the DsrMKJOP membrane complex (a membrane complex with putative disulfide/thiol reductase activity), in which two of the six electrons for reduction of sulfite derive from the membrane quinone pool. These results show that DsrC is involved in sulfite reduction, which changes the mechanism involved in sulfate respiration. This has important implications for models used to date ancient sulfur metabolism based on sulfur isotope fractionations.

3.2. Introduction

The dissimilatory reduction of sulfur compounds is one of the earliest energy metabolisms detected on Earth, at ~3.5 billion years ago [1-2]. At the end of the Archean (~2.7 billion years ago) the advent of oxygenic photosynthesis led to a gradual increase in the levels of atmospheric oxygen, which in turn caused an increasing flux of sulfate to the oceans from weathering of sulfide minerals on land [3]. As a consequence of this process, reduction of sulfate became a dominant biological process in the oceans, resulting in sulfidic anoxic conditions from about 0.6 billion to 02.5 billion years ago [3-4]. During this extended period, sulfate reducing prokaryotes were main players in marine habitats where most evolutionary processes were taking place. Today, these organisms are still today major contributors to the biological carbon and sulfur cycles and their activities have important environmental and economic consequences.

A key enzyme in sulfur-based energy metabolism is the dissimilatory sulfite reductase (dSiR), which is present in organisms that reduce sulfate, sulfite and other sulfur compounds. This enzyme is also found in some phototrophic and chemotrophic sulfur oxidisers, where it is proposed to operate in the reverse direction (reverse sulfite reductase, rSiR). The dSiR is minimally composed of two subunits, DsrA and DsrB, in a ~200kDa $\alpha_2\beta_2$ arrangement. The *dsrA* and *dsrB* genes are paralogous, and most likely arose from a very early gene duplication event that preceded the separation of the *Archaea* and *Bacteria* domains [5-8], in agreement with a very

early onset of biological sulfite reduction. The dSiR belongs to a family of proteins that also include the assimilatory sulfite (aSiR) and nitrite (aNiR) reductases, the monomeric low molecular mass aSiRs, and other dSiRs like asrC and Fsr [9-11]. This family has in common a characteristic cofactor assembly that includes an iron tetrahydroporphyrin of the isobacteriochlorin class, termed siroheme (Figure 1a) that is coupled through its cysteine axial ligand to a [4Fe4S] iron-sulfur cluster [12-14].

The aSiR and aNiR, found in plants, fungi and bacteria, are monomeric enzymes that display an internal two-fold symmetry of a module that is related to DsrA/DsrB, suggesting that these assimilatory proteins also resulted from a gene duplication event [9-10, 14]. Phylogenetic sequence analysis indicates that both dSiRs and aSiRs diverged from a common ancestral gene that was present in one of the earliest life forms on Earth [7, 10, 14].

Despite its central role in anaerobic metabolism many aspects of dSiRs remain poorly understood. One of these is the nature of their physiological product because *in vitro* they reduce sulfite to a mixture of trithionate, thiosulfate and sulfide in proportions that depend on the reaction conditions [15], in contrast to aSiRs, which reduce sulfite directly to sulfide. This has led to some controversy, still unresolved, over whether the biological mechanism of dissimilatory sulfite reduction involves the formation of thiosulfate and trithionate as necessary intermediates [15-16]. Another open question regarding dSiRs is the content and the actual nature of the cofactors present. It is not clear whether both DsrA and DsrB subunits contain the coupled siroheme-[4Fe4S] cofactor because its

characteristic binding site in DsrB is missing the first cysteine [5]. Both DsrA and DsrB contain a ferredoxin-like domain, not present in aSiRs, which should bind an extra [4Fe4S] cluster. Cofactor quantification of dSiRs is quite disparate, with studies reporting from 2 to 4 sirohemes and 10 to 32 non-heme irons per $\alpha_2\beta_2$ module [13, 17-19]. The nature of the catalytic cofactor has also been disputed with some studies proposing a cubane-siroheme arrangement similar to that found in aSiRs [13, 19], and other studies proposing the presence of higher nuclearity high-spin iron-sulfur clusters [18-20]. Finally, a most important and unresolved question is the nature of the physiological electron donor to dSiR.

Most studies of dSiRs have focused on desulfoviridin (Dvir), the dSiR of *Desulfovibrio* spp. This enzyme has a characteristic and redox-insensitive band at ~628 nm due to the presence of sirohydrochlorin, the iron-free form of siroheme (Figure 1b).

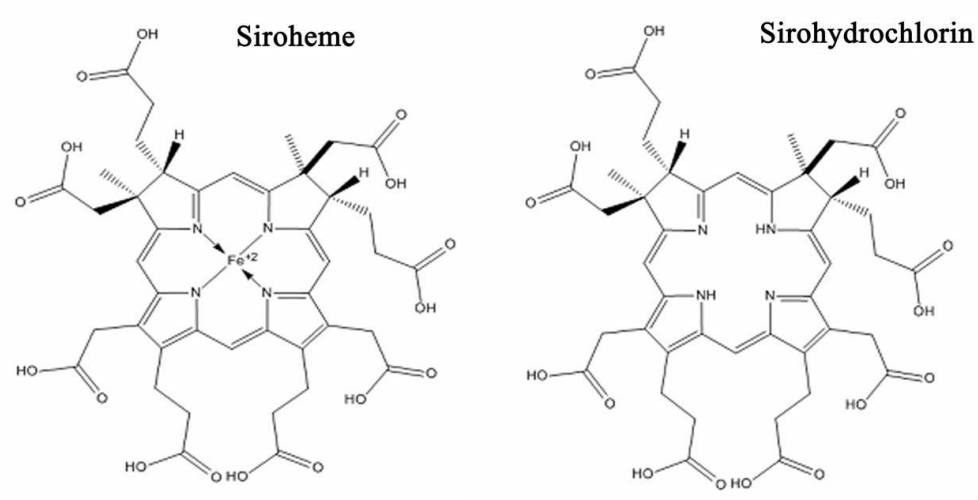

Figure 1 – Schematic representation of the siroheme and sirohydrochlorin molecules. Images generated in ChemBioDraw – version 11.0.1, CambridgeSoft – Life Science Enterprise Solutions.

It is reported that up to 80% of its siroheme lacks iron and is in the form of sirohydrochlorin [13, 18, 21], but this has been disputed [22]. Another particular feature of Dvir is that it forms a stable complex with DsrC, a small protein of 11 kDa. Initial reports described DsrC as a γ subunit of dSiRs present in a stoichiometry of $\alpha_2\beta_2\gamma_2$ [23]. However, the *dsrC* gene is located separately from *dsrAB* in several sulfate-reducing organisms, like *Desulfovibrio*

vulgaris Hildenborough, where their expression is not coordinately regulated [24]. There are also several dSiRs that do not include DsrC [5, 7], but all organisms that contain the *dsrAB* genes include also *dsrC*. These points indicate that DsrC is not a subunit of dSiR, but rather a protein with which it interacts. In several sulfur-oxidising and sulfite-reducing bacteria, *dsrC* is located in the same operon as *dsrAB* [25-27]. It is actually one of the few proteins, apart from DsrAB and the DsrMKJOP membrane complex (a membrane complex with putative disulfide/thiol reductase activity), to be conserved in both sulfur oxidisers and sulfate/sulfite reducers [27]. In addition, *D. vulgaris dsrC* is one of the most highly expressed genes in the cell with twice the expression level of *dsrAB* [28], pointing to an important role in cellular metabolism. Interestingly, homologues of DsrC, like YccK, are also present in organisms that do not contain dSiRs such as *Escherichia coli* and *Haemophillus influenzae*. YccK (renamed as TusE) was recently shown to be involved in sulfur-transfer reactions as part of the biosynthesis of thio-modifications of bacterial tRNA wobble positions [29]. This work provided the first functional assignment of a DsrC-like protein in sulfur metabolism, with important implications to the dissimilatory processes where the function of DsrC has not yet been elucidated. The functional part of DsrC seems to be a C-terminal flexible arm, which displays several strictly conserved residues including a cysteine that is the penultimate one [30].

In this work we report the structure of Dvir, the dSiR from *D. vulgaris* Hildenborough in which the DsrAB proteins are bound to DsrC. This structure resolves several long standing questions about

dSiRs, and suggests a function for DsrC that has important implications regarding the mechanism of sulfate reduction.

3.3 Experimental Procedures

3.3.1 Protein Crystallization and X-Ray Data

Dvir from *D. vulgaris* Hildenborough (DSM 644) was purified as previously described [31]. A detailed description of the crystallization and structure solution of Dvir by multiple-wavelength anomalous dispersion (MAD) based on the iron is presented in [31]. In summary, small dark green crystals were obtained in 12.5% PEG 4000, 0.1 M Tris-HCl pH 8.5, 0.2 M $MgCl_2$ and were cryoprotected with the crystallization solution supplemented with 20% glycerol. Crystals belong to the monoclinic space group $P2_1$ (a = 122.7, b = 119.4 and c = 146.68 Å, β = 110.0º) with two $\alpha_2\beta_2\gamma_2$ units per asymmetric unit corresponding to a solvent content of ~51%. A three-wavelength multiple-wavelenght anomalous dispersion data collection to 2.9 Å was carried out on the tunable beamline ID29 at the European Synchrotron Radiation Facility (ESRF), Grenoble.

Further efforts were undertaken to improve crystal X-ray diffraction, which included many crystallization set-ups with the same or similar experimental conditions to overcome low crystallization reproducibility and very poor crystal quality (low resolution, multiple and anisotropic diffraction patterns). Additional

X-ray data were later measured at ESRF ID23-2 beamline using an ADSC Q315 CCD detector. A data set with 300 images was collected at 0.933 Å, with an oscillation angle of 0.5º and an exposure time of 9 s/image. The X-ray data were integrated and scaled using the XDS program [32]. Data merging and conversion to structure factor amplitudes were carried out respectively with SCALA [33] and TRUNCATE [34] from the CCP4 suite [35]. Crystals diffract to 2.1 Å and belong to the same space group ($P2_1$) as the 2.9 Å data set, but with different cell parameters: *a* = 65.41, *b* = 118.91 and *c* = 132.25 Å, β = 104.1º with one $\alpha_2\beta_2\gamma_2$ assembly in the asymmetric unit and solvent content of ~50%.

3.3.2 Structure Determination and Refinement

Because the two measured crystals are not isomorphous, the 2.1 Å data set structure was solved by molecular replacement with MOLREP [36] using the 2.9 Å model as a template (two αβγ units were found). Further refinement (using NCS-restraints) was carried out with BUSTER [37] and model building using Coot [38]. 5% of reflections were randomly excluded from the refinement for cross-validation (R_{free} calculation). The electron density maps are generally well defined (better for chains ABC than DEF, as reflected by the higher average isotropic thermal motion parameters), except for some surface loops. The two αβγ units are very similar (rmsd of 0.2 Å for 919 aligned residues), so chains A, B and C will be used to

describe the Dvir structure. The final model comprises 1818 amino acid residues, 2 sirohemes, 2 sirohydrochlorins, 8 [4Fe4S] clusters, 2 sulfite ions and 1016 water molecules. The Ramachandran plot shows that 87.4% of the residues lie in most favored regions and only 0.4% fall in disallowed regions. Figures 1 to 4 were generated using PyMOL [39].

3.4. Results

3.4.1 The Crystal Structure of Dvir

The 2.1 Å final model of Dvir was refined to an R–factor of 19% (R-free of 21.9%). Statistics of data processing and refinement are listed in Table 1.

Table 1 - Crystallographic data processing and refinement statistics.

Data collection	
Wavelenght (Å)	0.933
Space Group	$P2_1$
Unit Cell Parameters (Å, º)	*a* = 65.41, *b* = 118.90, *c* =132.45 β=104.1
Resolution range (Å)	40.29 – 2.10 (2.21-2.10)
Unique reflections	112244 (14772)
I/σ (I)	13.2 (2.0)
R_{merge} (%)*	4.7 (44.9)
R_{pim} (%)#	3.8 (38.1)
Completeness (%)	98.1 (88.7)
Multiplicity	3.1 (2.4)
Wilson B ($Å^2$)	36.8

Refinement	
Nº of amino acid residues in a. u.	1818
Other moieties:	
- Siroheme (SRM)	2 (with Fe) + 2 (Fe-free)
- Fe_4S_4 clusters	8
- SO_3^{2-}	2
- Water	1016
R/R-free (%)	19.0 / 21.9
Average B-factor (main-chain) (Å^2)	
- chains A and B / C	31.9 / 42.9
- chains D and E / F	47.2 / 56.1
- solvent molecules	43.7
r.m.s. bond length deviation from ideal values (Å)	0.005
r.m.s. bond angle deviation from ideal values (º)	0.944

Values in parenthesis show the statistics of the highest resolution shell (2.21 - 2.10 Å).

* R_{merge} = Σh Σi |*I*i(h) - <*I*(h)>|/Σh Σi *I*i (h), # Rpim = Σh [1/(N-1)]1/2 Σi |*I*i(h) - <*I*(h)>|/Σh Σi *I*i (h)
, where *I* is the observed intensity, <*I*> is the average intensity of multiple observations from symmetry-related reflections, and N is redundancy.

This model contains two αβγ units (α: residues 2-437 of DsrA, chains A and D; β: residues 2-381 of DsrB, chains B and E and γ: residues 3-105 of DsrC, chains C and F) (Figure 2).

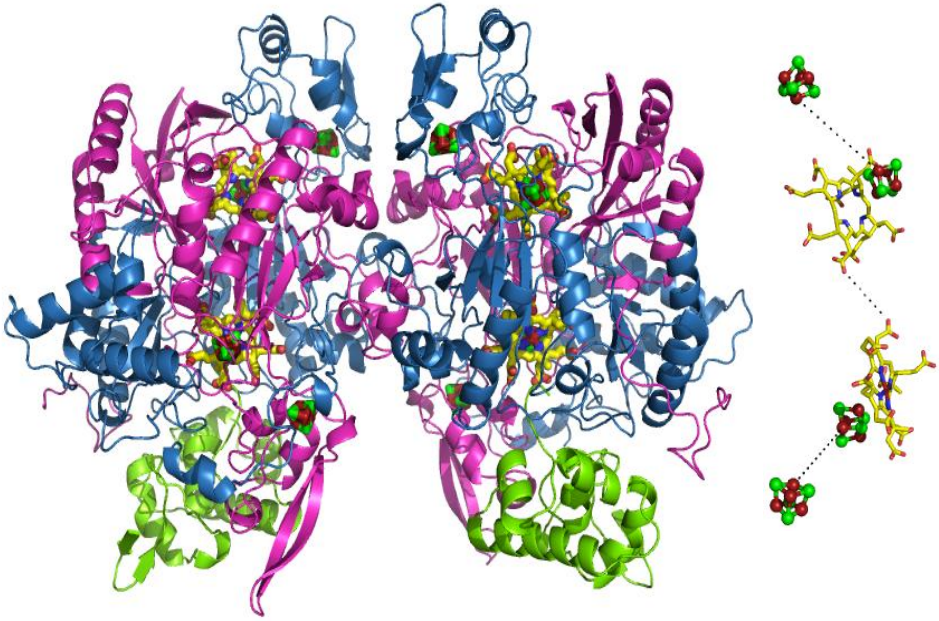

Figure 2 – Secondary structure representation of the $\alpha_2\beta_2\gamma_2$ assembly (DsrAB sulfite reductase bound to DsrC), with the cofactors in ball-and-stick mode. DsrA (chains A and D) is colored blue, DsrB (chains B and E) magenta and DsrC (chains C and F) green. The distance between the cofactors from one αβγ unit is displayed on the right side. Color code is C: yellow, O: red, N: blue, Fe: brown and S: green. **C)** Superposition of DsrA and DsrB.

The $\alpha_2\beta_2\gamma_2$ assembly has overall dimensions of ~ 125x100x60 Å and a total surface area of about 55,720 Å^2. The interface area between the two αβ units is 6,100 Å^2, which represents ~11% of the total dimer surface area. This interface is mainly hydrophilic with an important contribution from the DsrA C-terminal tail that embraces DsrB from the other αβ unit, and to a lesser extent the C-terminus of DsrB (Figure 3). This demonstrates a strong interaction between the two αβ units that corroborates the $\alpha_2\beta_2$ minimal composition proposed for all dSiRs.

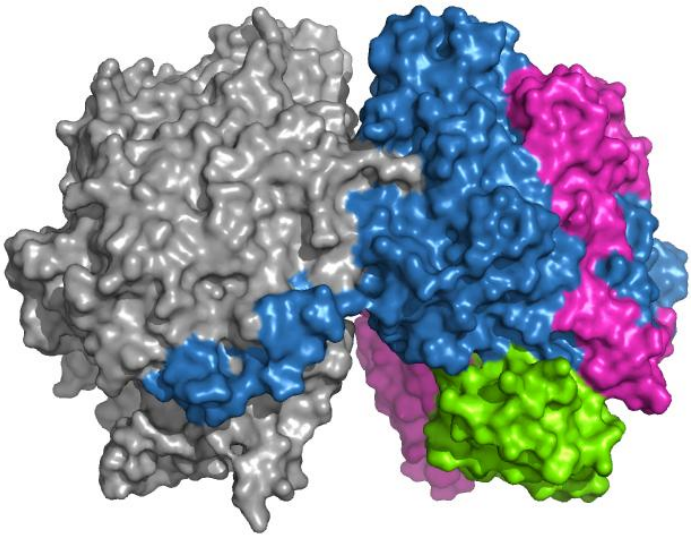

Figure 3 - Molecular surface of the $\alpha_2\beta_2\gamma_2$ assembly with one αβγ unit in gray and the other colored according to Figure 2.

3.4.2 DsrAB Structure and Cofactor Binding

The α, β and γ proteins correspond respectively to DsrA, DsrB and DsrC. The structures of the DsrA and DsrB subunits are very similar. Both proteins can be divided into three main domains (A1/B1, A2/B2, A3/B3), which can be superimposed with an rms deviation of 1.96 Å for 321 equivalent Cα atoms, despite sharing only 20% sequence identity (Figure 4). Apart from the three similar domains, the structures of DsrA and DsrB include N- and C-terminal tails that are distinct in the two proteins.

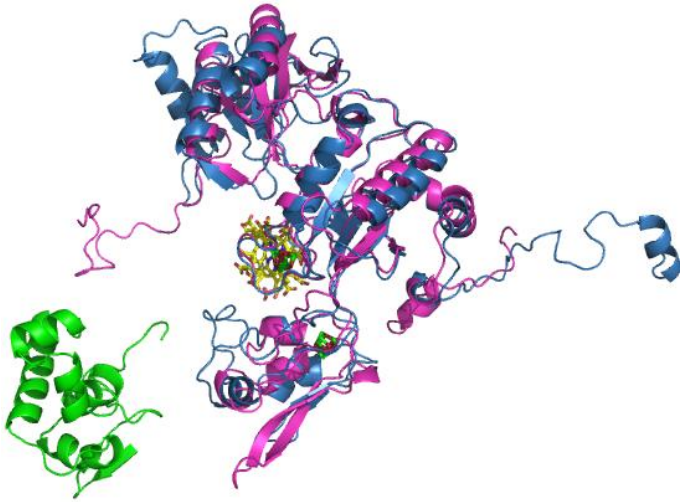

Figure 4 - Cartoon Superposition of DsrA and DsrB, using the same color code as Figure 2.

The A1 and B1 domains (residues 19A-168A and 24B-134B, respectively) show an antiparallel four- or five-stranded β-sheet, flanked by a pair of α-helices with two additional helices in the N-terminal region of the A1 domain. The A2 and B2 domains (residues 169A-241A and 323A-402A, and residues 135B-207B and 278B-365B, respectively) consist of a five-stranded β-sheet bundled with several α-helices. These domains bind a [4Fe4S] cluster (cluster 1) that is part of the siroheme-[4Fe4S] cofactor (Figure 2 and 4). In the A2 domain, this cluster is coordinated by four cysteines (Cys 177A, 183A, 221A, 225A), which are strictly conserved among dSiRs and form the $CX_5CX_nCX_3C$ motif previously identified as the sequence motif for binding of the siroheme-[4Fe4S] cofactor in both aSiRs and dSiRs [5, 40]. Notably, the [4Fe4S] cluster bound by DsrA is in close proximity to a sirohydrochlorin group, i.e. a siroheme that is demetallated (Figure 5A). The sirohydrochlorin is buried in the interior of the protein and sits on the interface between DsrA and DsrB. In the B2 domain the iron-sulfur cluster is also coordinated by four cysteines (Cys 151B, 188B, 189B and 193B) but in a different sequence motif CX_nCCX_3C. The absence of the $CX_5CX_nCX_3C$ motif in DsrB led to the idea that this protein would not bind a siroheme-[4Fe4S] cofactor, which is now shown not to be true. The CX_nCCX_3C motif responsible for binding the catalytic cluster 1 in DsrB is conserved in most dSiRs (with the exception of DsrB from *Pyrobaculum aerophilum*, which has the same $CX_5CX_nCX_3C$ motif in both DsrA and DsrB) and is quite unusual in having two consecutive cysteines ligating the cluster. There are only two examples where this has been reported structurally: for cluster N2 in the Nqo6

subunit of *Thermus thermophilus* complex I [41], and for *Pseudomonas aeruginosa* APS reductase [42]. Recently, tandem cysteine coordination of a novel [4Fe4S] cluster has also been proposed for a large family of CCG proteins (which includes DsrK) by site directed mutagenesis [43]. Close to cluster 1 of DsrB is a siroheme group that is coupled to the cluster through Cys193B, positioned at ~2.4 Å from both (Figure 5B).

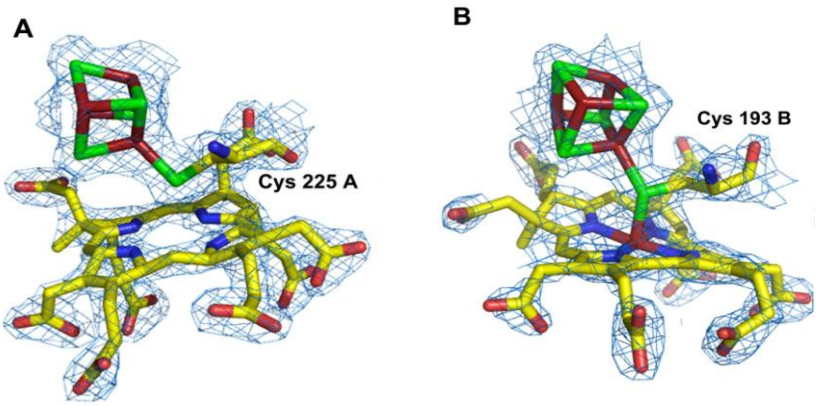

Figure 5. Electron density maps (2Fo-Fc contoured at 1.5 σ) around the **A)** sirohydrochlorin group and cluster 1 of DsrA; **B)** siroheme and cluster 1 of DsrB; The colour code is the same as in Fig 2, except for C atoms of substrate interacting residues (gray) and DsrC C-terminal arm (orange).

Thus, in Dvir the DsrB protein contains the typical exchange-coupled siroheme-[4Fe4S] cofactor previously identified in aSiRs, aNiRs and dSiRs as the catalytic site for sulfite or nitrite reduction

[9, 12-13], whereas the DsrA protein contains a demetallated siroheme that is obviously not catalytic.

The A1A2B1B2 domains of Dvir form a unit that is comparable to the structures of siroheme aSiR and aNiR. There are two structures of aSiRs described, the truncated hemoprotein SiRHP from *Escherichia coli* [14] and the monomeric NirA protein from *Mycobacterium tuberculosis* [44], and one structure of an aNiR from spinach [45]. Despite the low degree of sequence identity (below 25%), these three structures show an overall similarity in the folding arrangement and all contain one siroheme-[4Fe4S] cofactor. A structural comparison of Dvir with the aSiRs and aNiR shows that the domains A1A2 of DsrA can be superimposed with half of the parachute domain (domain 1 in aSiRs) and the siroheme binding domain (domain 2 in aSiRs), whereas the domains B1B2 of DsrB can be superimposed with the other half of the parachute domain and the [4Fe4S] coordinating domain (domain 3 in aSiRs). In this orientation, the catalytic siroheme-[4Fe4S] cofactor of Dvir is in a similar position to the aSiRs cofactors. Superposition of these Dvir domains with the aSiRs and aNiR structures yields rms values in the range 2.4-2.8 Å for the aligned Cα atoms. This similarity supports the proposals of a common ancestor for dSiRs, aSiRs and aNiRs [7, 10, 14].

The A2/B2 domains of DsrA/DsrB are interrupted by insertion of the A3/B3 domains (residues 242A-322A and 208B-277B) that display a typical ferredoxin fold. These domains fold into 2 two-stranded β-sheets surrounded by 3 α-helices and bind one [4Fe4S] cluster (cluster 2), coordinated by four cysteines (Cys 284A, 288A,

306A and 309A in DsrA, and 231B, 258B, 261B and 264B in DsrB) (Figure 2 and 4). Cluster 2 of the DsrB ferredoxin domain is 13 Å from the siroheme-coupled cluster 1, and 6.5 Å from the protein surface. This arrangement suggests that cluster 2 is positioned to transfer electrons from a yet unidentified external electron donor to cluster 1 of the catalytic cofactor. The way the ferredoxin domain interrupts the A2/B2 domain agrees with the proposal that a ferredoxin gene was inserted into an ancestral gene for a siroheme-[4Fe4S] binding reductase [5]. In this respect it is quite interesting to note that when the structure of a DsrAB dimer is aligned with the structure of the spinach aNiR (for which ferredoxin is the electron donor), with the two sirohemes superimposed, the ferredoxin domain of DsrB is in the actual position where spinach ferredoxin has been modeled to bind to the aNiR [45]. This indicates that the ancestral siroheme-[4Fe4S] binding reductase was probably made more efficient by incorporating its electron donor as another domain in its sequence.

The recently reported structure of the *A. fulgidus* dSiR [46] includes only the $\alpha_2\beta_2$ unit of DsrAB. Overall, this structure is quite similar to the structure of the DsrAB proteins from *D. vulgaris*, apart from some small differences in the N- and C-terminals of both subunits and two longer loops in the ferredoxin domains (Figure 6). The most noteworthy difference lies in the fact that dSiR from *A. fulgidus* has four sirohemes and no sirohydrochlorin.

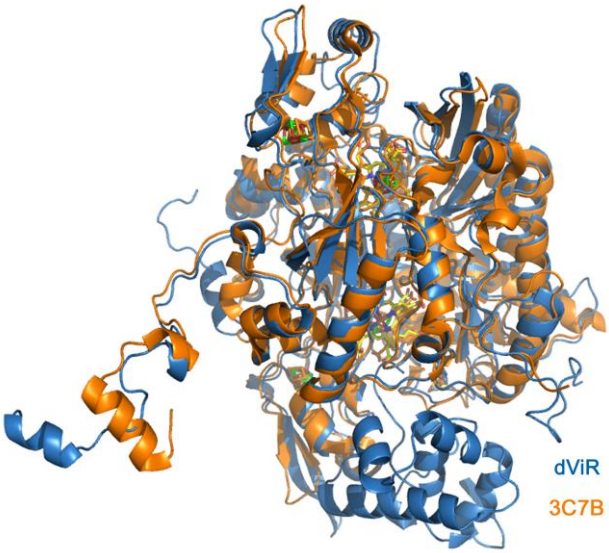

Figure 6 – Superposition of one αβγ unit of D. vulgaris dSiR (DsrAB and DsrC) in blue and A. fulgidus dSiR (DsrAB, PDB code: 3C7B model) in orange. The cofactors are color coded for Dvir and displayed in orange for 3C7B model.

3.4.3 The Catalytic Site

The siroheme and sirohydrochlorin groups are located in the interior of the molecule, in the interface between DsrA and DsrB, with the closest distance to the protein surface of ~14 Å. The catalytic siroheme is surrounded on the proximal side by residues that belong to DsrB. In contrast, the distal side of the heme, where the substrate will bind, is surrounded by basic residues that belong to DsrA, namely Arg83, Arg101, Arg172, Lys213, Lys215, Lys217, Arg231, Arg376 and Arg378. These residues are strictly conserved in dSiRs and create a positive pocket in the active site that favors the binding of the negatively charged sulfite, and may also be involved in providing some of the protons necessary for sulfite reduction. Moreover, several of these residues are establishing H-bonds or salt bridges with the siroheme carboxylate groups and are important for counter-balancing the negative charge of these groups and thus for protein stabilization. Residues Arg71, His150 and His152 of DsrB are also involved in this role. These features of the active site of Dvir are also present in the aSiRs and aNiR [14, 32, 33], and a structure-based sequence alignment shows conservation of the residues involved in forming the active site and stabilizing the siroheme carboxylates.

At the distal side of the catalytic siroheme, residual density is observed, indicating the presence of an axial ligand bound to the iron, which was assigned as a sulfite ion due to its trigonal pyramidal shape combined with the presence of positively charged residues oriented towards the negatively charged oxygen atoms of

the sulfite ion. The electron density was well fitted with sulfite as there were no significant residual negative or positive electron density peaks. It is quite clear that an atom lighter than sulfur (e.g., C, N, O) cannot be fitted at the central position. Sulfite is coordinating the siroheme iron through its sulfur atom (~2.4 Å), with its oxygen atoms establishing H-bonds with Arg101A, Arg172A, Lys213A, Lys215A and also with two water molecules (Figure 7). The four basic residues that interact directly with the substrate are strictly conserved in dSiRs and aSiRs, whereas in spinach aNir Lys215 is replaced by Asn226, which has been associated with a switch in substrate preference from sulfite to nitrite [44-45]. At the distal side of the sirohydrochlorin
group in Dvir, the crucial residues Arg172A and Lys213A of the active site are replaced by Ser140B and Pro181B (Ser130B and Met170B for the structural heme in *A. fulgidus* dSiR).

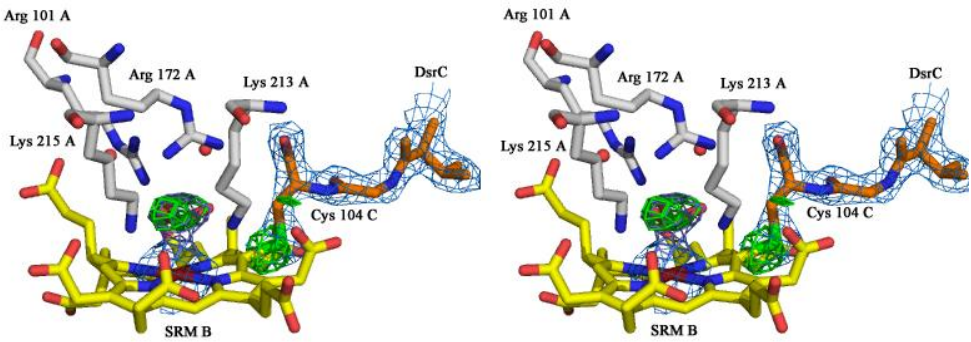

Figure 7 - Schematic view of siroheme from DsrB, bound SO_3^{2-} and C-terminal arm of DsrC (in stereo). The Fo-Fc OMIT map is shown for sulfite ion and Sγ of Cys104C (3.5 σ contour) and the 2Fo-Fc maps are show (1.5 σ contour) for the C-terminal DsrC. The amino acid residues and water molecules (red spheres) that are hydrogen bonded with sulfite are also displayed.

We have also identified a possible substrate channel (Figure 8A). The molecular surface of Dvir shows that the distal face of the catalytic siroheme B is solvent accessible through a channel (~ 9 Å wide, 6 Å high and 20 Å deep), with one side formed by residues 212A and loops 334A-336A and 374A-381A, and the other side by residues on helices 225B-230B and 263B-267B. The positive electrostatic potential at the entrance of this channel, which extends into the active site, facilitates the entrance of the negatively charged substrate molecule. This substrate channel is not present in the case of the DsrA sirohydrochlorin group, due to the presence of bulkier residues, such as Arg283A and Tyr334B, which

block the access to the demetallated siroheme in DsrA. In the *A. fulgidus* dSiR, the substrate binding site of the DsrA siroheme is blocked by a tryptophan residue that is sitting right above the iron. In addition, there is an extended loop that blocks access to this heme, which was proposed to have a structural role [31]. This loop is absent from Dvir, but in its place there is an extended loop from the DsrA ferredoxin domain (Gly257A to Asp275A) that also shields access to the sirohydrochlorin.

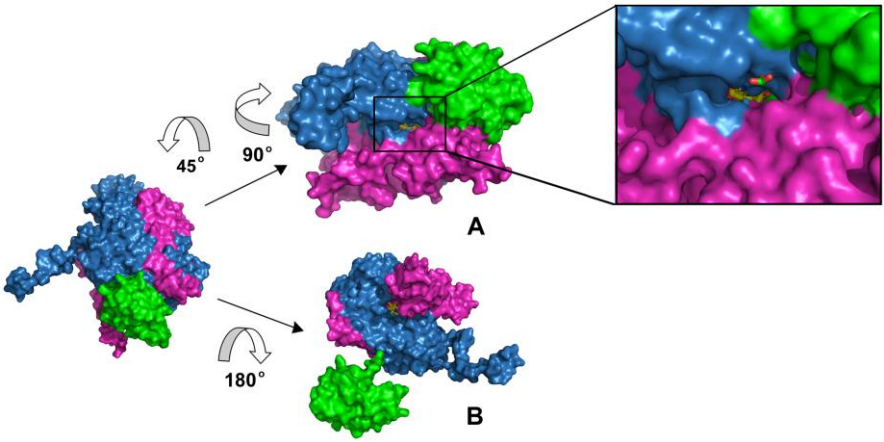

Figure 8. A) Molecular surface of one αβγ unit showing the substrate channel, with a zoomed view of the channel entrance, containing a randomly placed SO_3^{2-} ion for scale; the distal site of the siroheme (in yellow) is solvent accessible. The color scheme is as in Fig 2; **B**) Surface representation of DsrAB with DsrC displaced

from its binding position. The siroheme (in yellow) can be seen in the interior of the cleft formed between DsrAB.

3.4.4 Structure of DsrC Bound to DsrAB

Evidence so far available for DsrC indicates that it is likely to have an important role in sulfite metabolism, and there have been several proposals for its involvement in the sulfite reduction/sulfide oxidation pathway [25-26, 30, 47]. DsrC contains a highly conserved C-terminal sequence that includes two cysteines. The penultimate residue, Cys104C in *D. vulgaris*, is strictly conserved in all family members (including YccK/TusE), whereas the previous one (Cys93C) is conserved only in DsrC proteins that are involved in dissimilatory sulfur metabolism. This suggests the possible involvement of a disulfide bridge between these two cysteines as a redox-active center in the sulfite reduction pathway, and one of the proposals is that DsrC could act as an electron donor for DsrAB [30, 47].

The structure of DsrC bound to DsrAB comprises 105 residues (Glu3 to Val105) and has a mainly helical fold (six α-helices and one 3/10 helix) with a 2-stranded-β-sheet at the N-terminus (Figure 4). DsrC is enclosed in a cleft formed by the DsrA and DsrB subunits and establishes several hydrogen bonds with both (Figure 8B and 9). The C-terminal arm of DsrC extends into the interface between DsrA and DsrB, where it reaches the siroheme (Figures 7 and 9). DsrC and DsrAB are associated through a large interface area of 3,090 $Å^2$ that

corresponds to ~ 24% of the total area of DsrC, 4% of DsrA and only 2.4% of DsrB, which become inaccessible to solvent due to the complex formation. The DsrC-DsrAB interface has a pronounced polar character comprising several hydrogen-bonds (10 H-bonds between DsrC and DsrA and 3 H-bonds with DsrB), many water molecules and only a few hydrophobic contacts.

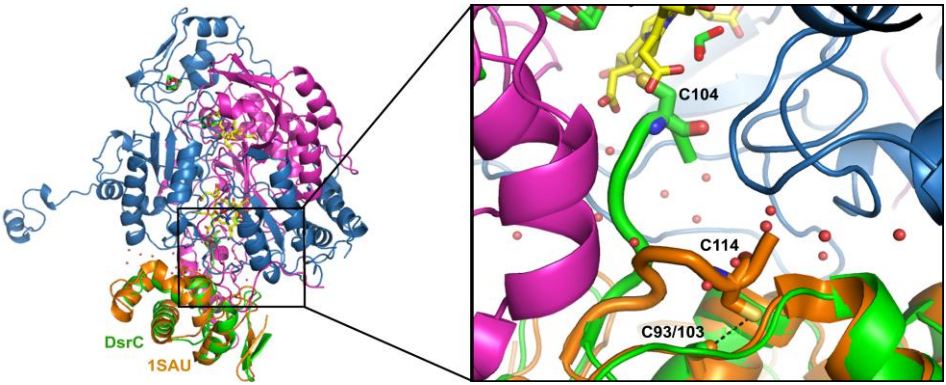

Figure 9 - Secondary structure view of one DsrABC unit with *A. fulgidus* DsrC (pdb code: 1SAU) superposed. The zoomed image shows the extended C-terminal arm of the *D. vulgaris* DsrC reaching the heme, and the retracted arm from *A. fulgidus* DsrC. The two conserved cysteines of each DsrC are represented in stick mode, a dashed black line showing the close contact between Cys103 and Cys114 in *A. fulgidus* DsrC. Some water molecules at the interface are displayed as red spheres. Colour code as the previous images.

The *D. vulgaris* DsrC structure is quite similar to the other known DsrC structures from: *P. aerophilum* [30], *A. fulgidus* [47],

and *Allochromatium vinosum* (PDB code:1YX3). The only major structural difference among these structures is in the C-terminal segment. In the NMR structures of *P. aerophilum* and *A. vinosum* DsrC the C-terminal arm is very disordered and in an extended configuration, whereas in the *A. fulgidus* crystal structure the C-terminal arm is retracted and in contact with the rest of the protein, such that the two conserved cysteines come in van der Waals contact (Figure 3C). Treatment with an oxidizing agent lead to the formation of a disulfide bond between them [47]. In the *D. vulgaris* model the extended C-terminal arm of DsrC has its Cys104C being positioned right next to the substrate binding side (Figures 2C and 3C). This configuration strongly suggests an involvement of Cys104C in the reduction of sulfite. Cys93C is 18 Å away from Cys104C, so a disulfide bond between the two is not possible in this configuration.

Remarkably, the Sγ of Cys104C is only 1.9 Å from the 20´-*meso* carbon of the porphyrin ring of siroheme B, indicating that there is a cross-link from Cys104C to the heme (Figure 2C). This observation is unexpected as it fixes the interaction between DsrC and DsrAB, and conflicts with the observation that for most dSiRs the DsrC protein is not found associated with DsrAB. Therefore, the interaction between Cys104C and siroheme B should be transient in nature. There are several possible mechanisms that could generate this cross-link, like formation of a □-cation radical in the siroheme, which could be quenched by reaction with the nearby Cys104C, or generation of a sulfenic acid on Cys104 followed by attack and displacement by the ring. Whatever its nature, this side-reaction is most probably caused by contact with oxygen during aerobic

purification of the enzyme, since it is highly unlikely that the link could be formed during normal turn-over conditions as it would be highly inhibitory. The observed DsrAB-DsrC cross-linked complex can explain the very low levels of activity of aerobically isolated Dvir compared to the activity of whole cells. This cross-link also explains why only sirohydrochlorin and not the siroheme can be extracted from Dvir [48].

3.5. Discussion

The structure of *D. vulgaris* Dvir shows that it contains two sirohemes, two sirohydrochlorins and 34 Fe *per* $\alpha_2\beta_2$ unit, finally settling the debate on the cofactor content of this protein. The nature of the catalytic site was confirmed to be a coupled siroheme-[4Fe4S] cofactor. The presence of the catalytic cofactor in DsrB rather than DsrA was unexpected, as well as the presence of fully demetallated siroheme in DsrA. To the best of our knowledge, this is the first time that a metal-free heme has been reported in a protein structure. However, it has long been reported that Dvir contained sirohydrochlorin in uncertain amounts [48], which is responsible for its characteristic absorption peak at ~628 nm. This peak is detected even in whole bacterial cells [49], revealing that the presence of this chromophore is not the result of iron loss

during protein purification. Several factors, such as the absence of a substrate channel and the lack of two of the four crucial positive residues conserved at the active site of the several siroheme-containing reductases, indicate that the cofactor in DsrA would not be not catalytic even if it had iron. Most dSiRs are reported to contain two sirohemes *per* $\alpha_2\beta_2$ unit (for example [5, 7, 13, 20]). However, apart from Dvir, no dSiR has the characteristic absorption at 628 nm, indicating that they do not contain sirohydrochlorin. Since only two sirohemes are catalytically active in Dvir, it is possible that only the two catalytic sirohemes are present in other dSiRs. The presence of four sirohemes in the structure of *A. fulgidus* dSiR was unforeseen, since siroheme quantification of this protein had yielded two hemes *per* $\alpha_2\beta_2$ unit [5]. This suggests that the heme quantification method is not reliable, so the actual number of sirohemes in other dSiRs is yet to be firmly established. Nevertheless, only two of the four *A. fulgidus* dSiR sirohemes are proposed to be catalytic, since in the other two the substrate binding site is blocked and some crucial positive residues are also missing. Therefore, for both dSiRs only two catalitically active sirohemes are present *per* $\alpha_2\beta_2$ unit, whereas in aSiRs the second catalytic heme that should be present was lost during evolution [9]. These observations suggest that in both families (aSiRs and dSiRs) the process of gene duplication was associated with loss of function from one of the catalytic sites. In aSiRs this center is no longer present, whereas in dSiRs it may still be present, but without a catalytic role. In the particular case of Dvir from *Desulfovibrio* spp. this center has no iron bound to the porphyrin. It is quite intriguing

why this iron is not present as this is an absolutely unprecedented situation. By comparing the structures of *A. fulgidus* and *D. vulgaris* dSiRs we could find no obvious difference surrounding the prosthetic group of DsrA that could explain why one retains the iron and not the other. Nothing is really known about how siroheme (or sirohydrochlorin) is inserted into proteins so it is difficult to speculate as to in which step iron is lost (or not inserted) into the DsrA heme of Dvir.

Regarding the positively charged active site of Dvir, it is quite striking that so many of its characteristics are shared with those of aSiRs, indicating that this is not the main factor affecting the difference in products observed between both types of enzymes. However, there are a few noteworthy differences in the active site residues of Dvir in comparison with the aSiRs. In particular, two positive residues of the aSiRs that are making salt bridges to the carboxylate groups of acetate 12' (Arg117 of *E. coli* aSiR) and acetate 18' of the siroheme (Arg214 of *E. coli* aSiR) are replaced by Thr136A and Tyr212A, respectively, two residues that are conserved in dSiRs (except in *P. aerophilum*). Also, a strictly conserved glutamine in aSiRs and aNiRs (Gln121 of *E. coli* aSiR), which is H-bonded with the carboxylate of propionate 3', is absent in dSiRs. A strictly conserved arginine of dSiRs, Arg83A in Dvir, is also making a salt bridge with the same carboxylate and is absent in aSiRs. These localized differences may affect the electronic density at the siroheme in such a way that may have an effect on the sulfite reduction mechanism of dSiRs relative to aSiRs. It is also interesting to compare the active site residues of dSiRs with the rSiRs, which in

theory catalyze the reverse reaction *i.e.* oxidation of sulfide to sulfite. It is striking that all of the residues highlighted above for Dvir are also conserved in rSiRs, with the exception of Arg376 of DsrA and His152 of DsrB, which are establishing H-bonds with acetates 18' and 2' of the siroheme. The acetate 2' has been proposed to contain an amide instead of a carboxylic group [50]. However, at the current resolution it is not possible to differentiate between oxygen and nitrogen atoms at this position.

The elucidation of the interaction between DsrAB and DsrC is a major step in our understanding of the role of this small protein in sulfite reduction. DsrC has a highly conserved C-terminus that is very disordered in solution, indicating it is a site of interaction with other proteins. In contrast, in the crystal structure of *A. fulgidus* DsrC, the C-terminus is found in a different conformation, close to the rest of the protein, such that the two strictly conserved cysteines come within bonding distance of each other. Our structure shows that when DsrC interacts with DsrAB its C-terminus is extended and inserts into a cleft between both proteins, in a way that brings its penultimate cysteine in close contact to the siroheme. The position of DsrC Cys104 near the siroheme active site is extremely relevant and has important implications for the mechanism of sulfite reduction. It is important to note that aSiRs, which do not interact with DsrC-like proteins, reduce sulfite directly to sulfide, whereas *in vitro* dSiRs display a very low activity (suggesting the need for partner proteins), and form a mixture of products that is probably not physiologic. The presence of Cys104C so close to the siroheme strongly suggests its involvement in

binding either the substrate or the product, or in the catalytic reaction. Given the difference in products between aSiRs and dSiRs, and the fact that a sulfite ion is found at the active site, it seems more likely that DsrC is involved in the catalytic reaction and/or binding the product. In turnover conditions the Sγ atom of Cys104C may be positioned right next to the substrate molecule, since a rotamer of Cys104C can be easily oriented towards the siroheme distal site, so that its Sγ atom is only 2.4 Å away from one of the oxygen atoms of the sulfite ion. We propose that in dSiRs the reduction of sulfite involves, not a six-, but a four-electron reduction to form an S^0 intermediate, which is then transferred to Cys104C of DsrC to form a persulfide (Figure 10). Once DsrC dissociates from DsrAB, Cys93C can reduce this persulfide, releasing H_2S and forming a Cys93-Cys104 disulfide in DsrC. This oxidised form of DrsC may then be reduced by the membrane-bound DsrMKJOP complex, which contains a cytoplasmic catalytic subunit (DsrK) similar to heterodisulfide reductases and has an unusual catalytic iron-sulfur center for putative reduction of disulfide bonds [26]. The reduced DsrC can then enter another catalytic cycle and bind to DsrAB.

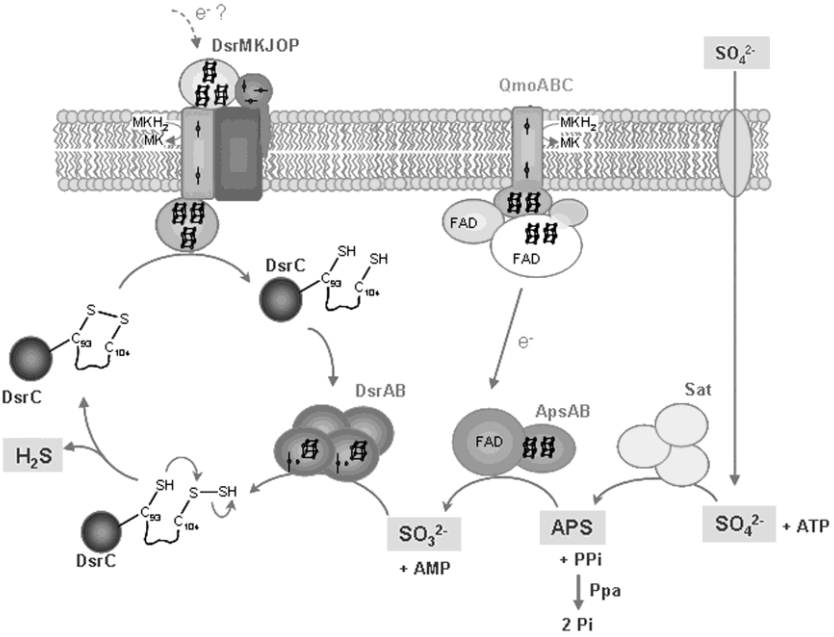

Figure 4. Schematic representation of the proposed sulfate reduction mechanism. Sat: sulfate adenylyltransferase; ApsAB: adenosine phosphosulfate reductase; DsrAB: sulfite reductase; QmoABC: membrane complex that is the probable electron donor to ApsAB; DsrMKJOP: membrane complex with putative disulfide/thiol reductase activity.

Thus, two of the electrons for sulfite reduction would derive from the quinone pool (*via* DsrMKJOP and DsrC) and the other four from the unknown electron donor to Dvir. The involvement of the

DsrMKJOP complex provides a link between membrane quinol oxidation and dSiR, which can explain the fact that proton translocation is observed upon reduction of sulfite [51]. Thus, a persulfide of DsrC would be a crucial intermediate in the reduction of sulfite. The involvement of persulfides as a form of "activated sulfur" is well known in several biological pathways such as the biosynthesis of FeS clusters and other cofactors [52]. In the DsrC homologue YccK/TusE, a persulfide of the cysteine corresponding to Cys104C is also involved in the sulfur transfer reactions performed by this protein [29]. The SoxYZ protein of sulfur oxidisers is another example of a protein that carries sulfur intermediates on an external mobile arm containing a conserved cysteine [53].

The observed cross-link between DsrC and the siroheme explains why in Dvir the association between this protein and DsrAB is stable, whereas in other dSiRs it must be transient. This unexpected feature may result from one of several possible mechanisms, most likely as a result of aerobic purification of the enzyme. One possibility is the formation of a π-cation radical in the siroheme. One of the characteristics of isobacteriochlorins (porphyrins in which two adjacent pyrrole rings are reduced, as sirohydrochlorin) relative to porphyrins and chlorins is the greater ease with which these macrocycles can be oxidized to generate a π-cation radical species [54]. In model compounds, ring oxidation in isobacteriochlorins occurs before oxidation of the metal. The possibility of forming a π-cation radical has been invoked as one of the reasons for which sirohemes may have been selected for the reduction of sulfite and nitrite, as it permits an extra electron to be

generated at the active site [55]. In the structure of the dSiR from *M. tuberculosis* an unusual covalent bond is also found between the side chains of Tyr69 and Cys161, in a position relative to the siroheme very similar to that of Cys104C [44]. We believe this covalent link may also be the result of oxidation by a π-cation radical species. There are other reports of the presence of cross-linked amino acids close to the active sites of redox metalloenzymes such as galactose oxidase, cytochrome *c* oxidase, catechol oxidase and others ([56] and references therein), for which the significance is mostly unknown. For example the Tyr-Cys cross-link present in galactose oxidase, forms spontaneously upon exposure to Cu(I) and oxygen, through a free radical mechanism [56]. Autocatalytic reactions are common in heme modifications like in heme oxygenase, mammalian peroxidases and cytochromes P450 [57]. However, covalent cross-links between porphyrin *meso* carbons and proteins are very unusual, but have been reported in hydroxylamine oxidoreductase and cytochrome P460 from *Nitrosomonas europea* [58]. To the best of our knowledge, this is the first time a covalent link is observed involving a heme *meso* carbon and a cysteine residue. The *A. fulgidus* dSiR, which was purified anaerobically, does not include DsrC [46]. We recently obtained crystals from anaerobically purified Dvir, which still showed the presence of the cross-link. However, it is not possible to discard the possibility of transient contact with oxygen during protein or crystal manipulations. Further work will be necessary to elucidate the conditions that lead to this unusual link between the siroheme and DsrC.

The mechanism proposed herein can explain several pending questions regarding the process of sulfite reduction, namely the role of DsrC and its two conserved cysteines, the role of the DsrMKJOP complex, and why *in vitro* the dSirs do not form sulfide but a mixture of products that depend on the reactions conditions (and are probably the result of sulfite reacting with semi-reduced species at the siroheme). It is interesting that in whole cell extracts of *D. vulgaris*, the product detected for reduction of sulfite was only sulfide, whereas after removal of the membrane fraction the mixture of products was observed [59]. It has also been reported that a form of Dvir purified from the membranes (possibly containing small amounts of the DsrMKJOP complex) forms sulfide as the major product, in contrast to the same protein isolated from the soluble fraction, which formed a mixture of products [60]. In the phototrophic sulfur oxidiser *A. vinosum* the DsrKJO proteins were co-purified with DsrAB and DsrC, supporting an association between these proteins also in the reverse pathway [25].

The elucidation of the way DsrAB interacts with DsrC has important implications, since it shows that this protein has a role in sulfite reduction. The involvement of other proteins besides the DsrAB may require a reassessment of the models used to date ancient sulfur metabolism on geological samples based on sulfur isotope fractionations. Since such fractionations depend on which steps limit the sulfate reduction process, the proposal of a new mechanism involving new proteins, may demand a re-evaluation of such models [61]. This will in turn require a more detailed understanding of the steps involved in sulfate and sulfite reduction.

3.6 Acknowledgements

This work was supported by the research grants PTDC/QUI/68368/06 and PPCDT/BIA-PRO/55621/2004 funded by Fundação para a Ciência e Tecnologia (FCT, MCES, Portugal) and FEDER program, and FCT-POCTI fellowships to TFO (SFRH/BD/29519/2006) and SSV (SFRH/BD/30648/2006). We also would like to thank ESRF for financial and technical support for data collections. CV would like to thank K. Cowtan for making an early version of BUCCANEER available.

3.7 References

1. Shen, Y., R. Buick, and D.E. Canfield, *Isotopic evidence for microbial sulphate reduction in the early Archaean era.* Nature, 2001. 410(6824): p. 77-81.
2. Philippot, P., et al., *Early Archaean microorganisms preferred elemental sulfur, not sulfate.* Science, 2007. 317(5844): p. 1534-7.
3. Canfield, D.E., K.S. Habicht, and B. Thamdrup, *The Archean sulfur cycle and the early history of atmospheric oxygen.* Science, 2000. 288(5466): p. 658-61.
4. Anbar, A.D. and A.H. Knoll, *Proterozoic ocean chemistry and evolution: a bioinorganic bridge?* Science, 2002. 297(5584): p. 1137-42.
5. Dahl, C., et al., *Dissimilatory sulphite reductase from Archaeoglobus fulgidus: physico-chemical properties of the enzyme and cloning, sequencing and analysis of the reductase genes.* J Gen Microbiol, 1993. 139(8): p. 1817-28.
6. Hipp, W.M., et al., *Towards the phylogeny of APS reductases and sirohaem sulfite reductases in sulfate-reducing and sulfur-oxidizing prokaryotes.* Microbiology, 1997. 143 (Pt 9): p. 2891-902.
7. Molitor, M., et al., *A dissimilatory sirohaem-sulfite-reductase-type protein from the hyperthermophilic archaeon Pyrobaculum islandicum.* Microbiology, 1998. 144 (Pt 2): p. 529-41.
8. Wagner, M., et al., *Phylogeny of dissimilatory sulfite reductases supports an early origin of sulfate respiration.* J Bacteriol, 1998. 180(11): p. 2975-82.

9. Crane, B.R. and E.D. Getzoff, *The relationship between structure and function for the sulfite reductases.* Curr Opin Struct Biol, 1996. 6(6): p. 744-56.
10. Dhillon, A., et al., *Domain evolution and functional diversification of sulfite reductases.* Astrobiology, 2005. 5(1): p. 18-29.
11. Loy, A., S. Duller, and M. Wagner, *Evolution and Ecology of Microbes Dissimilating Sulfur Compounds: Insights from Siroheme Sulfite Reductases*, in *Microbial Sulfur Metabolism*, C. Dahl and C. Friedrich, Editors. 2007, Springer Berlin Heidelberg. p. 46-59.
12. Janick, P.A. and L.M. Siegel, *Electron paramagnetic resonance and optical spectroscopic evidence for interaction between siroheme and Fe4S4 prosthetic groups in Escherichia coli sulfite reductase hemoprotein subunit.* Biochemistry, 1982. 21(15): p. 3538-47.
13. Moura, I., et al., *Characterization of two Dissimilatory Sulfite Reductases (Desulforubidin and Desulfoviridin) from the Sulfate-Reducing Bacteria. Mössbauer and EPR Studies.* Journal of the American Chemical Society, 1988. 110: p. 1075-1082.
14. Crane, B.R., L.M. Siegel, and E.D. Getzoff, *Sulfite reductase structure at 1.6 A: evolution and catalysis for reduction of inorganic anions.* Science, 1995. 270(5233): p. 59-67.
15. Peck, H.D. and J. LeGall, *Biochemistry of dissimilatory sulphate reduction.* Philos Trans R Soc Lond B Biol Sci, 1982. 298(1093): p. 443-66.
16. Akagi, J.M., *Reduction of bisulfite by the trithionate pathway by cell extracts from Desulfotomaculum nigrificans.* Biochem Biophys Res Commun, 1983. 117(2): p. 530-5.

17. Fauque, G., et al., *Purification and Characterization of bisulfite reductase (Desulfofuscidin) from Desulfovibrio thermophilus and its complexes with exogenous ligands.* Biochemical and Biophysica acta Pro., 1990. 1040(1): p. 112-118.
18. Pierik, A.J. and W.R. Hagen, *S = 9/2 EPR signals are evidence against coupling between the siroheme and the Fe/S cluster prosthetic groups in Desulfovibrio vulgaris (Hildenborough) dissimilatory sulfite reductase.* Eur J Biochem, 1991. 195(2): p. 505-16.
19. Marritt, S.J. and W.F. Hagen, *Dissimilatory sulfite reductase revisited. The desulfoviridin molecule does contain 20 iron ions, extensively demetallated sirohaem, and an S = 9/2 iron-sulfur cluster.* Eur J Biochem, 1996. 238(3): p. 724-7.
20. Arendsen, A.F., et al., *The dissimilatory sulfite reductase from Desulfosarcina variabilis is a desulforubidin containing uncoupled metalated sirohemes and S = 9/2 iron-sulfur clusters.* Biochemistry, 1993. 32(39): p. 10323-30.
21. Murphy, M.J., et al., *Reduced nicotinamide adenine dinucleotide phosphate-sulfite reductase of enterobacteria. II. Identification of a new class of heme prosthetic group: an iron-tetrahydroporphyrin (isobacteriochlorin type) with eight carboxylic acid groups.* J Biol Chem, 1973. 248(8): p. 2801-14.
22. Wolfe, B.M., S.M. Lui, and J.A. Cowan, *Desulfoviridin, a multimeric-dissimilatory sulfite reductase from Desulfovibrio vulgaris (Hildenborough). Purification, characterization, kinetics and EPR studies.* Eur J Biochem, 1994. 223(1): p. 79-89.

23. Pierik, A.J., et al., *The third subunit of desulfoviridin-type dissimilatory sulfite reductases.* Eur J Biochem, 1992. 205(1): p. 111-5.
24. Karkhoff-Schweizer, R., R.M. Bruschi, and G. Voordouw, *Expression of the gama-subunit gene of Desulfoviridin-type dissimilatory sulfite reductase and of the alfa and beta subunit gene is not coordinatellt regulated.* European Journal of Biochemistry, 1993. 211: p. 501-507.
25. Dahl, C., et al., *Novel Genes of the dsr Gene Cluster and Evidence for Close Interaction of Dsr Proteins during Sulfur Oxidation in the Phototrophic Sulfur Bacterium Allochromatium vinosum.* J Bacteriol, 2005. 187(4): p. 1392-404.
26. Pires, R.H., et al., *Characterization of the Desulfovibrio desulfuricans ATCC 27774 DsrMKJOP complex - a membrane-bound redox complex involved in sulfate respiration.* Biochemistry, 2006. 45(1): p. 249-262.
27. Sander, J., S. Engels-Schwarzlose, and C. Dahl, *Importance of the DsrMKJOP complex for sulfur oxidation in Allochromatium vinosum and phylogenetic analysis of related complexes in other prokaryotes.* Arch Microbiol, 2006. 186(5): p. 357-66.
28. Haveman, S.A., et al., *Gene expression analysis of energy metabolism mutants of Desulfovibrio vulgaris Hildenborough indicates an important role for alcohol dehydrogenase.* J Bacteriol, 2003. 185(15): p. 4345-53.
29. Ikeuchi, Y., et al., *Mechanistic insights into multiple sulfur mediators sulfur relay by involved in thiouridine biosynthesis at tRNA wobble positions.* Molecular Cell, 2006. 21(1): p. 97-108.

30. Cort, J.R., et al., *Solution structure of Pyrobaculum aerophilum DsrC, an archaeal homologue of the gamma subunit of dissimilatory sulfite reductase.* Eur J Biochem, 2001. 268(22): p. 5842-50.
31. Oliveira, T.F., et al., *Purification, crystallization and preliminary crystallographic analysis of a dissimilatory DsrAB sulfite reductase in complex with DsrC.* J Struct Biol, 2008. 164(2): p. 236-9.
32. Kabsch, W., *Automatic processing of rotation diffraction data from crystals of initially inknown symmetry and cell constants.* J. Appl. Crystallogr., 1993. 26: p. 795-800.
33. Evans, P.R., Joint CCP4 and ESF-EACBM Newsletter, 1997. 33: p. 22-24.
34. French S. and W. K., *On the treatment of negative intensity observations.* Acta Cryst. A, 1978. 34(4): p. 517-525.
35. *Collaborative Computational Project Number 4 - The CCP4 Suite: Programs for Protein Crystallography.* Acta Cryst. D, 1994. 50: p. 760-763.
36. Vagin A. and T. A., *MOLREP: an Automated Program for Molecular Replacement.* Journal of Applied Crystallography, 1997. 30(6): p. 1022-1025.
37. Blanc, E., et al., *Refinement of severely incomplete structures with maximum likelihood in BUSTER-TNT.* Acta Crystallogr D Biol Crystallogr, 2004. 60(Pt 12 Pt 1): p. 2210-21.
38. Emsley, P. and K. Cowtan, *Coot: model-building tools for molecular graphics.* Acta Crystallogr D Biol Crystallogr, 2004. 60(Pt 12 Pt 1): p. 2126-32.
39. DeLano, W.L., *The PyMOL Molecular Graphics System, Version 1.2r3pre, Schrödinger, LLC.* 2002.

40. Ostrowski, J., et al., *Characterization of the cysJIH regions of Salmonella typhimurium and Escherichia coli B. DNA sequences of cysI and cysH and a model for the siroheme-Fe4S4 active center of sulfite reductase hemoprotein based on amino acid homology with spinach nitrite reductase.* J Biol Chem, 1989. 264(26): p. 15726-37.
41. Sazanov, L.A. and P. Hinchliffe, *Structure of the hydrophilic domain of respiratory complex I from Thermus thermophilus.* Science, 2006. 311(5766): p. 1430-6.
42. Chartron, J., et al., *Substrate recognition, protein dynamics, and iron-sulfur cluster in Pseudomonas aeruginosa adenosine 5'-phosphosulfate reductase.* J Mol Biol, 2006. 364(2): p. 152-69.
43. Hamann, N., et al., *A cysteine-rich CCG domain contains a novel [4Fe-4S] cluster binding motif as deduced from studies with subunit B of heterodisulfide reductase from Methanothermobacter marburgensis.* Biochemistry, 2007. 46(44): p. 12875-85.
44. Schnell, R., et al., *Siroheme- and [Fe4-S4]-dependent NirA from Mycobacterium tuberculosis is a sulfite reductase with a covalent Cys-Tyr bond in the active site.* J Biol Chem, 2005. 280(29): p. 27319-28.
45. Swamy, U., et al., *Structure of spinach nitrite reductase: implications for multi-electron reactions by the iron-sulfur:siroheme cofactor.* Biochemistry, 2005. 44(49): p. 16054-63.
46. Schiffer, A., et al., *Structure of the dissimilatory sulfite reductase from the hyperthermophilic archaeon Archaeoglobus fulgidus.* J Mol Biol, 2008. 379(5): p. 1063-74.

47. Mander, G.J., et al., *X-ray structure of the gamma-subunit of a dissimilatory sulfite reductase: fixed and flexible C-terminal arms.* FEBS Lett, 2005. 579(21): p. 4600-4.
48. Murphy, M.J. and L.M. Siegel, *Siroheme and sirohydrochlorin. The basis for a new type of porphyrin-related prosthetic group common to both assimilatory and dissimilatory sulfite reductases.* J Biol Chem, 1973. 248(19): p. 6911-9.
49. Postgate, J.R., *Sulphate Reduction by Bacteria.* Annual Review of Microbiology, 1959. 13: p. 505-520.
50. Matthews, J.C., et al., *Siroamide: a prosthetic group isolated from sulfite reductases in the genus Desulfovibrio.* Biochemistry, 1995. 34(15): p. 5248-51.
51. Kobayashi K., et al., *Proton translocation associated with sulfite reduction in a sulfate-reducing bacterium, Desulfovibrio vulgaris.* FEBS Letters, 1982. 149(2): p. 235-237.
52. Kessler, D., *Enzymatic activation of sulfur for incorporation into biomolecules in prokaryotes* FEMS Microbiology Review, 2006. 30(6): p. 825-840.
53. Sauve, V., et al., *The SoxYZ complex carries sulfur cycle intermediates on a peptide swinging arm.* J Biol Chem, 2007. 282(32): p. 23194-204.
54. Chang, C.K., et al., *pi cation radicals of ferrous and free base isobacteriochlorins: Models for siroheme and sirohydrochlorin.* Proc Natl Acad Sci U S A, 1981. 78(5): p. 2652-6.
55. Young, L.J. and L.M. Siegel, *Superoxidized states of Escherichia coli sulfite reductase heme protein subunit.* Biochemistry, 1988. 27(16): p. 5984-90.

56. Whittaker, M.M. and J.W. Whittaker, *Cu(I)-dependent biogenesis of the galactose oxidase redox cofactor.* J Biol Chem, 2003. 278(24): p. 22090-101.
57. Colas, C. and P.R.O. de Montellano, *Autocatalytic radical reactions in physiological prosthetic heme modification.* Chemical Reviews, 2003. 103(6): p. 2305-2332.
58. Pearson, A.R., et al., *The crystal structure of cytochrome P460 of Nitrosomonas europaea reveals a novel cytochrome fold and heme-protein cross-link.* Biochemistry, 2007. 46(28): p. 8340-9.
59. Drake, H.L. and J.M. Akagi, *Dissimilatory reduction of bisulfite by Desulfovibrio vulgaris.* J Bacteriol, 1978. 136(3): p. 916-23.
60. Steuber, J., H. Cypionka, and P.M.H. Kroneck, *Mechanism of Dissimilatory Sulfite Reduction by Desulfovibrio-Desulfuricans - Purification of a Membrane-Bound Sulfite Reductase and Coupling with Cytochrome C(3) and Hydrogenase.* Archives of Microbiology, 1994. 162(4): p. 255-260.
61. Hoek, J. and D.E. Canfield, *Controls on isotope fractionation during dissimilatory sulfate reduction*. Microbial Sulfur Metabolism, ed. C. Dahl and C. Friedrich. 2007, Heidelberg: Spinger-Verlag.

Chapter 4

Structural insights into dissimilatory sulfite reductases: Structure of desulforubidin from *Desulfomicrobium norvegicum*

This Chapter was submitted to the Special Topic issue "The Microbial Sulfur Cycle" in *Frontiers in Microbial Physiology and Metabolism* (invited communication):

Oliveira, T. F.; Franklin, E.; Afonso J. P.; Khan, A; Oldham N. J.; Pereira, I. A. C.; Archer M., "Structural insights into dissimilatory sulfite reductases: Structure of desulforubidin from *Desulfomicrobium norvegicum*"

Note: TFO performed the last steps of protein purification and crystallized the protein, TFO measured and processed X-ray diffraction data, TFO determined and refined the structure with the help MA. TFO, IACP and MA analyzed the structure and wrote the manuscript.

4.1 Abstract

Dissimilatory sulfite reductases (dSiRs) are crucial enzymes in bacterial sulfur-based energy metabolism, which is likely to have been present in some of the earliest life forms on Earth. Several classes of dSiRs have been proposed on the basis of different biochemical and spectroscopic properties. Here, we describe the first structure of a dSiR from the desulforubidin class isolated from *Desulfomicrobium norvegicum*. The desulforubidin structure has a $\alpha_2\beta_2\gamma_2$ unit, in which two DsrC proteins are bound to the core $DsrA_2DsrB_2$ unit, as reported for the desulfoviridin structure from *Desulfovibrio vulgaris*. In contrast to desulfoviridin, four sirohemes and eight [4Fe-4S] clusters are present in desulforubidin, but only two of the coupled siroheme-[4Fe-4S] cofactors are likely to be catalytically active. Mass spectrometry studies of purified desulforubidin and desulfoviridin show that both proteins may present different oligomeric complex forms that bind two, one or no DsrC proteins, providing an explanation for conflicting spectroscopic and biochemical results in the literature. Pyruvate:ferredoxin oxidoreductase and Ferredoxin I were tested as electron donors to desulfoviridin, but no evidence for this role could be obtained.

4.2 Introduction

Microorganisms play an important role in sulfur transformations and are a critical component of sulfur cycling on our planet. Many Bacteria and Archaea have the ability to use sulfur compounds in a series of oxidation or reduction reactions, thereby generating metabolic energy in the process of dissimilatory metabolism. Data from isotopic analysis suggests that dissimilatory sulfate reduction is an extremely ancient process which began 3.5 billion years ago, and became of global significance after sulfate concentrations significantly increased in the Precambrian oceans approximately 2.5 billion years ago [1] [2].

A key enzyme in the reduction of sulfate/sulfite is the dissimilatory sulfite reductase (dSiR), which is responsible for the six electron reduction of sulfite to sulfide. dSiRs belong to a redox enzyme super family, characterized by the presence of a coupled siroheme-[4Fe-4S] cluster cofactor, which include assimilatory sulfite (aSiRs) and nitrite reductases, and other types of sulfite reductases [3-5]. The dSiR is composed of two subunits, DsrA and DsrB, in a ~200 kDa $\alpha_2\beta_2$ arrangement. The *dsrA* and *dsrB* genes are paralogous and probably originated from duplication of an early *dsr* gene before the separation of the *Archaea* and *Bacteria* domains [6-8]. The aSiRs, which generate sulfide for incorporation into amino-acids and cofactors, are monomeric enzymes with an internal two-fold symmetry of a unit that is related to DsrA/DsrB, which indicates

that they also originated from gene duplication, followed by gene fusion of an ancestral sulfite reductase gene that was present in a very early life form [3-4, 9]. After the early divergence of the aSiR and dSiR genes there was incorporation of a ferredoxin domain in the *dsr* gene before separation into the *dsrA* and *dsrB* genes [6]. Evolutionary analysis of the *dsrAB* genes indicates they were mainly inherited via vertical transmission, except for a few events of lateral gene transfer, namely in the archaeal genus *Archaeoglobus*, which has *dsrAB* genes of bacterial origin, in the thermophilic genus *Thermodesulfobacterium*, and Gram-positive bacteria of the *Firmicutes* phylum like *Desulfotomaculum* species [5, 8, 10-11]. In contrast to aSiRs, which reduce sulfite directly to sulfide, the *in vitro* product of dSiRs is not sulfide, but a mixture of products including trithionate, thiosulfate and sulfide [12], suggesting other proteins may be required for the complete reduction to sulfide.

Biochemical studies of dSiRs led to a classification in four different classes based on their UV/visible absorption and other molecular characteristics [13]: Desulfoviridin (Dvir), a green protein (characteristic absorption peak at 628 nm) present in *Desulfovibrio* spp. [14-18]; Desulforubidin (Drub), a reddish-brown protein (characteristic absorption peak at 545 nm) present in *Desulfomicrobium* and *Desulfosarcina* spp. [15, 19-21]; Desulfofuscidin (characteristic absorption peak at 576 nm) present in *Thermodesulfobacterium* spp. [22-23]; and the brown colored P-582 protein (characteristic absorption peak at 582 nm) present in *Desulfotomaculum* spp. [24]. All these dSiRs are proposed to have

an $\alpha_2\beta_2$ structural arrangement, but the type and content of the cofactors is, however, the subject of some controversy [13].

After many years of failed attempts, the first X-ray structures of dSiRs were recently determined, including the Dvir from *Desulfovibrio vulgaris* Hildenborough [25], and dSiR from *Archaeoglubus fulgidus* [26] (at 2.10 Å and 2.04 Å resolution, respectively), showing an $\alpha_2\beta_2$ arrangement with similar overall folds, and finally shedding light on the cofactor composition of these proteins. Four sirohemes and eight [4Fe-4S] clusters are present in *A. fulgidus* dSiR, whereas two sirohemes, two sirohydrochlorins (the metal-free form of siroheme) and eight [4Fe-4S] clusters are present in *D. vulgaris* Dvir. Nevertheless, only two sirohemes per $\alpha_2\beta_2$ unit are proposed to be catalytically active in both proteins. The sequence-based predictions of a similar fold to aSiRs, and of a separate ferredoxin domain containing a [4Fe-4S] cluster that transfers electrons to the active site, were confirmed by these structures. In addition, the crystal structure of *D. vulgaris* Dvir provided important functional information, because in this protein the DsrAB subunits are complexed to the DsrC protein in a $\alpha_2\beta_2\gamma_2$ arrangement. DsrC was originally thought to constitute a third subunit of dSiR [27], but has subsequently been recognized as an independent protein that interacts with DsrAB [28-33], and which is homologous to the TusE protein involved in biosynthetic sulfur-relay reactions [34-35]. In the structure of the *D. vulgaris* DsrAB-DsrC complex, the strictly conserved Cys at the C-terminus of DsrC is positioned right next to the substrate-binding site pointing to the involvement of DsrC in the reduction of sulfite [25].

In this work we determined the three-dimensional structure of a dSir from a different class, the Drub isolated from *Desulfomicrobium norvegicum*. The structure determined at 2.5 Å resolution, shows strong similarities to the one of Dvir, including the presence of DsrC in a $\alpha_2\beta_2\gamma_2$ arrangement. Mass spectrometry studies showed that both purified Drub and Dvir present different oligomeric forms, which may include, or not, the DsrC protein. Finally, ferredoxin and pyruvate-ferredoxin oxidoreductase (PFOR) have been investigated as possible electron donors to dSiR.

4.3 Methods:

4.3.1 Protein Purification

Desulfomicrobium norvegicum (formely known as *Desulfovibrio desulfuricans* strain Norway 4 or *Desulfovibrio baculatus* strain Norway 4) was grown in lactate/sulfate medium and cell extracts prepared as previously described [36]. The purification protocol was performed aerobically at 6ºC. The soluble fraction was loaded on a DEAE-Sepharose fast flow XK50/30 column (GE Healthcare) equilibrated with 20 mM Tris-HCl pH 7.6 buffer. A stepwise gradient of increasing NaCl concentration (0 to 1 M, incremental steps of 0.05 M) was performed. The fraction eluted with 300 mM NaCl was dialyzed against 20 mM Tris-HCl pH 7.6. The

protein was then concentrated and loaded onto a Q-Sepharose 26/10 ion exchange column (GE Healthcare), and a similar procedure was performed. The protein sample was then subjected to size exclusion chromatography on a Sephycryl S-200 HR (GE Healthcare). Finally, the protein was dialyzed in 20 mM Tris-HCl pH 7.6 and loaded onto a Mono Q 5/50 GL column (GE Healthcare) and eluted using the same NaCl step gradient as outlined above. All purification steps were monitored by SDS-PAGE and UV-visible spectroscopy analysis.

4.3.2 Crystallization

The concentrated protein 8 $mg.ml^{-1}$ was used in a number of crystallization trials using a TTP LabTech's mosquito nanolitre pipetting crystallization robot. Several screenings were tested such as: PEG´s from Qiagen; Structure Screen, Pact Premier I and II and JSCG from Molecular Dimensions; Wizard I and II and JBS screen HTS L I and II from Jena Biosciences, with some initial crystals being obtained. Crystal optimization was complicated due to poor crystal reproducibility between different batches of purified protein, and protein degradation over time. Thin needle crystals were obtained using the hanging drop vapor diffusion method at 291 K with a reservoir volume of 500 μl of 20% PEG 3350, 0.1 M BisTris Propane pH 7.5 and 0.2 M K/Na Tartrate. Crystals grew using a protein: precipitant ratio of 2:1 (total volume of 3 μl) over two months with dimensions of 0.15 x 0.03 x 0.03 mm. Prior to X-ray data collection, crystals were cryo-protected by being briefly dipped into a reservoir

solution supplement with 25% glycerol, and immediately flash-frozen in liquid nitrogen (100 K).

4.3.3 Data collection and structure determination

X-ray diffraction data were collected at 0.933 Å at ID14-2 beamline, ESRF - Grenoble, France, to 2.5 Å resolution. A total of 340 images were measured with an oscillation range of 0.6^{o} and exposure time of 10 s/per image. Data were processed with *MOSFLM* [37]; and scaled with *SCALA* [38] from the *CCP4* program suite (Colaborative Computational project, Number 4, 1994). The sequence information for *Dm. norvegicum dsrAB* genes is incomplete at their termini. They do however share 99% sequence identity with the corresponding genes of *Dm. baculatum* (strain DSM 4028). This high identity allowed completion of the Drub *dsrAB* sequences based on those from *D. baculatum*: 62 amino acid residues were added at the N-terminus of DsrA and 115 residues at the C-terminus of DsrB.

A sequence alignment of the composite Drub with Dvir from *D. vulgaris* revealed a high degree of sequence similarity, with DsrA and DsrB subunits sharing both 73% and 81% of sequence identity over the DsrC subunit. Molecular Replacement was done with *PHASER* [39] using the *D. vulgaris* Dvir (PDB code: 2V4J) as a search model. One *PHASER* run was performed searching independently for 2 molecules of each Dsr- A, B and C subunits. One solution with rotation function (RFZ) and translation function (TFZ) of 22.9 and

23.1 respectively and a refinement log-likelihood gain LLG of 662.90 was obtained.

A first model building cycle was performed with *BUCANEER* [40]. Electron-density map inspection and manual model building were carried out using *COOT* [41]. Further refinement was done with *REFMAC5* [42] within the *CCP4* program suite. For the refinement a subset (5%) of the reflections were randomly excluded for cross validation (R_{free} calculation). All structural figures were drawn with *PyMOL* [43].

4.3.4 Mass Spectrometry studies

Purified *Dm. norvegicum* Drub and *D. vulgaris* Dvir were subjected to preparative 9% native gel electrophoresis. Each band was excised from the gel and the protein extracted by electro-elution as described in [44]. Nanoflow electrospray ionization-mass spectrometry was performed on the proteins thus obtained. Experiments were executed on a Waters Synapt High Definition Mass Spectrometer (Manchester, UK) – a hybrid quadrupole/ion mobility/orthogonal acceleration time of flight (oa-TOF) instrument – equipped with a nanospray source and operated in TOF mode. Protein samples were buffer-exchanged into 1 M ammonium acetate pH 7.5 buffer using Vivaspin 500 centrifugal filters with 10 kDa molecular weight cutoff (Sartorius, Göttingen, Germany), diluted to a final concentration of 5 μM and electrosprayed from thin wall Nanoflow Probe Tips (Waters, Manchester, UK).

Experiments were conducted at a capillary voltage of 1.5 kV, nanoflow gas pressure of 0.3 Bar, source temperature of 323 K and sample cone voltage of 30 V, with the source operating in positive ion mode. Backing pressure was maintained between 5.0 and 6.0 mBar to provide collisional cooling of ions in the intermediated vacuum region of the instrument. The collisional energies were 50-70 V in the trap and 30-50 V in the transfer, with a trap gas flow of 10 ml min^{-1} resulting in a pressure of 5.2 x 10^{-2} mBar. Tandem mass spectrometry experiments were performed with trap voltages between 60-120 V. The oa-TOF-MS was operated over the scanning range of m/z 500-15000. Spectra were acquired and processed using Masslynx 4.1 software (Waters, Manchester, UK).

4.3.5 Electron transfer assays

Dvir from *D. vulgaris* Hildenborough was used in experiments to test potential electron donors, since it can be purified with much higher yields than Drub from *Dm. norvegicum*. Direct protein-protein interactions were probed using the surface plasmon resonance technique (Biacore T100 GE Healthcare). Two possible electron donors were tested: ferredoxin-I (FDX; DVU3276) isolated from *D. vulgaris* Hildenborough, and pyruvate ferredoxin oxido-reductase (PFOR) isolated from *D. africanus* (as the *D. vulgaris* one is very unstable and shows 69/82% sequence identity/homology

with *D. vulgaris protein*). A CM5 (carboxymethylated dextran) chip from GE Healthcare was used for the immobilization of dSiR *D. vulgaris*, and FDX and PFOR were tested as analytes. In one of the cases, the reverse coupling was performed, with FDX being coupled to the CM5 chip and dSiR D. vulgaris used as analyte.

Reduction of sulfite by Dvir with pyruvate/PFOR as electron donors was followed by spectroscopic measurement of hydrogen sulfide, using an adaptation of the methylene blue method [45], where this is produced when sulfide reacts with N,N'-dimethyl-p-phenylenediamine (DPD) and ferric chloride under acidic conditions. For the assay, a reaction mixture containing 10 mM sodium pyruvate, 100 μM coenzyme A, 22.5 nM PFOR, 625 nM Dvir, and 200 μM sodium sulfite in a total volume of 200 μl was started with sulfite addition and stopped at various time points (30´, 1 h, 2 h, 3 h, 4 h and 12 h) by addition of 50 μl of the DPD/$FeCl_3$ mixture (prepared in 50% HCl). After 10 minutes incubation for color development, the absorbance was measured at 670 nm in a 96 well plate on a SpectraMax Plus384 spectrophotometer.

4.4 Results and Discussion:

4.4.1 Drub crystal structure

Analysis of the purified *Dm. norvegicum* Drub by SDS-PAGE showed that the DsrC protein is also present, as observed for Dvir from several organisms [27-28]. Crystals of Drub were obtained using PEG3350 as precipitant (pH ~7.5) and diffracted to ~ 2.5 Å. Drub crystals belonged to the orthorhombic space group ($P2_12_12_1$) with unit cell dimensions of a = 99.3, b = 135.1 and c = 178.0 Å (Figure 1).

Figure 1 . Crystal of *D. norvegicum* dSiR obtained by the hanging drop vapor diffusion method to final dimensions of 0.15 x 0.03 x 0.03 mm.

The Matthews coefficient [46] was 2.7 $Å^3Da^{-1}$, consistent with the presence of 1 molecule ($\alpha_2\beta_2\gamma_2$) in the asymmetric unit and 53.3% of solvent content. The structure of Drub was determined by molecular replacement (Figure 2).

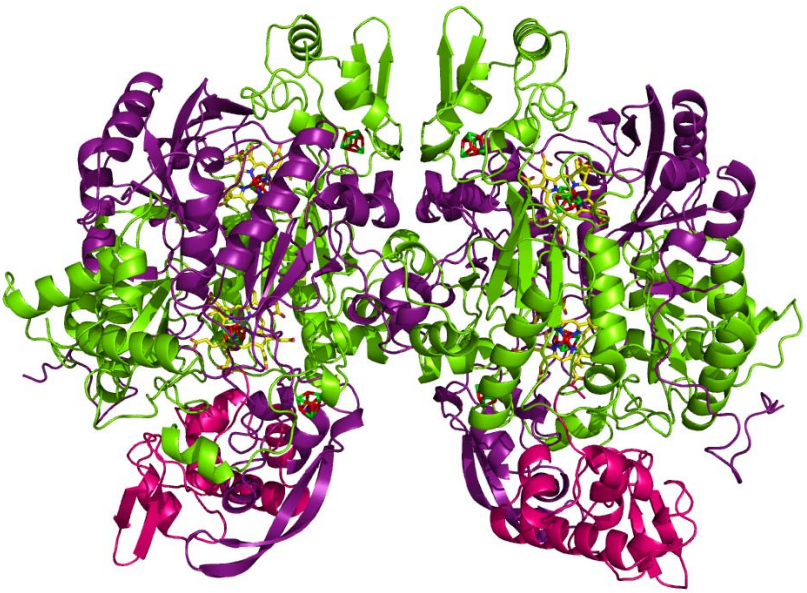

Figure 2. Cartoon representation of the overall $\alpha_2\beta_2\gamma_2$ structure of Drub from *Dm. norvegicum*. α (DsrA), β (DsrB) and γ (DsrC) are colored in green, purple and pink respectively. Siroheme, [4Fe4S] cluster and SO_3 are represented in ball and stick in the following color code: C, yellow; S, green; Fe, dark red; N, blue; Oxygen, red.

The final model comprised 1850 amino acid residues out of 1856, 4 sirohemes and 8 [4Fe-4S] clusters, 2 sulfite ions, 1 glycerol and 1051 water molecules. The $\alpha_2\beta_2\gamma_2$ unit corresponding to $[DsrA]_2[DsrB]_2[DsrC]_2$ is composed of the α subunit comprising residues 2-437 of chains A and D, the β subunit consisting of residues 2-386 from chains B and E, and the γ subunit containing residues 2-105 of chains C and F. Final refinement values for R and R_{free} are 15.1% and 20.5%, respectively, with the entire model fitting the generally well defined electron density map.

The deposited sequences for *Dm.* norvegicum *dsrA* and *dsrB* genes are incomplete at the N-terminal of *dsrA* and C-terminal of *dsrB*. The sequences were completed using those of *Dm. baculatum dsrAB* genes, which share a very high sequence identity. On inspection of the inserted residues extrapolated from the sequence of *Dm. baculatum* six residues are observed which do not fit the experimental electron density and thus are not conserved in the *Dm. norvegicum* sequences. Residues 33A, 57A and 59A were refined manually with serine providing the best fit at these positions, residue 35A was refined as Gln, and residues 323B and 364B as Ser and Ile, respectively. These predictions are expected to be robust, but nevertheless potential misassignments will not have major implications for the structural model due to the nature and position of these residues. Structure analysis and validation of the model was achieved using *PROCHECK* [47] from CCP4 indicating good stereochemistry. The Ramachandran plot shows that the majority of the residues lie in favored regions with only 0.3% falling

in disallowed regions. The relevant statistics for data processing and structure refinement are displayed in Table 1.

Table 1: Data collection and refinement statistics. Values in parentheses are for the outer shell.

Data collection and processing	
Beamline	ID14-2 ESRF, Grenoble
Wavelength (Å)	0.933
Resolution range (Å)	45.10-2.53 (2.67-2.53)
No of images	340
Space group	$P2_12_12_1$
Unit cell parameters (Å)	a = 99.3, b = 135.1, c = 178.0
Mosaicity (°)	0.4
No. of molecules in asymmetric unit	1 ($\alpha_2\beta_2\gamma_2$)
R_{merge} (%)[a]	11.4 (28.6)
R_{pim} (%)[b]	4.2 (11.1)
I/σ (I)	12.8 (5.8)
Multiplicity	8.1 (7.4)
Completeness (%)	99.4 (96.9)
Total Reflections	649457 (82716)
Unique Reflections	79925 (11215)
Wilson B ($Å^2$)	33.5
Refinement	
Nor of amino acid residues	1850
Other molecules - Siroheme (SRM) - [4Fe4S] - SO_3^{2-} - Glycerol - water molecules	 4 8 2 1 1051
R (%) (working + test set)	15.1
R_{free} (%)	20.5
Ramachandran plot, residues in - most favored regions (%) - additional allowed regions	 88.5 11.0

(%)	0.3
- generously allowed regions (%)	0.3
- disallowed regions (%)	
Average B-factor (Å^2)	
- main chain DsrA	13.4
DsrB	13.7
DsrC	26.7
- side chain DsrA	14.8
DsrB	14.9
DsrC	28.7
- solvent molecules	18.0
r.m.s deviation from ideal values	
bond length (Å)	0.021
angles length (°)	2.040

(a) R_{merge} = $\Sigma h \Sigma I \left| Ii(h) - \langle I(h) \rangle \right| / \Sigma h \Sigma i Ii(h)$, where *I* is the observed intensity, $\langle I \rangle$ is the average intensity of multiple observations from symmetry-related reflections, and N is redundancy.

(b) R_{pim} = $\Sigma h[1/(N-1)] / (\Sigma i \left| Ii(h) - \langle I(h) \rangle \right| / \Sigma h \Sigma i Ii(h))$, where *I* is the observed intensity, (*I*) is the average intensity of multiple observations from symmetry-related reflections, and *N* is redundancy.

4.4.2 Overall Drub Architecture and Cofactors

The overall structure of dSiR of *Dm. norvegicum* is very similar to the dSiR structure of *D. vulgaris* [25]. It consists of a dimer of a $\alpha\beta\gamma$ unit with the C-terminal arms of DsrA (405-437A/D) extending towards DsrB from the other monomer (DsrB*), and establishing several hydrogen bonds with amino-acid residues from this subunit, important for dimer stabilization. Both DsrA and DsrB proteins are formed by three domains ($A_1A_2A_3/B_1B_2B_3$) as observed in *D. vulgaris* (PDB 2V4J) and *A. fulgidus* (PDB 3MMC) dSiRs. The Drub structure is formed by a conserved four domain core ($A_1A_2B_1B_2$, where A_1 corresponds to residues 19A-168A, A_2 to 169A-241A and 135B-207B, B_1 to residues 24B-134B, and B_2 to residues 323A-402A and 283B-370B) that is similar to the structures of aSiRs and aNiR [9, 48-49]. A third ferredoxin domain A_3/B_3 is present in both DsrA and DsrB, where A_3 consists of residues 242A-322A, and B_3 to residues 208B-282B.

Each of the A_2/B_2 domains binds a siroheme-[4Fe-4S] cofactor, giving a total of four sirohemes per $\alpha_2\beta_2$ unit as described for the dSiR of *A. fulgidus* (Figure 3).

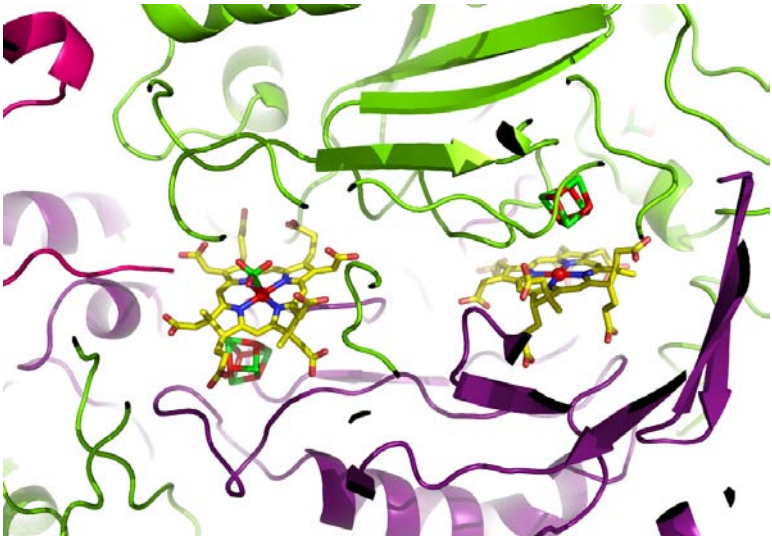

Figure 3 – Ball and Stick representation of the two siroheme-[4Fe4S] clusters in DsrA (green) and DsrB (purple), where a red sphere representing the iron atom is visible. A SO_3^{2-} molecule is found at the active site. (Color code: carbon: yellow; nitrogen: blue; iron: dark red; sulfur: green, oxygen: red).

In contrast, dSiR from *D. vulgaris* has two sirohemes and two sirohydrochlorins per $\alpha_2\beta_2$ unit. The [4Fe-4S] cluster of the coupled siroheme cofactor in A_2 is coordinated by the strictly conserved Cys-X_5-Cys-X_n-Cys-X_3-Cys motif (Cys residues 177A, 183A, 221A and 225A), and as in *D. vulgaris* dSiR, a different cysteine motif (C-X_n-C-C-X_3-C) is observed in the B_2 domain (Cys residues 151B, 188B, 189B and 193B). In each motif two cysteine residues (225A and

193B) share the coordination of the [4Fe-4S] cluster and the siroheme. In the A_3/B_3 ferredoxin domains the [4Fe-4S] cluster is coordinated by cysteines 283A, 303A, 306A and 309A and 231B, 263B, 266B and 269B, respectively.

Previous cofactor quantifications of dSiRs from the desulforubidin class indicated a content of 2.2±0.3 mol of siroheme and 21±2 mol of iron per mol of *Dm. baculatum* Drub [15], and 2 sirohemes and approximately 15 irons for *Desulfosarcina variabilis* Drub [19]. The present structure indicates these values were underestimated with a total of four sirohemes, 36 irons and 32 sulfurs present in the *Dm. norvegicum* Drb $\alpha_2\beta_2$ unit.

4.4.3 The Catalytic Site

Despite the presence of four siroheme-[4Fe-4S] cofactors in Drub, only two of them (bound by DsrB) should be catalytically active, as described for *D. vulgaris* and *A. fulgidus* dSiRs. At the distal side of the catalytic DsrB siroheme, several conserved positive residues are found (Arg 71, 83, 101, 172, 231, 376 and 378 from chain A, Lys 213, 215 and 217 also from chain A and His 150 and 152 from chain B), which create a positive pocket for binding the negatively charged sulfite and are involved in protein stabilization through H-bonds and salt-bridges with the siroheme carboxylate groups. In contrast, some of these crucial substrate residues are missing at the distal side of the DsrA siroheme-[4Fe-4S] cluster. Furthermore, a positive electrostatic potential that extends through a channel can be identified. This channel leads to the catalytic DsrB siroheme, being similar to the one identified in the Dvir structure. Through this narrow channel (formed by the conserved residues Tyr212A, residues 334A-336A, 374A-381A, 225B-230B and 268B-272B), the distal side of the catalytic siroheme is solvent accessible, allowing access of sulfite to the active site. This substrate channel is not present in the non-catalytic siroheme group due to the presence of obstructing residues which block access to the siroheme in DsrA (Tyr339B, Arg283A and a loop comprising residues 257A to 275A). Finally, the interaction with DsrC is only observed at the catalytic siroheme (see below).

Inspection of the catalytic site reveals a positive electron density indicating the presence of an axial ligand bound to the

siroheme iron. Due to its pyramidal shape and the presence of no residual negative or positive electron density peaks during refinement, a sulfite ion was well fitted into this blob, with its sulfur atom pointing towards the siroheme moiety. Thus, the previously observed presence of only two catalytically active sites per $\alpha_2\beta_2$ unit in dSiRs [25-26] is confirmed in the structure of *Dm. norvegicum* Drub.

4.4.4 DsrC fold and complex Interaction

In some dSiRs, namely Dvirs, the small DsrC protein copurifies with DsrAB [27-28], whereas in other dSiRs it does not [6-7]. The structure of *D. vulgaris* Dvir showed that the C-terminal arm of DsrC inserts into a cleft formed at the interface between DsrA and DsrB, positioning the strictly conserved C-terminal DsrC Cys residue next to the catalytic siroheme, providing evidence for a direct role of DsrC in the sulfite reduction mechanism [25]. In contrast, solution structures of isolated DsrC show the C-terminal arm to be disordered [29-30], whereas in a crystal structure it is retracted and in contact with the rest of the structure [32]. In Drub, DsrC adopts a conformation identical to that observed in *D. vulgaris* Dvir, with the C-terminal arm (98C-105C) inserting into the cleft formed by DsrA and DsrB and establishing several hydrogen bonds with both subunits. Also, as observed for Dvir, a covalent bond is present between the Sγ of Cys 104C and the 20 -meso carbon of the catalytic siroheme porphyrin ring. This nonphysiological bond

probably results from an autocatalytic side-reaction, quite common in heme proteins [50].

4.4.5 Structural comparison of Drub with others dSiRs

Superposition of Drub with other dSiRs structures with PDBeFold [51] showed an r.m.s.d. of 0.73 Å for *D. vulgaris* Dvir (1830 aligned Cα) and 1.37 Å for *A. fulgidus* dSiR (1500 superposed Cα atoms). The higher structural similarity of Drub with Dvir reflects a higher amino acid sequence identity - 74% for DsrA and DsrB with *D. vulgaris* Dvir, *versus* 53 and 50%, respectively, for *A. fulgidus* dSiR.

Although the overall fold of dSiRs is quite conserved (Figure 4), there are some relevant localized differences.

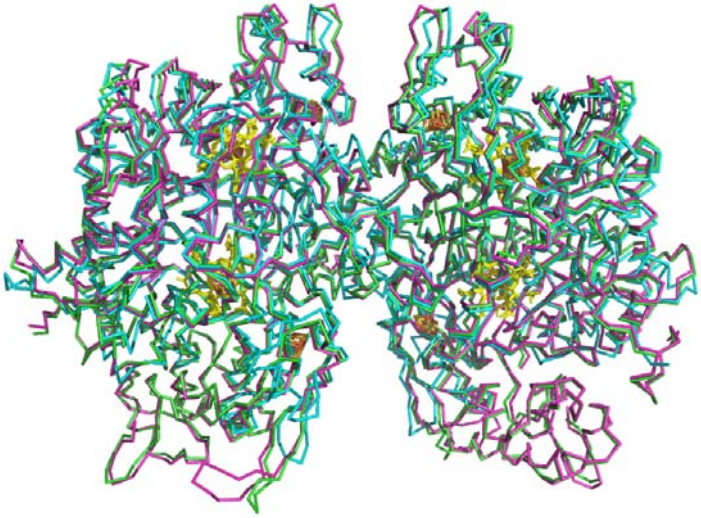

Figure 4. – Cα representation of the overall structure superposition of the dSiRs from *D. norvegicum* (magenta), *D. vulgaris* Hildenborough (green), *A. fulgidus* (cyan). A ball and stick illustration of the cofactors SRM (yellow) and [Fe_4S_4] clusters (orange) is also displayed.

In Drub, DsrB has an inserted segment formed by residues 239B and 254B (5 residues longer than in Dvir and 11 residues longer than *A. fulgidus* dSiR), which corresponds to a longer two anti-parallel stranded β-sheet followed by a 3-residue-H-bonded turn. Moreover, the DsrB N-terminus is also 11-residues longer in Drub, as in Dvir, than in *A. fulgidus* dSiR. It adopts an extended conformation and interacts with DsrA residues: 39-41A (Cα 3B-41A is 5.9 Å) located in a bending loop and 147-151A sited in a α-helix

(Cα 6B-151D is 5.3 Å), and with DsrC (e.g. O atom of Pro 10B is 5.9 Å apart from Oε1 Glu 35C, Cγ of Pro 13B is 4.7 Å away from Cα Gly 38C). Interestingly, both of these inserted segments, not present in *A. fulgidus* dSiR, are flanking DsrC in Drub and Dvir and probably play a role in stabilizing the interaction between DsrAB and DsrC in these proteins.

In Drub and DVir, DsrA shows a 16-residue-insertion (257 to 274A with a 3_{10}-helix), which is replaced by a 2 residues B sheet inserted by a 5 loop long (119-125B: A. fulgidus numbering). In spite of similar length, the C-terminus of DsrA of both Drub and Dvir show a different conformation compared to *A. fulgidus*. In Drub the DsrA C-terminal arm extends along DsrB* (chain E, e.g. distances between Cα atoms: 404A-378E is 4.0 Å, 414A-264E is 4.9 Å, 435A-86D is 5.4 Å) until it reaches DsrA* (chain D) and close to DsrC* (chain F), whereas in *A. fulgidus* the C-terminal arm is more "wrapped" around itself and only in closer contact with DsrB*. These C-tails start diverging after residue 420A (Drub numbering).

Although no 3D structure is yet available for dSiRs belonging to either Desulfofuscidin or P582 classes, we expect similar overall folds for these proteins based on the high sequence identity (ranging from ≈50 to 70%) and similarity (ranging from ≈65 to 80%) among them. *Dm. norvegicum* Drub shows highest sequence identity to *D. vulgaris* Dvir (73%), followed by P582 proteins (≈65%), and lastly *A. fulgidus* dSiR and Desulfofuscidins (≈50%). The DsrA and DsrB cysteine motifs required for binding the [4Fe-4S] cluster of the coupled cofactor, well as the cysteine residues coordinating the ferredoxin domain [4Fe-4S] cluster, are strictly conserved among

the analyzed Desulfofuscidin or P582 dSiRs. In addition, most positively charged residues around the catalytic siroheme and surrounding the substrate channel are also conserved in Desulfofuscidin and P582 proteins. Furthermore, the non conservation of some substrate interacting residues around the non-catalytic DsrA siroheme is also observed in the Desulfofuscidin or P582 dSiRs, which indicates that the presence of a single catalytically active siroheme is a shared characteristic of the different classes of dSirs

4.4.6 Analysis of *D. vulgaris* and *Dm. norvegicum* dSiR oligomeric states

As previously reported by other authors [18, 20, 52-53], we observed that purification of Dvir [44] and Drub on ion-exchange chromatography originates two or three peaks that cannot be distinguished by several analytical techniques including SDS-PAGE, UV-Visible spectroscopy and enzyme activity. Separation by ion-exchange chromatography suggests these peaks have quite different isoelectric points. Native gel analysis of the purified *Dm. norvegicum* Drub showed three different bands, indicating the protein is still present in different states (Figure 5-B). A similar situation was reported for the Dvir from *D. vulgaris* where only two bands are observed (Figure 5-A) [44, 52], and crystals could only be

obtained from the faster migrating band 1. In order to clarify the difference between the different forms, nanoflow electrospray ionization mass spectrometry studies of the bands isolated from preparative native gel electrophoresis of *D. vulgaris* and *Dm. norvegicum* dSiRs were carried out.

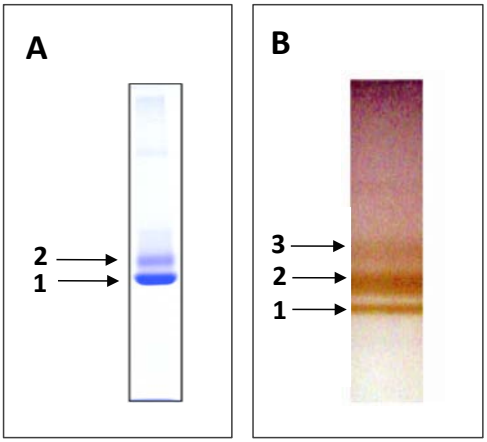

Figure 5: Native polyacrylamide electrophoresis of purified *D.vulgaris* Dvir stained with Coomassie (A) and purified *Dm. norvegicum* Drub unstained (B).

The MS-plot for *D. vulgaris* Dvir band 1 produced well defined peaks corresponding to a Mw of 213.8 kDa, indicating the presence of a single species (Figure 6-a). Analysis of Dvir band 2 from the same gel, provided less definition across the peaks, and a mixture of three species with Mw of 213.4 kDa, 200.5 and 105.9 kDa is observed (Figure 6-b). Molecular weight calculations for the

different possible stoichiometries between *D. vulgaris* DsrA, DsrB and DsrC, including cofactors, gives a theoretical Mw of 213.3 kDa for the *D. vulgaris* $\alpha_2\beta_2\gamma_2$ form, 200.5 kDa for $\alpha_2\beta_2\gamma$, and 106.6 kDa for $\alpha\beta\gamma$ forms (Table 2).

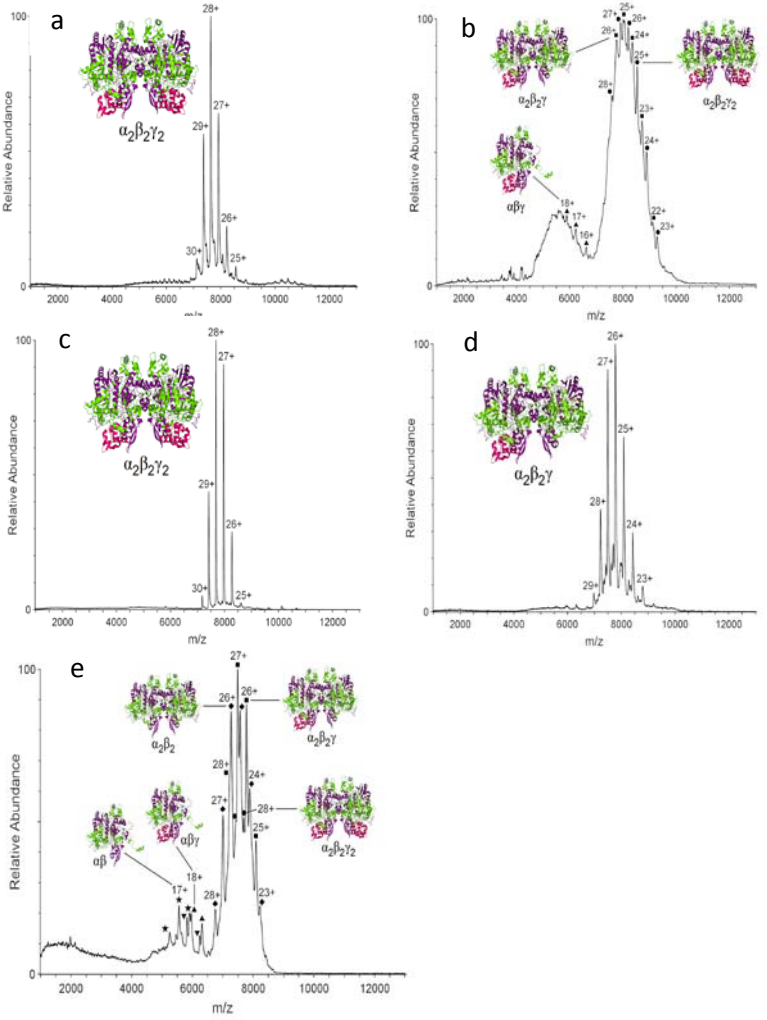

Figure 6. Nanospray ionization mass spectrometry plots of mass-to-charge ratio (m/z) versus signal intensity from the purified dSiRs bands after native gel electrophoresis; *D. vulgaris* Dvir a) band 1, b) band 2; *Dm. norvegicum* c) band 1, d) band 2 and e) band 3.

Table 2. Predicted and observed molecular weight of the different oligomeric forms of *D. vulgaris* Dvir and *Dm. norvegicum* Drub.

	Predicted Complex Stoichiometry	**Predicted Cofactors**	**Theoretical MW (kDa)**	**Obtained MW (kDa)**
Dvir band 1	$\alpha_2\beta_2\gamma_2$	2 SRM + 2 SRHC + 8 [4Fe4S]	213.3	213.8
Dvir band 2	$\alpha_2\beta_2\gamma_2$ $\alpha_2\beta_2\gamma$ $\alpha\beta\gamma$	2 SRM + 2 SRHC + 8 [4Fe4S] 1 SRM +2 SRHC + 8 [4Fe4S] 1 SRM +1 SRHC + 4 [4Fe4S]	213.3 200.5 106.7	213.4 200.5 105.9
Drub band 1	$\alpha_2\beta_2\gamma_2$	4 SRM + 8 [4Fe4S]	215.5	215.1
Drub band 2	$\alpha_2\beta_2\gamma$	3 SRM + 8 [4Fe4S]	202.8	202.0
Drub band 3	$\alpha_2\beta_2\gamma_2$ $\alpha_2\beta_2\gamma$ $\alpha_2\beta_2$ $\alpha\beta\gamma$ $\alpha\beta$	4 SRM + 8 [4Fe4S] 3 SRM + 8 [4Fe4S] 2 SRM + 8 [4Fe4S] 2 SRM + 4 [4Fe4S] 1 SRM + 4 [4Fe4S]	215.5 202.8 190.0 107.8 95.0	215.1 202.3 189.1 107.2 94.5

From these theoretical masses we can conclude that the fast migrating band 1 of Dvir comprises a single $\alpha_2\beta_2\gamma_2$ species, which is in agreement with the crystal structure obtained. In contrast, the slower migrating Dvir band 2 includes a mixture of three different forms, $\alpha_2\beta_2\gamma_2$ and $\alpha_2\beta_2\gamma$ and $\alpha\beta\gamma$, which explains why it could not be crystallized.

For *Dm. norvegicum* Drub, the bands 1 and 2 produced well defined peaks at 215.1 kDa and 202.0 kDa, respectively, corresponding to single complex forms $\alpha_2\beta_2\gamma_2$ (band 1) and $\alpha_2\beta_2\gamma$ (band 2). In the slower migrating band 3, a mixture of peaks at 215.1, 202.3, 189.1, 107.2 and 94.5 kDa is observed, suggesting the presence of an heterogeneous sample corresponding to $\alpha_2\beta_2\gamma_2$, $\alpha_2\beta_2\gamma$, $\alpha_2\beta_2$, $\alpha\beta\gamma$, and $\alpha\beta$ complex compositions.

Tandem MS experiments were then carried out to try to test dissociation of DsrC from DsrAB in the single species samples, by gradually increasing the trap voltage (Figure 7). At 60 V no dissociation is observed, whereas from 80 to 120 V we can detect dissociation of free DsrC, siroheme-bound DsrC as well as siroheme, from the $\alpha_2\beta_2\gamma_2$ and $\alpha_2\beta_2\gamma$ forms of Drub and the $\alpha_2\beta_2\gamma_2$ form of Dvir. The fact that both free DsrC and siroheme are dissociated from these forms indicates that, in solution, not all molecules include the DsrC-siroheme cross-link observed in the crystal structures.

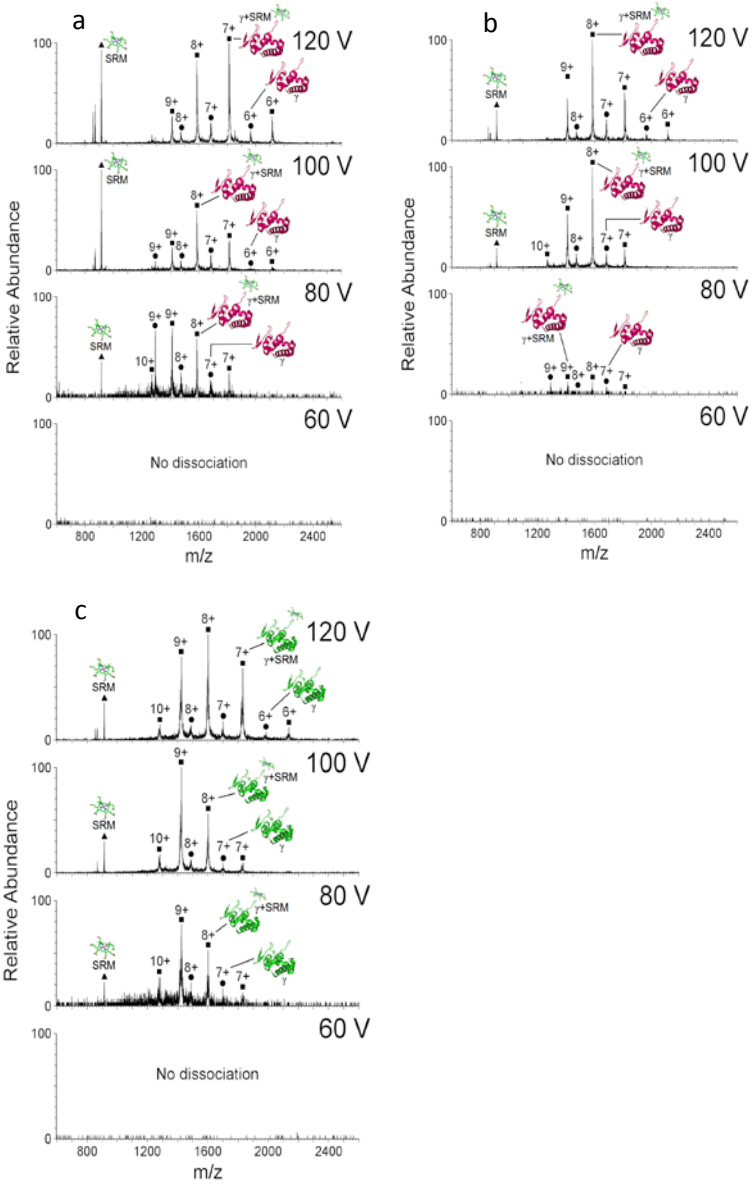
a
b
c
120 V
100 V
80 V
60 V
No dissociation
SRM
γ+SRM
γ
Relative Abundance
m/z
800
1200
1600
2000
2400

Figure 7. Partial complex dissociation of band 1 (a) and 2 (b) from dSiR *Dm. norvegicum* and for band 1 from *D. vulgaris* (c), showing the presence of isolated DsrC and SRM and DsrC-SRM complex.

These results are important because they show clearly that the purified dSiRs from *D. vulgaris* and *Dm. norvegicum*, which seem homogeneous by SDS-PAGE analysis, are in fact a mixture of oligomeric states, even after purification. A similar situation is likely to occur for other purified dSiRs described in the literature, which explains the disparate results in terms of cofactor content and spectroscopic properties [13], the appearance of several peaks with different pIs in ion exchange chromatography, and also why this protein resisted attempts at crystallization for so long. The major species present in both Dvir and Drub are the $\alpha_2\beta_2\gamma_2$ and $\alpha_2\beta_2\gamma$ forms. These forms can be separated on ion-exchange chromatography, but the resulting fractions still have some of the other form, probably due to gradual dissociation of the DsrC protein. In addition, the MS results indicate that the crystallization process selects for the cross-linked $\alpha_2\beta_2\gamma_2$ form, since other forms are present in the Drub protein solution used for crystallization, and non-cross-linked forms of the $\alpha_2\beta_2\gamma_2$ complex should also be present in the Dvir solution. The presence of the cross-link is likely to make the whole structure more stable and enable crystallization. Finally, these results provide evidence that, as expected, not all DsrAB dimers are bound to DsrC physiologically, and that DsrC is not a subunit of dSiR, but a protein with which DsrAB interacts during sulfite reduction [25].

4.4.7 Search for the dSiR electron donor

The direct involvement of DsrC in the reduction of sulfite by DsrAB, as revealed by the *D. vulgaris* Dvir structure, led us to propose a mechanism for sulfite reduction in which reduced DsrC is a co-substrate of DsrAB, with oxidized DsrC (with a disulfide bond between the two C-terminal conserved Cys) being formed as a product [25]. The oxidized DsrC is proposed to be reduced by the membrane-bound DsrMKJOP complex, with the result that two of the six electrons required for sulfite reduction probably originate from the quinone pool. This still leaves a requirement for another electron donor to deliver the remaining four electrons to dSiR, but this donor has not yet been identified. It is known that ferredoxin is the electron donor for the assimilatory sulfite and nitrite reductases. However, in dSir structures, a ferredoxin domain was incorporated in DsrA and DsrB during dSir evolution [4, 6]. This incorporation suggests that the external electron donor may be a ferredoxin-reducing protein.

Using biochemical and biophysical techniques we have tried to examine two potential electron donors to dSiRs: Pyruvate-ferredoxin oxidoreductase (PFOR), and ferredoxin I. We first generated a model for the *D. vulgaris* Hildenborough PFOR based on the structure of PFOR from *D. africanus* (PDB code 1BOP) [54], since the proteins share 69% sequence identity. The surface electrostatic potential was calculated for both *D. vulgaris* Dvir and PFOR structures, to detect possible interaction sites. On the *D. vulgaris* Dvir surface, a negatively charged region is observed in the

ferredoxin domain of chain B, which is a likely region for interaction with an electron donor. In contrast, an overall positive charge along the surface of the ferredoxin domain is observed in PFOR. Using modeling tools in Pymol, the PFOR ferredoxin domain can be placed in the vicinity of the *D. vulgaris* Dvir ferredoxin domain positioning the iron-sulfur clusters of the two domains at ~ 15 Å from each other. This suggests that electron transfer from the PFOR [4Fe-4S] cluster to the Dvir ferredoxin [4Fe-4S] cluster is possible, so PFOR looks like a plausible candidate electron donor.

We analyzed protein-protein interactions between the *D. vulgaris* Dvir and potential donors using the surface plasmon resonance technique. However, we could detected no direct binding between immobilized Dvir and either PFOR or Fd-I. We cannot exclude that this technique may be hampered by the transient nature of the interaction between PFOR and Dvir. In addition to the direct protein-protein interaction assays, we also tested an activity-based assay for reduction of sulfite by Dvir with pyruvate/PFOR as electron donors. The assay was based on the measurement of sulfide production by the methylene blue method. Again, we could detect no reduction of sulfite from pyruvate. These results suggest that PFOR or Fd-I may not be physiological electron donors to dSiRs, or alternatively, the system may need other components to allow the enzyme to complete the catalytic cycle. Further work is necessary to elucidate the nature of the electron donor to dSiR.

4.5 Concluding remarks

In conclusion, the structure of a Drub determined herein shows that it is very similar to the structure of *D. vulgaris* Dvir, with the difference in spectral properties being explained simply by the presence of both sirohydrochlorin and siroheme in Dvir, whereas only siroheme is present in Drub. Since the Drub sirohemes corresponding to the sirohydrochlorins are nonetheless not catalytic, there seems to be little justification for classifying Drub and Dvir as two different classes of dSiRs.

Using MS studies we established that purified Dvir and Drub are still present in different oligomeric forms with two, one or no DsrC molecules bound. The relative proportions of these species are likely to be highly dependent on the preparation, finally providing an explanation for the conflicting results in terms of cofactor content and spectroscopy results for these proteins. In addition, we obtained evidence for the fact that not all DsrC molecules in the DsrABC complexes have a covalent bond to the siroheme. Our preliminary attempts to discover the physiological electron donor to dSir have proved unsuccessful, and future studies will be required to elucidate this important point in dissimilatory sulfate reduction.

4.6 Acknowledgements

This work was supported by research grant PTDC/QUI-BIQ/100591/2008 funded by Fundação para a Ciência e Tecnologia (FCT, MCTES, Portugal). We also would like to thank FCT for the FCT-POCTI fellowships to TFO (SFRH/BD/29519/2006) and ESRF for financial and technical support for data collections.

4.7 References

1. Canfield, D.E., M.T. Rosing, and C. Bjerrum, *Early anaerobic metabolisms.* Philos Trans R Soc Lond B Biol Sci, 2006. **361**(1474): p. 1819-34; discussion 1835-6.
2. Canfield, D.E. and R. Raiswell, *The Evolution of the Sulfur Cycle.* American Journal of Science, 1999. **299**: p. 627-723.
3. Crane, B.R. and E.D. Getzoff, *The relationship between structure and function for the sulfite reductases.* Curr Opin Struct Biol, 1996. **6**(6): p. 744-56.
4. Dhillon, A., et al., *Domain evolution and functional diversification of sulfite reductases.* Astrobiology, 2005. **5**(1): p. 18-29.
5. Loy, A., S. Duller, and M. Wagner, *Evolution and Ecology of Microbes Dissimilating Sulfur Compounds: Insights from Siroheme Sulfite Reductases*, in *Microbial Sulfur Metabolism*, C. Dahl and C. Friedrich, Editors. 2007, Springer Berlin Heidelberg. p. 46-59.
6. Dahl, C., et al., *Dissimilatory sulphite reductase from Archaeoglobus fulgidus: physico-chemical properties of the enzyme and cloning, sequencing and analysis of the reductase genes.* J Gen Microbiol, 1993. **139**(8): p. 1817-28.
7. Molitor, M., et al., *A dissimilatory sirohaem-sulfite-reductase-type protein from the hyperthermophilic archaeon Pyrobaculum islandicum.* Microbiology, 1998. **144 (Pt 2)**: p. 529-41.
8. Wagner, M., et al., *Phylogeny of dissimilatory sulfite reductases supports an early origin of sulfate respiration.* J Bacteriol, 1998. **180**(11): p. 2975-82.

9. Crane, B.R., L.M. Siegel, and E.D. Getzoff, *Sulfite reductase structure at 1.6 A: evolution and catalysis for reduction of inorganic anions.* Science, 1995. **270**(5233): p. 59-67.
10. Klein, M., et al., *Multiple lateral transfers of dissimilatory sulfite reductase genes between major lineages of sulfate-reducing prokaryotes.* J Bacteriol, 2001. **183**(20): p. 6028-35.
11. Zverlov, V., et al., *Lateral gene transfer of dissimilatory (bi)sulfite reductase revisited.* J Bacteriol, 2005. **187**(6): p. 2203-8.
12. Peck, H.D. and J. LeGall, *Biochemistry of dissimilatory sulphate reduction.* Philos Trans R Soc Lond B Biol Sci, 1982. **298**(1093): p. 443-66.
13. Rabus, R., T. Hansen, and F. Widdel, *Dissimilatory Sulfate- and Sulfur-Reducing Prokaryotes*, in *The Prokaryotes*, M.e.a. Dworkin, Editor. 2007, Springer-Verlag, http://link.springer-ny.com/link/service/books/10125/. New York. p. 659-768.
14. Lee, J.P. and H.D. Peck, *Purification of the Enzyme Reducing Bisulfite to Trithionate from Desulfovibrio gigas and its Identification as Desulfoviridin.* Biochemical and Biophysical Research Communications, 1971. **45**(3): p. 583-589.
15. Moura, I., et al., *Characterization of two Dissimilatory Sulfite Reductases (Desulforubidin and Desulfoviridin) from the Sulfate-Reducing Bacteria. Mössbauer and EPR Studies.* Journal of the American Chemical Society, 1988. **110**: p. 1075-1082.
16. Pierik, A.J. and W.R. Hagen, *S = 9/2 EPR signals are evidence against coupling between the siroheme and the Fe/S cluster prosthetic groups in Desulfovibrio vulgaris*

(Hildenborough) dissimilatory sulfite reductase. Eur J Biochem, 1991. **195**(2): p. 505-16.

17. Steuber, J., H. Cypionka, and P.M.H. Kroneck, *Mechanism of Dissimilatory Sulfite Reduction by Desulfovibrio-Desulfuricans - Purification of a Membrane-Bound Sulfite Reductase and Coupling with Cytochrome C(3) and Hydrogenase.* Archives of Microbiology, 1994. **162**(4): p. 255-260.
18. Wolfe, B.M., S.M. Lui, and J.A. Cowan, *Desulfoviridin, a multimeric-dissimilatory sulfite reductase from Desulfovibrio vulgaris (Hildenborough). Purification, characterization, kinetics and EPR studies.* Eur J Biochem, 1994. **223**(1): p. 79-89.
19. Arendsen, A.F., et al., *The dissimilatory sulfite reductase from Desulfosarcina variabilis is a desulforubidin containing uncoupled metalated sirohemes and S = 9/2 iron-sulfur clusters.* Biochemistry, 1993. **32**(39): p. 10323-30.
20. Lee, J.P., et al., *Isolation of a New Pigment, Desulforubidin, from Desulfovibrio desulfuricans (Norway Strain) and Its Role in Sulfite Reduction* Journal of Bacteriology, 1973. **115**(1): p. 453-455.
21. DerVartanian, D.V., *Desulforubidin: dissimilatory, high-spin sulfite reductase of Desulfomicrobium species.* Methods Enzymol, 1994. **243**: p. 270-6.
22. Hatchikian, E.C., *Desulfofuscidin: dissimilatory, high-spin sulfite reductase of thermophilic, sulfate-reducing bacteria.* Methods Enzymol, 1994. **243**: p. 276-95.
23. Hatchikian, E.C. and J.G. Zeikus, *Characterization of a new type of dissimilatory sulfite reductase present in Thermodesulfobacterium commune.* J Bacteriol, 1983. **153**(3): p. 1211-20.

24. Akagi, J.M., M. Chan, and V. Adams, *Observations on the bisulfite reductase (P582) isolated from Desulfotomaculum nigrificans.* J Bacteriol, 1974. **120**(1): p. 240-4.
25. Oliveira, T.F., et al., *The crystal structure of Desulfovibrio vulgaris dissimilatory sulfite reductase bound to DsrC provides novel insights into the mechanism of sulfate respiration.* J Biol Chem, 2008. **283**(49): p. 34141-9.
26. Schiffer, A., et al., *Structure of the dissimilatory sulfite reductase from the hyperthermophilic archaeon Archaeoglobus fulgidus.* J Mol Biol, 2008. **379**(5): p. 1063-74.
27. Pierik, A.J., et al., *The third subunit of desulfoviridin-type dissimilatory sulfite reductases.* Eur J Biochem, 1992. **205**(1): p. 111-5.
28. Steuber, J., et al., *Molecular properties of the dissimilatory sulfite reductase from Desulfovibrio desulfuricans (Essex) and comparison with the enzyme from Desulfovibrio vulgaris (Hildenborough).* Eur J Biochem, 1995. **233**(3): p. 873-9.
29. Cort, J.R., et al., *Solution structure of Pyrobaculum aerophilum DsrC, an archaeal homologue of the gamma subunit of dissimilatory sulfite reductase.* Eur J Biochem, 2001. **268**(22): p. 5842-50.
30. Cort, J.R., et al., *Allochromatium vinosum DsrC: solution-state NMR structure, redox properties, and interaction with DsrEFH, a protein essential for purple sulfur bacterial sulfur oxidation.* J Mol Biol, 2008. **382**(3): p. 692-707.
31. Dahl, C., et al., *Novel Genes of the dsr Gene Cluster and Evidence for Close Interaction of Dsr Proteins during Sulfur Oxidation in the Phototrophic Sulfur Bacterium*

Allochromatium vinosum. J Bacteriol, 2005. **187**(4): p. 1392-404.

32. Mander, G.J., et al., *X-ray structure of the gamma-subunit of a dissimilatory sulfite reductase: fixed and flexible C-terminal arms.* FEBS Lett, 2005. **579**(21): p. 4600-4.
33. Pires, R.H., et al., *Characterization of the Desulfovibrio desulfuricans ATCC 27774 DsrMKJOP complex - a membrane-bound redox complex involved in sulfate respiration.* Biochemistry, 2006. **45**(1): p. 249-262.
34. Ikeuchi, Y., et al., *Mechanistic insights into multiple sulfur mediators sulfur relay by involved in thiouridine biosynthesis at tRNA wobble positions.* Molecular Cell, 2006. **21**(1): p. 97-108.
35. Numata, T., et al., *Structural basis for sulfur relay to RNA mediated by heterohexameric TusBCD complex.* Structure, 2006. **14**(2): p. 357-66.
36. Pereira, P.M., et al., *The Tmc complex from Desulfovibrio vulgaris hildenborough is involved in transmembrane electron transfer from periplasmic hydrogen oxidation.* Biochemistry, 2006. **45**(34): p. 10359-67.
37. Leslie, A.G.W., *Joint CCP4 + ESF-EAMBC.* Newsletter on Protein Crystallography, 1992. **26**.
38. Weiss, M., *Global Indicators of X-ray data quality.* Journal of Applied Crystallography, 2001. **34**(2): p. 130-135.
39. McCoy, A.J., et al., *Phaser crystallographic software.* J Appl Crystallogr, 2007. **40**(Pt 4): p. 658-674.
40. Cowtan, K., *The Buccaneer software for automated model building. 1. Tracing protein chains.* Acta Crystallogr D Biol Crystallogr, 2006. **62**(Pt 9): p. 1002-11.

41. Emsley, P. and K. Cowtan, *Coot: model-building tools for molecular graphics.* Acta Crystallogr D Biol Crystallogr, 2004. **60**(Pt 12 Pt 1): p. 2126-32.
42. Murshudov, G.N., A.A. Vagin, and E.J. Dodson, *Refinement of macromolecular structures by the maximum-likelihood method.* Acta Crystallogr D Biol Crystallogr, 1997. **53**(Pt 3): p. 240-55.
43. DeLano, W.L., *The PyMOL Molecular Graphics System, Version 1.2r3pre, Schrödinger, LLC.* 2002.
44. Oliveira, T.F., et al., *Purification, crystallization and preliminary crystallographic analysis of a dissimilatory DsrAB sulfite reductase in complex with DsrC.* J Struct Biol, 2008. **164**(2): p. 236-9.
45. Fogo, J.K. and P. Milton, *Spectrophotometric Determination of Hydrogen Sulfide.* Analytical Chemistry, 1949. **21**(6): p. 732-734.
46. Matthews, B.W., *Solvent content of protein crystals.* J Mol Biol, 1968. **33**(2): p. 491-7.
47. Laskowski, R.A., et al., *PROCHECK: a program to check the stereochemical quality of protein structures.* Journal of Applied Crystallography, 1993. **26**(2): p. 283-291.
48. Schnell, R., et al., *Siroheme- and [Fe4-S4]-dependent NirA from Mycobacterium tuberculosis is a sulfite reductase with a covalent Cys-Tyr bond in the active site.* J Biol Chem, 2005. **280**(29): p. 27319-28.
49. Swamy, U., et al., *Structure of spinach nitrite reductase: implications for multi-electron reactions by the iron-sulfur:siroheme cofactor.* Biochemistry, 2005. **44**(49): p. 16054-63.

50. Colas, C. and P.R.O. de Montellano, *Autocatalytic radical reactions in physiological prosthetic heme modification.* Chemical Reviews, 2003. **103**(6): p. 2305-2332.
51. Krissinel, E. and K. Henrick, *Secondary-structure matching (SSM), a new tool for fast protein structure alignment in three dimensions.* Acta Crystallogr D Biol Crystallogr, 2004. **60**(Pt 12 Pt 1): p. 2256-68.
52. Seki, Y., K. Kobayashi, and M. Ishimoto, *Biochemical studies on sulfate-reducing bacteria. XV. Separation and comparison of two forms of desulfoviridin.* J Biochem, 1979. **85**(3): p. 705-11.
53. Marritt, S.J. and W.F. Hagen, *Dissimilatory sulfite reductase revisited. The desulfoviridin molecule does contain 20 iron ions, extensively demetallated sirohaem, and an S = 9/2 iron-sulfur cluster.* Eur J Biochem, 1996. **238**(3): p. 724-7.
54. Chabriere, E., et al., *Crystal structure of the free radical intermediate of pyruvate:ferredoxin oxidoreductase.* Science, 2001. **294**(5551): p. 2559-63.

Chapter 5

Conclusion

5.1 Conclusion

Sulfate reducing bacteria (SRB) have been studied for more than a century, but we still do not have a molecular understanding of how energy conservation is achieved by using sulfate as terminal electron acceptor. The genomics revolution has provided an opportunity to have a more general view of proteins present in these bacteria, thus enabling microbiologists to obtain more detailed insights into the ecology and biotechnology of these important microorganisms. Understanding how these microorganisms co-evolved and operate together with others to create electron flows that predominate today on Earth´s surface remains a grand challenge. Understanding biogeochemical co-evolution is critical to the survival of humans as we continue to influence the fluxes of matter and energy on a global scale. Microbial life can easily live without us; we, however, cannot survive without the global catalysis and environmental transformations it provides.

The X-ray structure of dissimilatory Sulfite Reductase (dSiR) from *D. vulgaris* Hildenborough, a member of the desulfoviridin class was important to reveal the dSiR architecture and cofactor content showing an $\alpha_2\beta_2$ assembly with 2 sirohemes, 2 sirohydrochlorins and 34 Fe *per* $\alpha_2\beta_2$ unit, confirming the presence of a coupled siroheme-[4Fe-4S] cofactor. The structure also showed a fully demetallated siroheme (sirohydrochlorin) in the DsrA subunit

which is responsible for its characteristic absorption peak at ~628 nm. The putative substrate channel leading this DsrA sirohydrochlorin is blocked and two conserved residues assumed to be crucial at the active site of DsrB siroheme are not present in DsrA. Therefore, dSiRs only have two catalytically active sirohemes present *per* $\alpha_2\beta_2$ unit, whereas in aSiRs the second catalytic heme was lost during evolution.

The 3D structure of *Desulfomicrobium Norvegicum* sulfite reductase from the desulforubidin class of dSiRs is very similar to the one of *D. vulgaris*. It has, however, 4 siroheme-[4Fe-4S] cofactors (no demetallated sirohydrochlorin), but the siroheme at the DsrA subunit is also not catalytic active. Structural analysis of *D. vulgaris* and *Dm Norvegicum* dSiRs and amino-acid sequence alignment with members of other classes, namely desulfofuscidin or P582, suggests similar assemblies and properties for dSiRs of these classes.

The most relevant contribution from the work described in this thesis, was the elucidation of how the small molecular weight protein DsrC interacts with DsrAB. The DsrC C-terminus inserts into a cleft formed at the interface of DsrA and DsrB, placing its conserved penultimate cysteine in close contact to the substrate binding site at the catalytic siroheme, providing strong evidence of its involvement in sulfite reduction. A structure-based mechanism is proposed where DsrC plays a crucial role in this reduction and overall in the energetic metabolism. In this proposal a four, and not

six, electron reduction of sulfite occurs, forming an S^0 intermediate that is transferred to the C-terminal cysteine of DsrC with the formation of a persulfide. This persulfide then gives origin to an oxidized form of DsrC with a disulfide bond between its two conserved cysteines. This oxidized DsrC form is proposed to be a substrate for the membrane-bound complex DsrMKJOP. According to the proposed mechanism two electrons would derive from the quinone pool and the other four from an unknown electron donor to dSiR, thus providing a direct link between the quinone pool and sulfite reduction and suggesting a possible mechanism to explain energy conservation. Many efforts were devoted to identify the unknown electron donor of dSiR, unfortunately without success. Thus, further work is still required for a better understanding of the pathways involved in sulfate and sulfite reduction. This task will be one of the main goals for a near future.